Volume 6, Number 2
September, 1960

THE SOVIET JOURNAL OF

ATOMIC ENERGY

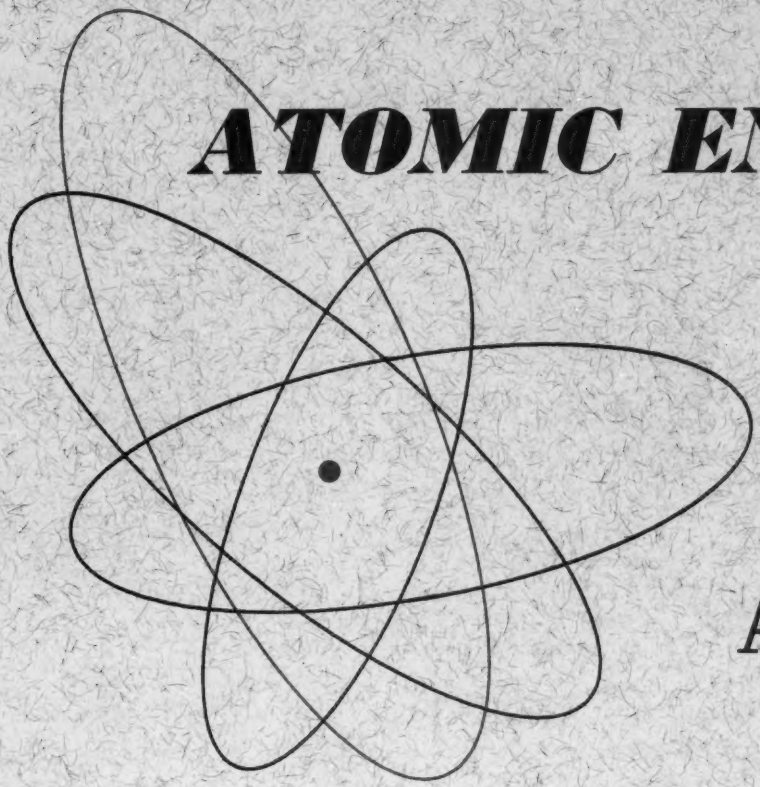

Атомная энергия

TRANSLATED FROM RUSSIAN

CONSULTANTS BUREAU

EQUIPMENT FOR A MODERN LABORATORY... A NEW CONCEPT IN DESIGN

Apparatus Drawings Project (ADP)

Sponsored by the American Association of Physics Teachers and the American Institute of Physics under a grant from the National Science Foundation

ADP has been designed to present physics teachers and laboratory workers in the field with **complete** data and drawings concerning **over 30 unique and economical pieces of apparatus** developed in the physics laboratories of some of America's leading colleges and universities.

The equipment described in ADP was developed as up-to-date teaching apparatus for laboratory experiments and lecture demonstrations. The drawings make available to other departments designs for apparatus which would otherwise be difficult to obtain. The reports contained in this series document original equipment which can be duplicated in your shop – **economically** – often by your students.

AN INVALUABLE TEACHING AID!
USEFUL IN RESEARCH!

PLENUM PRESS will publish and distribute the entire series which will cover over 30 different pieces of apparatus. You will be sent 10 reports in the first mailing. Printed on flat sheets (11 x 17, one side) for working convenience, the sheets fit into a durable cardboard case for safe storage.

THE CASE WILL BE SENT TO YOU AT NO EXTRA CHARGE!

Approximately 10 reports will be sent to you each mailing until you have received the complete set. Then (and at no extra charge) you will receive a clothbound (8½ x 11) book which will contain all the material in the reports in handy reference form for your desk or library.

The series of over 30 reports, the attractive cardboard storage case, and the desk-size manual will be sent to you for the single subscription price of only $25.00.

The full-size drawings and the book are not sold separately.

The first ten reports will consist of	Developed at
1. **Balmer Series Spectrum Tube**	**Massachusetts Institute of Technology**
2. **Magnetic Field of a Circular Coil**	**Rensselaer Polytechnic Institute**
3. **Air Suspension Gyroscope**	**Massachusetts Institute of Technology**
4. **Resolution of Forces Apparatus**	**Massachusetts Institute of Technology**
5. **Simple Mass Spectrometer**	**Swarthmore**
6. **Bragg Diffraction Apparatus**	**Rensselaer Polytechnic Institute**
7. **Versatile Mass Spectrometer**	**Dartmouth**
8. **Driven Linear Mechanical Oscillator**	**Bryn Mawr**
9. **Simple Kinetic Theory Demonstration**	**Princeton**
10. **Air Suspended Pucks for Momentum Experiments**	**Massachusetts Institute of Technology**

Equipment designed at other leading universities and colleges will be included in future reports.

YOU MAY SEND FOR A SAMPLE PAGE

FOR FURTHER DETAILS, CONTACT MR. CHARLES KNOWLES

PLENUM PRESS 227 WEST 17TH STREET, NEW YORK 11, N. Y.

THE SOVIET JOURNAL OF

ATOMIC ENERGY

A translation of ATOMNAYA ÉNERGIYA,
a publication of the Academy of Sciences of the USSR

(Russian original dated February, 1959)

Vol. 6, No. 2 September, 1960

CONTENTS

Annual subscription $75.00
Single issue 20.00
Single article 12.50

CONTENTS (continued)

NOTE

The Table of Contents will continue to list all material which appeared in Atomnaya Energiya, but those items which originated in the English language and are therefore not included in the translation are enclosed in brackets. Whenever possible, the source from which English copies of the omitted reports can be obtained will be given.

Consultants Bureau Enterprises, Inc.

INDUSTRIAL METHODS OF PROCESSING POOR URANIUM ORES

G. E. Kaplan, B. N. Laskorin, and B. V. Nevskii

In recent years great progress has been achieved in the technology of processing uranium ores. A method of extracting uranium from solutions by means of absorption on resins, developed comparatively recently, now makes it possible to obtain more than 70% of the total extractable uranium. The extraction of uranium with liquid extractants also finds wide application, especially in plants using acid leaching of uranium.

The normal methods of mechanical enrichment (gravitation, flotation, etc.) play a comparatively small part. However, with complex and poor ores being used, mechanical enrichment in the processing of uranium ores assumes greater importance. Radiometric enrichment is particularly progressive and this makes use of the radioactivity of uranium minerals for separating them from barren rock.

Introduction

Before the Second World War, due to the small scale use of uranium and its compounds, only rich ores were processed and mainly for the extraction of radium, while uranium compounds were obtained as by-products.

The establishment of a large uranium industry after the Second World War in connection with its use in military technology and nuclear power as well as the exhaustion of reserves of rich ores have made it necessary for most countries to undertake large scale processing of poor raw materials, usually characterized by a diversity of uranium-containing components, and a fine dispersion of the uranium minerals.

Due to the change-over to the use of extremely poor raw material, interest in the mechanical enrichment of uranium-bearing ores grows each year. However, if one judges by the literature on the subject, methods of enriching uranium ores have comparatively limited use at present, largely due to the difficulties of enriching most ores as a result of the character of uranium mineralization mentioned above.

The relative importance of the various processes in the treatment of uranium ores (in %) is as follows [1]:

Acid leaching and sorption extraction of uranium. .	73
including sorption from solutions	51
" " from pulp.	22*
Acid leaching with chemical methods for uranium extraction (mainly phosphate precipitation) . . .	11
Acid leaching and extractive recovery of uranium from solutions.	4
Carbonate leaching with chemical methods of uranium precipitation	10
Mechanical enrichment methods	2

Mechanical Enrichment

Intensive scientific investigations are being carried out in many countries to find the most efficient methods of enriching poor uranium ores [2,3]. In the USA, Britain, Canada, Australia, South Africa, and other countries special scientific research institutes and laboratories have been set up for developing methods of processing uranium ores.

Mechanical enrichment to extract waste tailings is used only for extremely poor ores (containing not more than 0.05 – 0.1% of uranium). Mechanical enrichment is also used occasionally for richer ores, but, as a rule, in this case a rich concentrate is separated and sent to central plants for processing, while the poor industrial product is usually processed on the spot by hydrometallurgical methods. In particular, such a method is used at Port Radium, Canada, and in the Belgian Congo [4].

The principal methods of enrichment which are used in industry are: gravitation enrichment, including those in heavy suspensions using hydrocyclones (Kvarnsdorp plant in Sweden and the Radium Hill factory in Australia), radiometric enrichment (at the present time scintillation counters are being used in the factory at Port Radium), and in some cases, flotation, selective pulverization, and magnetic separation.

GRAVITATION ENRICHMENT METHODS. Such methods are apparently used by several plants, but are described in detail only for the factory at Port Radium, where, according to the scheme given, the ore is enriched by the use of jigging and flotation in a closed cycle with crushers, screens, and graders (Scheme 1).

Numerous investigations on gravitation enrichment show that the greatest enrichment is achieved for ores containing complex uranium-bearing titanoniobates, for which, 90% extraction is achieved with a high degree of concentration (up to 100).

The enrichment of ores containing pitchblende is usually less efficient due to its fine dispersion in the minerals of the bearing rock; extraction of uranium into the concentrate does not exceed 70 – 75%, but occasionally quite rich concentrates may be obtained. Thus, for example, there are in the plant at Port Radium, starting ores containing about 1% of uranium yield concentrates with a uranium content of up to 20%, which are flown to the USA and to the plant at Port Hope (Canada). The enrichment tailings are not a waste product as they contain about 0.2 – 0.3% of uranium and are reprocessed on the spot by sulfuric acid leaching [4].

ENRICHMENT IN HEAVY SUSPENSIONS. Enrichment in heavy suspensions for example, of magnetite and of ferrosilicon is described for Swedish shale and for the separation of davidite concentrates (a uranium-bearing titanium mineral) at the Radium Hill mine. Investigations on the enrichment of relatively finely dispersed uranium ores, using heavy suspensions in hydrocyclones, are also described. This enrichment method gives quite satisfactory results with a number of Canadian ores, even when they are pulverized to 0.3 – 0.5 mm.

* Used only in the USA in processing carnotite-bearing sand of the Colorado Plateau.

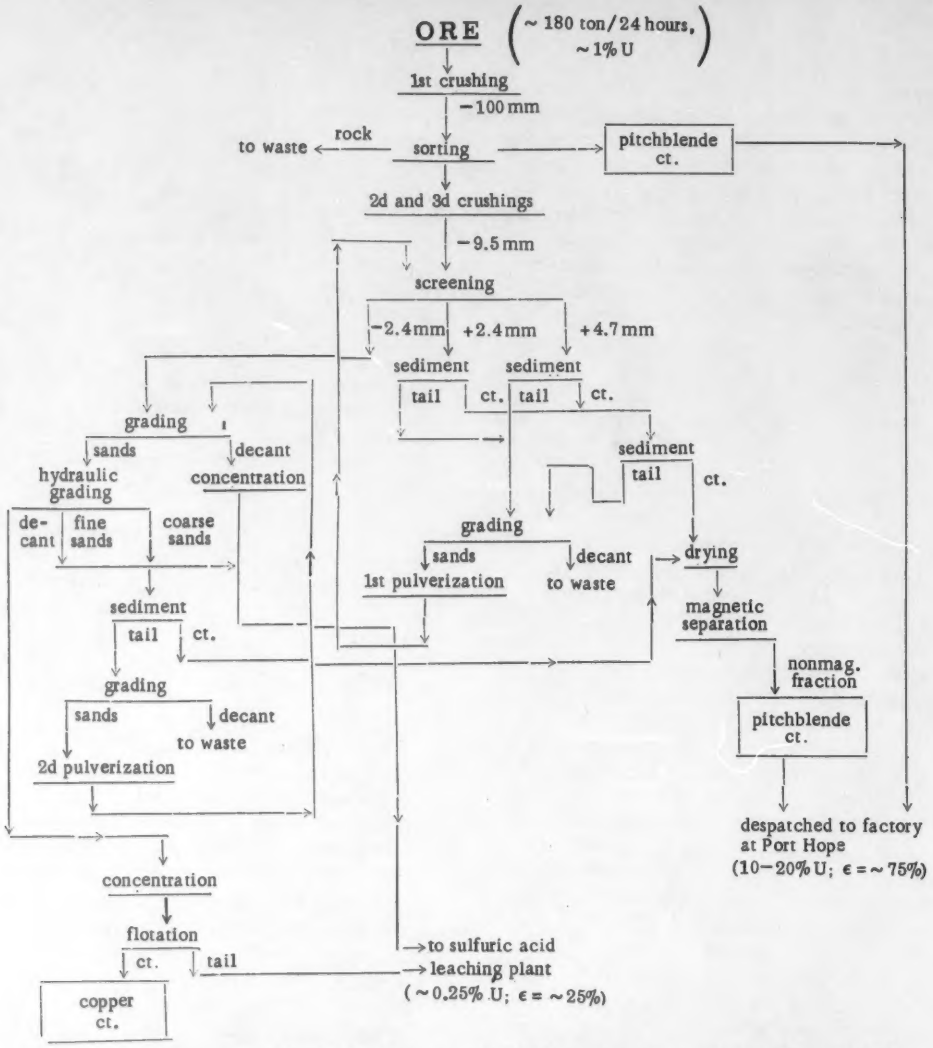

Fig. 1. Typical scheme of gravitational enrichment of pitchblende ores (plant at Port Radium, Canada).

RADIOMETRIC SORTING (Manual and Automatic). This method is apparently used in some mines but is described in detail only for the Port Radium plant, where machines are set up for piece grading to separate the barren rock from the rich concentrate. Radiometric sorting is also used in Australian and other establishments.

FLOTATION ENRICHMENT. This method is used also for extracting certain side components from ores (before uranium leaching) or, more often, from tailings (after leaching) [5].

Recently data have appeared on the use of flotation for the separation of uranium concentrates with the extraction of waste tailings, for example, the use of flotation for the enrichment of uranium ores in France (parsonite – uranium and lead phosphate) and also for carnotites of the Colorado Plateau, combined with selective pulverization [6].

Flotation enrichment is used in some plants in South Africa for extracting uranium and pyrite minerals from very poor tailings, from cyanation of gold ores, and for extracting pyrites (for sulfuric acid production) from tailings after uranium leaching [2,5].

Flotation of davidite is used at the Radium Hill mine, where a + 1.65 mm product is enriched in a heavy suspension and a −1.65 mm product by flotation. The uranium-bearing phosphorites from Florida are also enriched by flotation combined with washing. Their enrichment scheme does not differ from the accepted scheme for the enrichment of normal phosphorite ores. The bulk of the uranium thus passes into the phosphorite concentrate and is extracted from the latter during processing of the concentrate for fertilizer.

In the Rum Jungle (Australia) mine, the tailings from sulfuric acid leaching of uranium ores undergo flotation to produce a copper concentrate. In the plant at Port Radium, after gravitation enrichment of uranium minerals, flotation is used on the tailings to extract a silver-cobalt concentrate [4]. Occasionally selective pulverization is used for the enrichment, for example, of carnotite ores in some plants on the Colorado Plateau. At one of the mines enrichment by selective pulverization is combined with chemical processing, which consists of washing the sands in graders with a very weak solution of a mixture of sulfuric and hydrochloric acid, which extracts waste tailings.

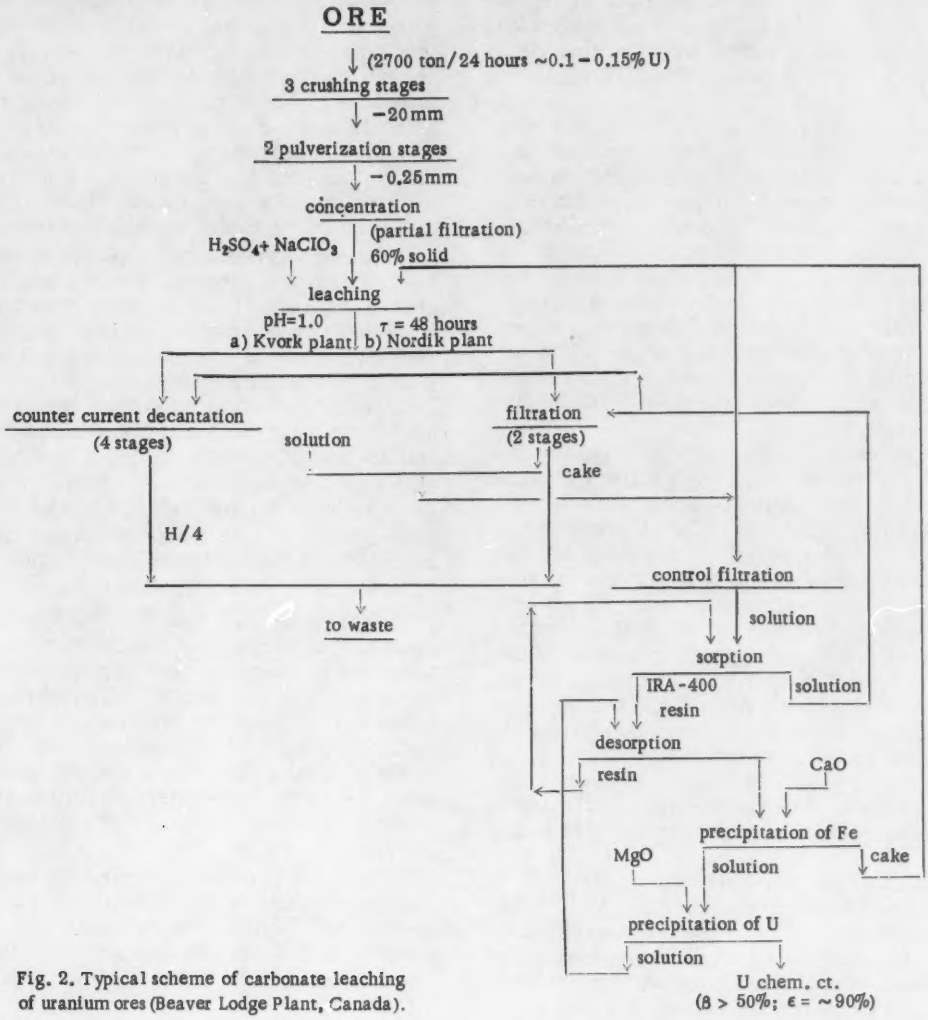

Fig. 2. Typical scheme of carbonate leaching of uranium ores (Beaver Lodge Plant, Canada).

There are papers describing investigations of other enrichment methods, for example, electromagnetic separation. This method is used at the Port Radium plant (Canada) for directly removing magnetite which does not bear uranium from the ores before enrichment and also from the gravitational concentrates. Investigations are being made of the electrostatic enrichment of complex uranium-bearing ores.

Pyrometallurgical Processes

Pyrometallurgical processes for the treatment of uranium-bearing raw material have a limited use (mainly as subsidiary processes followed by hydrometallurgical processing). Thus, uranium-vanadium ores are usually first sintered with sodium chloride and recirculating vanadium pentoxide and followed by the leaching of the vanadium with water and the uranium with a solution of acid or sodium carbonate. Clayey uranium ores are sometimes first sintered at about 500° to improve their concentrating and filtering properties. Uranium-bearing coal and other ores with organic compounds are often fired first to remove the organic substances.

Hydrometallurgical Processes

LEACHING. Solutions of acids or sodium carbonate are used as leaching agents. Some stubborn uranium-bearing minerals (phosphorites, titanates, niobates, zirconium minerals, etc.) are decomposed only by concentrated acids with heat and, in certain cases, the use of special additives or preliminary fusion with salts. In this method, the raw material is processed in a complex way with extraction of uranium and side components, phosphorus, tantalum, niobium, etc.

At the present time there are two plants in the USA processing uranium-bearing phosphorites and a plant for the processing of complex tantalum-niobium uranium-bearing concentrates.

The main and more economical process for the leaching of commercial uranium ores is at present acid leaching (90% of total ore tonnage). Ores with a low uranium content are leached with acid solutions of low concentration (mainly sulfuric acid) with a pH of 1 to 2. Leaching is carried out without heating for a long period (24 or more hours) [6,7], usually with mixing and, as a rule, continuously (Fig. 2). Regulated automatically by a pH meter the acid is usually introduced for

the leaching in portions, into the first and subsequent reactors. Pneumatic mixers of the Pachuca type (South Africa and Australia) and pneumomechanical agitators of the Dorr type (Canada) are used. A percolation method is used in individual cases (Swedish shale and carnotite ores).

Sometimes, leaching by a batch method is used after the dry pulverization of the ore, with the mixed mass being kept for several hours. Such leaching requires lower acid consumption, especially for ores with a considerable carbonate content (Shiprock plant, USA).

Manganese dioxide (South Africa and Australia) and sodium chlorate (Canada) are used as oxidants for converting uranium from the hexavalent to the tetravalent form. The oxidants are also introduced in portions, automatically regulated by the value of the oxidation-reduction potential. When manganese dioxide is used, it is occasionally recovered from solutions after sorption of the uranium [8].

Rich ores and concentrates with high uranium contents (1 – 50%) are treated with strong acids, for example, nitric acid, at the plants at Springfield (Britain), Le Bouchet (France), Port Hope (Canada), etc.

The ores are pulverized to 0.3 – 1 mm before acid leaching. To keep the water content to a minimum during the process for the elimination of water-soluble impurities, the pulp is concentrated and sometimes filtered (plants in Nordik, Kvork, etc.; Canada) [9,10].

A new type of mill, the Aerophol, has recently been used for the same purpose, dry pulverization, (also, two plants in South Africa and an experimental establishment in Canada) with the ore being pulverized by falling freely in large diameter drums without balls. Such mills were found to be more economical than the usual kind, due to the smaller consumption of steel and energy.

In a number of cases during leaching, part of the solution is returned to the head of the process in order to economize on acid and increase the uranium concentration in the final solutions. The apparatus for leaching is usually made of ordinary steel and is protected from corrosion by rubber lining or ceramic tiling. Concrete and wood are also used. Stainless steel is used comparatively rarely.

A method has been proposed for the processing of sulfide ores, which consists of the treatment of pulverized ores with water and air or oxygen, with the latter heated to 120° at a pressure of 10 atm and with a pulverization degree of 50 – 65% up to -74 μ. The pulp density is 65% solid. 90 – 95% of the uranium is extracted. In this case no acid is used in the leaching, but is obtained from the sulfides during leaching [11,12]. We should mention reports on the extraction of uranium from solution by treatment of ores with sulfur dioxide and on the method of chlorination with gaseous chlorine in the presence of a reducing agent at 700 – 1000°. Sodium carbonate leaching is used mainly for high-carbonate ores as acid leaching is not suitable due to the high consumption of acid [13].

Prior to selective uranium extraction with carbonate leaching, the ores are pulverized to -0.2 – 0.15 mm in a sodium carbonate solution and, as a rule, part of the solution is returned to the head of the process to lower the sodium carbonate consumption and raise the uranium concentration in the solutions. Leaching is carried out with heating and with a mixture of sodium carbonate and bicarbonate. The leaching time varies from several hours for ores with secondary uranium minerals to ten times that, for pitchblende ores. Apparatus with pneumatic mixing are usually used as in this case air is a uranium oxidant [14] (scheme 3). In some cases of sodium carbonate leaching, chemical oxidants are introduced, in particular, potassium permanganate. Since 1953, the foreign literature has included a series of articles describing carbonate leaching of uranium from ores using pressurized oxygen as oxidant. In addition to technological data, these publications contain the results of physicochemical investigations [13].

In recent years, several plants using this process have been built and tested. The first section of the plant at Beaver Lodge (Canada) uses carbonate leaching in autoclaves with air at several atmospheres pressure and separation of uranium from solutions by precipitation with sodium hydroxide. The second section of the plant operates on the carbonate process without the use of pressure, but with a long leaching process (about 100 hours) and intensive aeration (in Pachucas, scheme 3). Carbonate leaching at low pressure is also used in the plant at Bluewater (USA) [10,15].

Separation of uranium from solutions using pressurized hydrogen in the presence of a catalyst is described only in the data of laboratory investigations.

CONCENTRATION AND FILTRATION. In most technological schemes of uranium extraction from solutions, preliminary separation of solids from liquids is required. In the case of a badly filtering pulp, a concentration process is used and for pulp that filters well, filtration is used (South Africa). With relatively large-grained pulps, the sands are usually separated after leaching on classifiers and hydrocyclones and are then washed on 3 or 4 classifiers or horizontal vacuum filters.

In the case of solution separation by concentration, usually a system of countercurrent decantation with 3 to 4 stages is used. Filtration is in 2 – 3 stages, depending on the uranium content and nature of the ore (amount of residual moisture after concentration and filtration).

Various combinations of concentration and filtration are used, for example, one stage of concentration and two of filtration or two of concentration and one of filtration, etc. Normal condensers are usually used, though sometimes double- or triple-level ones are employed (Canada). During concentration, special coagulants of the synthetic polyelectrolyte type (separane, etc.) are often added.

The concentrators for acid pulps are made of wood or steel, protected with rubber lining. In most cases drum-type filters are used as they allow washing of the cake and thus decrease the number of filtration stages required (usually up to two).

The cake is usually removed from them using a series of continuous belts and this raises the efficiency of the filters, increases the life span of the fabric and improves the washing out of the uranium (due to the absence of flushing). Disc filters are used more rarely as they require a larger number of filtration stages (the solution is only washed by repulping) and sometimes automatic filter presses of various designs are employed (Burt, Eimko, etc.). Reports have recently appeared on the use of vacuum filters with horizontal surfaces (carousel, ribbon, and drum types with upper input), mainly for relatively large-grained materials.

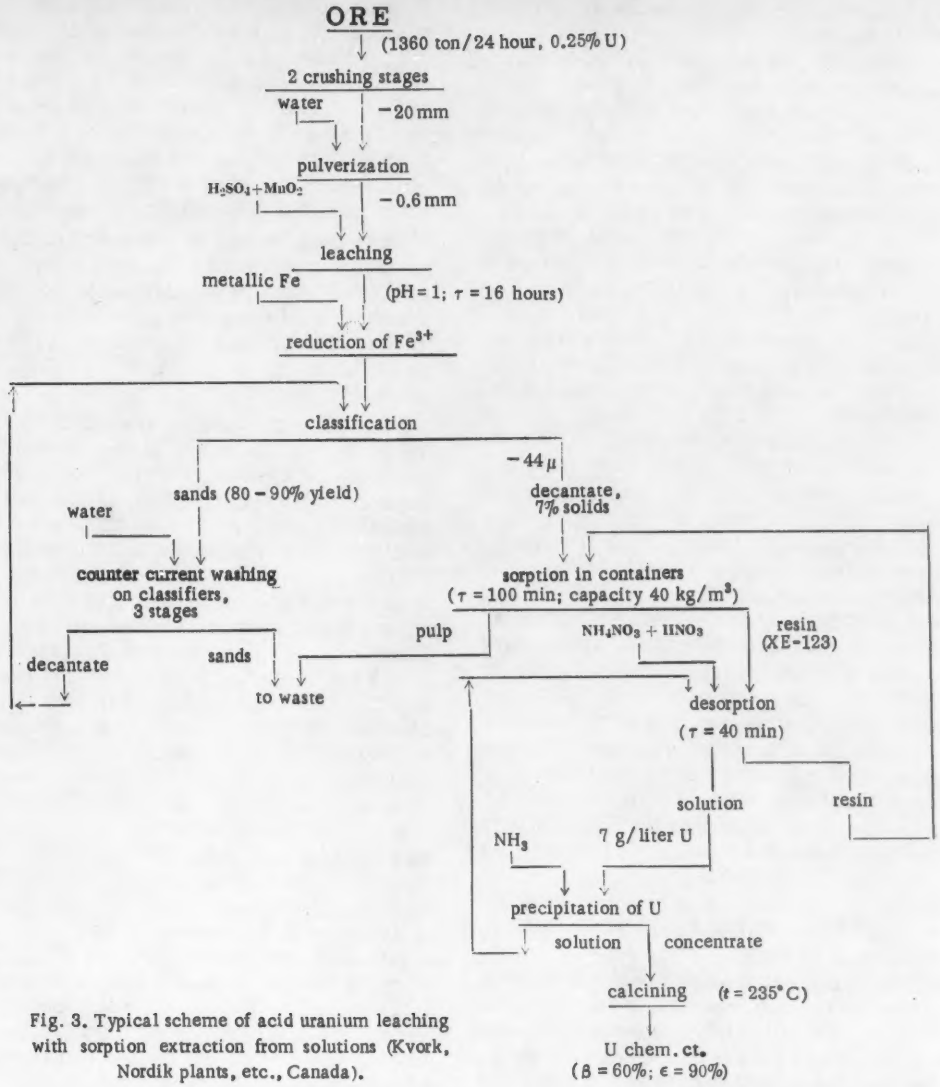

Fig. 3. Typical scheme of acid uranium leaching with sorption extraction from solutions (Kvork, Nordik plants, etc., Canada).

Framed vacuum clarifiers, filter presses, and sometimes sand clarifiers (South Africa) are mainly used for control filtration. Special flocculants are also used in the filtration: these include animal glue and synthetic polyelectrolytes for acid pulps and alkali-treated starch and synthetic flocculants for sodium carbonate pulps. Due to this, the capacity of the filters often reaches 5-6 tons of solid per m^2 of surface per day. The fabric on the filters is mainly synthetic and made from new types of hydrophobic fibers (nylon, perchlorovinyl, etc.) [16,17]. Sometimes fabrics are used which have first been covered with readily filterable powders such as kieselguhr.

SEPARATION OF URANIUM FROM SOLUTIONS. Uranium is comparatively rarely separated from acid solutions by certain chemical methods, which precipitate the uranium as phosphates, arsenates, vanadates, etc. (the plant at Port Radium and several plants in the USA). Sorption and extraction methods of separating uranium from acid solutions and pulps (excluding energy-consuming and difficult filtration and repulping operations) are used more widely [18,19].

Before the Geneva Conference of 1955, no investigations had been published on uranium sorption from industrial solutions and pulps. There were only some data on the use of ion exchange methods for analytical purposes and fragmentary information on the use of ionites for uranium extraction from industrial solutions in South African plants, but the type of sorbent and the apparatus used for the process were not mentioned. The first detailed data on these problems were published at the Geneva Conference of 1955. According to these data, sorption from acid solutions and acid ore pulps is carried out exclusively with anionites of the quaternary ammonium base type such as Dowex-1, Amberlite IRA-400 and IRA-410, Deacidite FF, etc. In addition, laboratory data were given at the 1955 conference on uranium sorption from sodium carbonate solutions [14,20].

Kunin, Price, Arden, and others stated that anion exchange resins could not be used for selective uranium sorption from solutions and indicated that due to the discovery in 1949 of the capacity of uranyl ions for forming negatively charged complexes in sulfuric acid

media, it had become possible to use anionites for selective uranium sorption.

It should be noted that Dietrich was the first to establish (in 1892) the existence of an anion form of uranium in sulfuric acid solutions. Kunin and Price report that anionites with weakly basic functional groups also sorb uranium, but their capacity and selectivity are not as great as those of strongly basic resins; Grensted, Ellis, and Olson maintain the opposite point of view.

Uranium sorption from solutions under dynamic conditions is widely used on an industrial scale in many establishments in South Africa, Canada, USA, and Australia. The full sorption and desorption cycle is accomplished in 3 to 4 consecutively connected columns, in one of which the resin is regenerated, while in the rest, uranium is absorbed [5,16,17]. Weak solutions of hydrochloric or nitric acids, mixed with their ammonium salts are used for the desorption; a mixture of sulfuric acid and sodium chloride is also used.

Some authors note that the capacity of strongly basic resins for uranium decreases by a factor of 6 with a decrease in the solution's pH from 2 to 0.5. The presence of such anions as vanadate, phosphate, cyanide, molybdate, titanium, ferric iron, etc. in the solution, lowers the sorption capacity of the resins. Such chemical poisons as cobalt cyanide, polythionate, elementary sulfur, and silicic acid present a serious danger to South African plants.

In 1955 Hollis and McArthur expounded the basis for a filtrationless method of uranium sorption from ore pulps. The first industrial tests of this method were begun in the USA in 1953. At present, plants in the USA which process carnotite sand ores by the filtrationless sorption method use anionites like Amberlite IRA-400 or Dowex-1 [21,22].

The process is as follows: the pulp, with particles less than 43 (after removal of sands on classifiers and hydrocyclones) and not more than 7 – 8% solids passes successively through a series of baths in which are placed mesh containers, one-third full of resin, which rise and fall vertically. When a container moves down, the resin is loosened and is in a suspended state, while the reverse motion settles it. After passing the chain of baths, the impoverished pulp is dumped. Each chain for uranium sorption consists of 6 – 8 baths, each of which contains four containers of $183 \times 183 \times 183$ cm^3. The containers hold up to 1.4 m^3 of resin in a swollen state, with a sorbent grain size of 0.8 – 1.6 mm. The full cycle of sorption and desorption is accomplished in 14 baths: sorption in six, and resin regeneration in six with two baths held in reserve. The sorption capacity of the resin at pH = 1.5 and of processing ores with a uranium content of 0.3% is 100 kg/ton. Uranium extraction from pulps is over 99%. The sorption and desorption process uses the countercurrent principle. The total loss of resin during two years of plant operation was 25%. while the sorption capacity decreased by only 10%.

After sorption, the uranium from the regenerator is usually precipitated with ammonia or magnesium oxide (Canada). The concentrate obtained is repulped and filtered on drum filters 2 or 3 times to wash it free from chlorine and other impurities as the resin is usually regenerated with a solution of sodium chloride. The chemical concentrates are dried in a mechanical rake dryer of the muffle type. The largest South African sorption plant has 45 columns [23].

Foos considers that in the future the filtrationless method will replace the method of sorption from clarified solutions, but he points out that many new flocculents have been developed for solving the problem of filtration and concentration, and these agents make it possible to clarify solutions inexpensively. Due to this, countercurrent decantation and sorption for solutions will, according to the author, compete with uranium sorption from pulp in certain cases [24].

Yzzo reports that by the end of 1956, 12 uranium ore processing plants in the USA used an ion exchange process. The largest plant in Moab, Utah (scheme 4), which started operating in 1956 by the method of sorption from pulp, has a capacity of 1360 tons of ore per day with a uranium content of – 0.25%. This plant employs 175 persons.

Some authors give detailed data on the operation of 16 large plants in the Union of South Africa with a capacity of 1000 to 7000 tons of ore per day, which reprocess the tailings from the plants of the gold industry which possess a uranium content of 0.006 – 0.1% (tailings with a uranium content of less than 0.01 – 0.015% are first enriched by flotation). Since 1950, at a number of plants the ores have been processed by the sorption method from clarified solutions under dynamic conditions using strongly basic resins with a grain size of 0.3 – 0.9 mm and a pH of 1 – 1.5. The pulps are filtered on drum filters (in two stages). The solutions are clarified on frame vacuum filters. Animal glue is added to the pulp to increase the filtering rate. Three consecutively connected columns (sorption in two and resin regeneration in one) are used for sorption from the clarified solution. Each column is 3.36 m high, 2.25 m in diameter, and has a 1.525 m resin bed; the current rate is 6 – 10 m/hour during sorption and -1 – 1.5 m/hour during regeneration. The capacity of fresh resin is 48 kg/m^3 at a uranium concentration in the starting solution of 0.5 g/liter and pH = 1.5. The maximum uranium concentration in the regenerated solution is 30 g/liter. Nitric acid mixtures containing ammonium nitrate are used for regeneration. It is stated that minute amounts of chlorides and nitrates in the starting materials lower the capacity of resins for uranium. A chlorate ion lowers the resin capacity especially sharply [5,23].

The paper by Shinker et al. describes laboratory experiments on uranium sorption from industrial and artificially prepared sodium carbonate solutions with a strongly basic anionite of the IRA-400 type. It states that the sorption capacity of the resin decreases with an increase in the carbonate content of the solution. Organic materials are absorbed by the resin and lower its capacity for uranium. Such anions as phosphates, arsenates, and vanadates are hardly absorbed by the sorbent. The resin is regenerated with a solution containing sodium nitrate and carbonate; the average uranium content of the regenerated solution is 20 – 25 g/liter [25].

A number of reports were given at the 1955 Geneva Conference on the use of extraction methods in industry. Thus, for example, Grensted reported that a US experimental plant used an extraction method for processing sulfuric acid pulps with an S : L ratio of 1 : 1 and a uranium content of 1% in the starting ore. A 2% solution of mono- and dialkyl phosphate in kerosene was used as extractant.

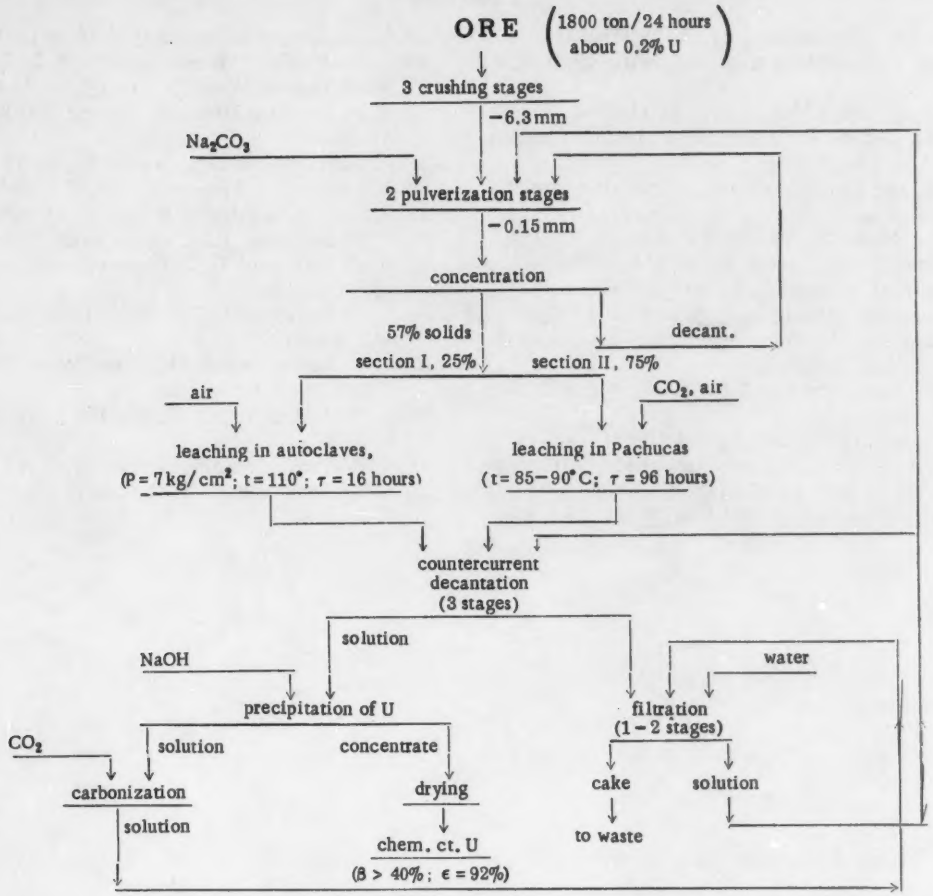

Fig. 4. Typical scheme of acid leaching with uranium sorption from pulp (plant at Moab, USA).

The report by Long describes the extraction of uranium from phosphoric acid solutions with a uranium content of up to 1 g/liter in the solution using alkyl pyrophosphates.

After the 1955 Geneva Conference, numerous papers appeared describing various extraction systems for recovering uranium [26 – 28].

The extraction method has been used most widely for recovering uranium from phosphoric acid solutions. Several plants in the USA produce uranium as a by-product in the processing of phosphorites; the extraction uses solutions of mono- and dialkyl phosphates and also higher amino compounds in kerosene.

A number of plants in the USA use an extraction method for recovering uranium from sulfuric acid solutions. A 3% solution of di- and dodecylphosphoric acid in kerosene is used as extractant. A solution of di-2-ethylhexylphosphoric acid (with a small amount of tributyl phosphate added) in kerosene is also used for extraction from sulfuric acid solutions.

Due to the large losses of pyroalkyl phosphates and their hydrolysis products (from 3 to 10 g/g of uranium), some plants extract the ores with nitric acid and extract the uranium from nitric acid solutions with tributyl phosphate.

The literature also mentions work carried out in the USA on uranium extraction from dense sulfuric acid and hydrochloric acid pulps under laboratory conditions. Belt extractors are used for the extraction. Acetone, tributyl phosphate, and solutions of mono- and dialkyl phosphate in methyl isobutyl ketone and other oxygen-containing organic oxidizers are being tested as extractants. The extraction of hydrochloric acid pulps yielded a 20 – 30% uranium concentrate. The main impurities were vanadium, iron, and calcium [26].

Received August 25, 1958

Literature

1. R. H. Kennedy, Mines Mag. 47, 9, 22 (1957).
2. T. V. Lord, Can. Mining and Met. Bull. 49, 526, 91 (1956).
3. E. J. Duggan, Mines Mag. 46, 3, 99 (1956).
4. R. L. Behan and D. F. Lillie, Can. Mining and Met. Bull. 49, 528, 254 (1956).
5. Journal of the South African Inst. Mining Met. 57, 3–11 (1956/57).
6. Chem. Eng. News 34, 25, 2968 (1956).
7. A. Linz, Chem. Eng. Prog. 52, 5, 205 (1956).
8. A. M. Gandin, J. Metals 8, 8, 1065 (1956).
9. W. L. Lenneman, Mining Eng. 8, 6, 622 (1956).
10. Symposium: The Uranium Industry of Canada Mining J. 77, 6, 123 (1956).
11. A. H. Ross, Can. Mining Met. Bull. 49, 532, 570 (1956).
12. R. A. Foos, Mining Eng. 8, 9, 893 (1956).
13. Symposium: Technology of Processing Uranium Ores. Mining Eng. 9, 9, 973 (1957).
14. T. V. Arden, Mine and Quarry Eng. 22, 12, 88 (1956).
15. W. A. Gow, Can. Mining J. 78, 3 (1957).
16. J. N. Botsford, West. Miner 30, 3, 37 (1957).
17. N. W. Byrne, West. Miner 30, 4, 71 (1957).
18. H. N. Dunkin, Chem. Eng. and Mining Rev. 51 (1957).
19. H. L. Hazen, Mining World 19, 5, 44 (1957).
20. Y. Dasher, J. Metals 9, 1, 185 (1957).
21. S. Dayton, Mining World 9, 2, 36 (1957).
22. T. Yzzo et al., Eng. and Mining J. 158, 1, 90 (1957).
23. W. Q. Hull and E. T. Pinkney, Ind. and Eng. Chem. 49, 1, 1 (1957).
24. R. F. Hollis and C. K. McArthur, Mining Eng. 9, 4, 442 (1957).
25. T. V. Arden and A. Himsley, West. Miner 30, 9, 51 (1957).
26. R. H. Bailes and Y. E. Magner, Mines Mag. 47, 6, 51 (1957).
27. G. V. Argall, Mining World 19, 8, 44 (1957).
28. R. S. Olsen and M. T. McCarty, Mining Congr. J. 43, 7, 50 (1957).

THE USE OF "GASEOUS" FLUORINATION IN THE PRODUCTION OF URANIUM TETRAFLUORIDE

Yu. V. Gagarinskii

On the basis of foreign reports to the Second International Conference on the Peaceful Uses of Atomic Energy (Geneva, 1958), we present a short description of methods used in industry and developed in laboratories for the production of UF_4 by the action of gaseous HF on UO_2 at high temperature.

At the present time, "gaseous" fluorination of uranium dioxide is accomplished in horizontal apparatuses with screw mixing. Methods have been developed for use in the fluorination of reduced uranium concentrates in a boiling bed (with subsequent preparation of UF_6) and in the fluorination of agglomerated dioxide in a countercurrent hydrogen fluoride layer in vertical apparatuses (with subsequent preparation of metallic uranium). The last method is considered to be the more promising.

The fluorination of uranium dioxide with gaseous hydrogen fluoride at a high temperature (so-called "gaseous" fluorination) has been used in the production of uranium tetrafluoride for quite a long time. In 1949 a process was developed for continuous fluorination by a countercurrent method in horizontal apparatuses with screw mixing [602]*. UO_3 (the end-product of uranium purification) was first reduced in the same apparatuses. Subsequently it was shown that fluorination of dioxide, obtained by reduction of UO_3 in a "boiling" bed, is achieved considerably more rapidly since, due to better heat exchange between the solid phase and the gas, sintering of the particles occurs to a lesser extent. Now, uranium dioxide is obtained by reduction of UO_3 in a "boiling" bed at the factory in Paducah, producing uranium hexafluoride [1840], and a factory starting up at Weldon Spring at the beginning of 1958, producing metallic uranium [602]. Uranium tetrafluoride is produced from the dioxide at these plants in horizontal apparatuses with screw mixing. In Canada, apparatuses with shelving and screw mixing are used for the same purpose [229].

On an experimental apparatus, a method was tested [1552, 542] for fluorination of reduced uranium concentrates with gaseous HF in a "boiling" bed to produce uranium tetrafluoride, suitable for processing into UF_6. A factory being constructed in Metropolis will operate on this principle [1552].

The fluorination of agglomerated uranium dioxide with gaseous HF in a moving bed was also studied [229, 1015]† under laboratory conditions and on experimental apparatuses. The process is accomplished by a countercurrent method in vertical apparatuses with movement of the agglomerated solid phase from top to bottom and of the hydrogen fluoride from bottom to top. An industrial apparatus operating on this principle is being constructed [229]. A short description of the gaseous fluorination methods listed is given below.

Fluorination of Uranium Dioxide Powder in Horizontal Apparatuses With Screw Mixing

The general scheme of the automated process in the Paducah plant is presented in Fig. 1 [1840]. The process is controlled from a control point, to which all the necessary technological indexes are supplied. The technological scheme for the preparation of tetrafluoride at Weldon Spring is largely the same. The dioxide is fluorinated in three horizontal inconel apparatuses set one above the other and connected in series. Freshly prepared uranium dioxide is fed in at the top of the apparatus, moved along inside it by means of screw-type mixers, poured over into the following apparatus, etc. Gaseous HF, first heated to 80 – 120°, is fed into the end of the lowest apparatus and travels countercurrent to the movement of the fluorinated product. The construction of such an apparatus [602] is seen in Fig. 2‡. The diameter of the reaction tube of the apparatus is 400 mm and the length somewhat more than 6 m. The mixer of the apparatus has several blades bent into steeply pitched spirals and fixed semirigidly to a shaft on struts. The temperature inside the fluorination apparatuses is kept at 290 – 340° at the UO_2 input and at 540 – 590° at the UF_4 output (the lower values refer to

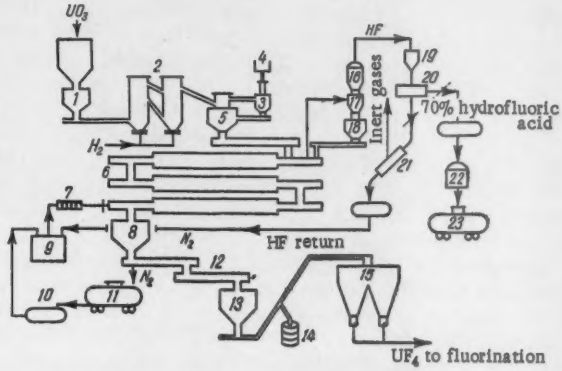

Fig. 1. Plan of technological process for UO_3 reduction and UO_2 fluorination in the Paducah plant:
1) hermetically sealed hopper; 2) column for UO_3 reduction in a "boiling" bed; 3) and 17) cyclones; 4) combustion of hydrogen; 5) hopper for UO_2; 6) fluorination apparatus; 7) heater; 8) and 18) hermetically sealed hopper for UF_4; 9) HF evaporator; 10) HF reservoir; 11) tank with anhydrous HF; 12) cooled screw-conveyor; 13) hopper for weighing tetrafluoride; 14) packing; 15) hopper for transfer to fluorination to UF_6; 16) filter; 19) return filter; 20) partial condensation; 21) total condensation; 22) reservoir; 23) tank for hydrofluoric acid.

* The numbers of the reports presented at the conference are given in brackets.

† See Atomic Technology Abroad No. 2, 69 (1959).

‡ Stuffing boxes of teflon wool, compressed with graphite and flushed with carbon dioxide are used in the Fed. Ger. Rep. for horizontal rotating furnaces, used for producing UF_3 [1001].

the Paducah plant and the higher ones to the one at Weldon Spring). Due to the high heat evolution in the fluorination reaction and the poor thermal conductivity of the $UO_2 - UF_4$ mixture, it is necessary to cool the working apparatus and this is done in zones.

The output of such a unit is about 660 kg of UF_4 per hour [1840]. The tetrafluoride of the Paducah plant contains 95% UF_4 and 2.5% UO_2F_2; the tetrafluoride of the Weldon Spring plant contains 96.2% UF_4, 2.0% UO_2F_2 and 1.8% uranium oxides. The packed weight of the tetrafluoride is 3.5 g/cc and the impurity content in it (%): $Fe - 5.5 \cdot 10^{-3}$, $Ni - 3.5 \cdot 10^{-3}$, $Cr - 9 \cdot 10^{-4}$, $Mn < 1 \cdot 10^{-3}$, $Cd < 1 \cdot 10^{-5}$, $Mo < 1 \cdot 10^{-3}$.

In the Paducah plant the irrecoverable uranium losses are less than 0.01%. The gases from the fluorination apparatuses pass through a cyclone and a charcoal filter. The 70% hydrofluoric acid, condensing at 68°, is marketed. The anhydrous HF, passing the cyclones is then condensed and reused for fluorination.

As can readily be calculated from its concentration in the condensate, the consumption of HF in fluorination in horizontal apparatuses exceeds 200% of the stoichiometric amount. The efficiency of HF use, quoted by the author of report [602], equals 99%, apparently refering to the amount of HF consumed after deduction of the condensate.

In report [179] it is stated that in the production of uranium tetrafluoride in a rotating steel furnace, lined with magnesium, with a capacity of 10 kg/hour, the consumption of hydrogen fluoride is 200% of the stoichiometric amount. On the basis of 3 – 4 years experimental work, the authors (Sweden) recommend the use of such units in industry.

The constructional materials used [1840] for work at a temperature below 54° with anhydrous HF and 70% hydrofluoric acid are low-carbon steels (seamless steel tubes and steel valves with monel plating) and for work at high temperatures with anhydrous HF and hydrofluoric acid at concentrations below 70%, monel and inconel (the latter where great heat stability is required).

Fluorination of Uranium Dioxide Powder in a "Boiling" Bed.

As stated above, this method is proposed for use in the preparation of UF_4 in a factory processing uranium concentrates into UF_6. The uranium is freed from impurities in the concentrates due to: 1) the formation of volatile hydrides by certain impurities, in particular, the conversion of sulfate sulfur into H_2S, during reduction of the concentrates; 2) the formation of volatile fluorides by silicon, boron, and arsenic and partly (depending on the composition of the concentrates) by molybdenum, vanadium, and phosphorus during the treatment of the reduced concentrates with hydrogen fluoride; and 3) the separation of elements forming in volatile fluorides in the preparation of UF_6 by the action of fluorine on UF_4 and the separation of elements forming volatile fluorides under these conditions by the fractional distillation of UF_6. The fact that the preparation of the final product (UF_6) simultaneously serves as a purification operation is an important positive factor since it decreases the probability of contamination of the final product due to corrosion of the apparatus.

An extremely important disadvantage of the method of fluorinating uranium dioxide in a "boiling" bed is the necessity for preliminary processing of the concentrates so that they have a definite grain size. Satisfactory results are obtained in "boiling" bed fluorination when the starting concentrate has a grain size of 30 – 325 mesh with a small content of the fine fractions. A concentrate with a small grain size undergoes preliminary treatment consisting of agglomeration with subsequent pulverization and dispersal.

The plan of an experimental apparatus for the reduction of concentrates and fluorination with gaseous HF in a "boiling" bed is presented in Fig. 3. Further processing of the UF_4 with fluorine for the preparation of UF_6 was also carried out in a "boiling" bed. The five-stage apparatus for fluorination had a diameter of 150 mm. The fluorination temperature in the upper stage was 350° and in the lower, 600°. The time that the product was kept in the apparatus was five hours. During fluorination there is a slight decrease in grain size. The finest fractions of the powder, consisting of only a

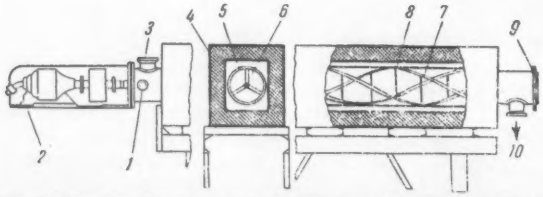

Fig. 2. Plan of horizontal apparatus with screw stirring for uranium tetrafluoride production:
1) powder input; 2) motor; 3) gas outlet; 4) furnace; 5) body of apparatus; 6) struts; 7) bladed rake; 8) vaned agitator; 9) gas input; 10) powder output.

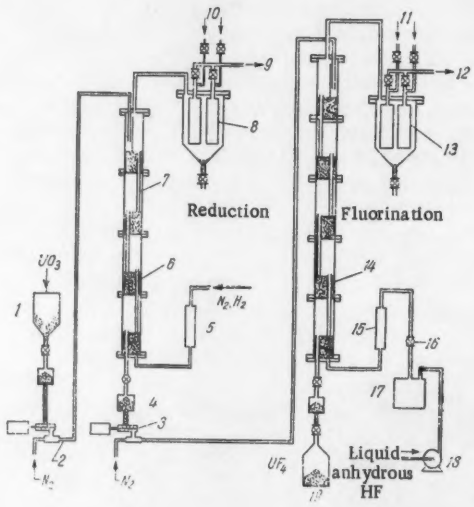

Fig. 3. Plan of experimental apparatus for the production of uranium tetrafluoride in a "boiling" bed: 1) loading hopper; 2) pneumatic powder feed; 3) screw conveyor; 4) observation glass; 5) and 15) heaters; 6) "boiling" bed of UO_2; 7) drain tube; 8) porous stainless steel filter; 9) to exhaust system; 10) and 11) flushing gas; 12) into condenser and scrubber; 13) porous monel metal filter; 14) "boiling" bed of UF_4; 16) gas meter; 17) HF evaporator; 18) feed pump; 19) receiver.

Degree of Purification of Uranium in the Reduction of Certain Concentrates and the Preparation of UF_4

Source of concentrates	State	Impurity content, 10^{-2}%						
		S	As	B	Mo	P	Si	V
South Africa	Before processing	80	40	1	1	5	960	<5
	After *	28	<1	<0,1	<0,2	<5	1	<2
New Mexico*	Before processing	780	—	—	1,5	75	230	25
	After **	7	<1	<0,1	0,4	<5	1,5	<1

*With acid leaching operations.

few percent of the product weight, are removed in a cyclone and held by the filters. The capacity of the apparatus is of the order of 210 kg/hour per m^3 of bed. The authors of the reports [1552 and 542] did not give the consumption of HF on a multistage apparatus. In the best case, the consumption of HF on a single stage apparatus was 125 – 130% of the stoichiometric amount. Experiment showed that fluorination was largely complete in the first two stages and it was not necessary to construct apparatuses with a greater number of stages. It should, however, be kept in mind that the required retention time for the material to be fluorinated in a multistage apparatus is considerably less than in a single stage unit (for example, with three stages this time is a factor of 4 less than with one stage).

The degree of fluorination on a multistage apparatus exceeds 97% with a UO_2F_2 content of from 1 – 2.5% in the finished tetrafluoride in most experiments. The degree of purification of the uranium in the reduction and fluorination to UF_4 in a continuous process is shown in the table for certain forms of raw material.

Tests were also made on vibrating shelf apparatuses for the fluorination of reduced concentrates [1552]. These apparatuses gave satisfactory results in the fluorination of concentrates free from sodium and no preliminary treatment of the concentrates to adjust the grain size was required. In the fluorination of sodium-containing concentrates, sintering* occurred and hindered the normal course of the process.

Fluorination of Agglomerated Uranium Dioxide in a Moving Bed

The authors of report [1015] consider that the advantage of this fluorination method over other methods is the possibility of ensuring reliable contact of the solid phase with gaseous HF and reducing the consumption of the latter to a minimum and also the simplicity of construction of the reaction apparatus and the low cost of its fabrication and operation. This method is evaluated [229] as the most promising one; its disadvantage is the need for agglomeration of the starting material.

Paper [1015] described the agglomeration of trioxide, mixed with aqueous ammonia, by extrusion through openings 6 mm in diameter. After drying and sieving out of the fines, the particle size of the agglomerated product was 3 – 12 mm with a porosity of 40%. According to paper [229], the agglomeration is performed by pressing the trioxide, mixed with water, into holes in a rubber belt with subsequent drying and dispersion. The particle size of the agglomerated product is 3 – 13 mm.

The plan of a countercurrent experimental apparatus for the reduction of agglomerated UO_3 and fluorination of UO_2 in a moving bed [1015] is presented in Fig. 4. The lower part of the conical reaction apparatus for fluorination is made from monel and heated electrically. The upper part of the apparatus can be cooled with cold gas (nitrogen or a mixture of nitrogen and hydrogen). A graph is given in report [1015] on the temperature dependence of the equilibrium concentration of HF in the gas phase in the reaction of HF with UO_2†. The decrease in this concentration with a fall in temperature is one of the factors, which makes it necessary to keep the temperature at the gas outlet from the apparatus lower than that in the main fluorination zone for better use of the HF.

In the opinion of the authors of report [1015], the successful operation of such an apparatus depends in the first instance on the following factors: 1) uniform distribution of gas and solid phase and also a uniform

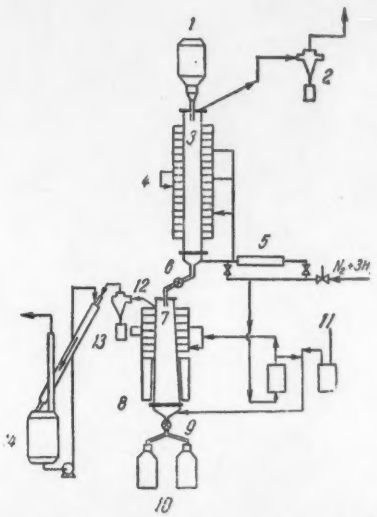

Fig. 4. Plan of experimental apparatus for the fluorination of agglomerated uranium dioxide: 1) loading hopper for UO_3; 2) and 12) cyclones; 3) reduction apparatus; 4) gas distribution; 5) heater; 6) and 9) multiway cocks; 7) fluorination apparatus; 8) electric heater; 10) receiver for UF_4; 11) anhydrous HF input; 13) scrubber-condenser; 14) reservoir with KOH.

*Apparently due to the formation of the NaF – UF_4 eutectic, which has a melting point of 618° [1015].

†On this problem see also Acad. Sci., Paris, 228, 1591–1592 (1949).

rate of their transfer along the apparatus; 2) maintenance of the required temperatures inside the apparatus (300 – 400° in the upper part and 500 – 600° in the lower). The first condition is achieved at an input rate of the solid phase of more than 10 kg : mole per hour per m^2 of cross section. According to a calculation made in the work on the basis of results from tests on the experimental apparatus, a fluorination apparatus with a capacity of 5000 tons of uranium per year must have a diameter of 600 mm and a height of 13.5 m.

The Canadian fluorination apparatus with a capacity of 45 kg of UF_4/hour [229] is in the form of a cylinder with a diameter of 200 mm and a height of 7.3 m. The fluorination temperature in the upper part of the apparatus is 200°, and 650° in the lower part; before admission to the apparatus the hydrogen fluoride is heated to 500°. The temperature of each zone of the apparatus (a total of 6 zones) is maintained by the input of cold nitrogen into the zone. The loading hopper is connected to the apparatus by a tube 2.44 m high and 76 mm in diameter, which acts as a seal. Nitrogen is fed into the tube from the top to the bottom.

During fluorination the volume of the agglomerated solid phase increases by 27% [229]. The product passes through the fluorination apparatus in 12 hours. A degree of fluorination of 98% is achieved. The HF consumption is 110% of the stoichiometric amount. Approximately 1% of dioxide and the same amount of UO_2F_2 remain in the tetrafluoride obtained.

According to the data in paper [229], the advantage of establishing a temperature gradient down the fluorination apparatus with the highest temperature below on the UF output is that this gives the most complete fluorination, the required plasticity of the $UO_2 - UF_4$ mixture is achieved and the increase in volume of the agglomerated solid phase is spread down the greatest length of the apparatus.

Received November 10, 1958.

ASPECTS OF THE METALLURGY OF URANIUM AND CONSTRUCTIONAL METALS

G. A. Meerson

On the basis of foreign material presented at the Second International Conference on the Peaceful Uses of Atomic Energy (Geneva, 1958), we examine aspects of uranium production (reductive melting, casting, pressure treatment, and powder metallurgy); zirconium metallurgy (new data on the technological scheme, the nature of sponge and the dimensions of ingots); the production of the new constructional metals, niobium and vanadium (comparison of various methods for their preparation; metallothermal, vacuum carbo-thermal, electrolytic refining and the quality of production); the production of thin-walled beryllium tubes for fuel element sheaths; the use of zirconium hydride as a moderator and of zirconium–uranium–hydrogen alloys for fuel element cores.

Reports on metallurgy at the Second Geneva Conference largely dealt with separate problems in which considerable progress has been made over the last three years or noted certain essential changes, innovations, etc.

URANIUM PRODUCTION. In most cases, the principle technological scheme of the latter stages of uranium production has been set on the basis of the following basic processes: reduction of trioxide to dioxide, "gaseous" fluorination with the production of uranium tetrafluoride and metallothermal reduction of the fluoride [602], [1433], [1252], [1001], [179]*.

As previously, uranyl nitrate is purified by an extraction method (tributyl phosphate), but, for example, as reported in [602], in an American factory operating since 1957 kerosene has been replaced by n-hexane as a solvent for tributyl phosphate. As a result the organic phase became less viscous in the extraction process and had a lower specific gravity, which improved the conditions for mixing and separating the phases and accelerated the extraction process.

UO_3 is reduced to UO_2 with decomposed ammonia (or hydrogen) in "boiling" bed furnaces. The dioxide is fluorinated with dry, gaseous HF†.

Both in the USA and in Britain now, UF_4 is reduced with magnesium and not with calcium. The use of oxygen and moisture free fluoride, obtained by dry fluorination, eliminates the danger of explosions in the magnesium-thermal reduction in a hermetically sealed bomb and decreases the amount of oxygen slag inclusions in the metal, which is also helped by the use of magnesium fluoride bomb linings instead of the dolomite linings described at the First Geneva Conference.

By the beginning of 1958, the process of magnesium-thermal reduction of uranium tetrafluoride [602] for single charges of two tons of uranium fluoride had been developed. The amount of fine magnesium turnings used is very close to theoretical (300 kg), which also decreases the possibility of high pressures developing in the bomb. Before the reaction, the bomb with charge is heated to 625 – 675° in a 400 kw resistance furnace. The whole operation lasts for 10 – 14 hours. The hot magnesium fluoride slag, accumulating above the ingot, retards the cooling of the upper part of the ingot and creates conditions for directed crystallization from bottom to top. A large charge and prolonged heating of the furnace lining cause slow cooling and crystallization and give the best separation of metal from slag. This makes it easier to use the ingot for pressure treatment directly after reduction and eliminates the operation of refining by vacuum remelting. To remove surface slag inclusions, the ingot is milled to a length of about 432 mm and a diameter of about 445 mm (a weight of 1225 kg, which represents 82% of the uranium content of the original fluoride). In the machining for removal of the external layers, containing slag inclusions, the following control method was used: the machined surface was periodically heated with the flame of a gas burner and when inclusions were absent, the color of the heated place was uniform and when they were present, it was spotted.

In the initial experiments on the direct pressure treatment of ingots after reduction (dingot ‡ process), attempts were made to use forging as the first process. However, due to the inconvenient form of the ingot (diameter slightly greater than the height), now the first pressure treatment operation used is hot extrusion in the γ-phase of a rod-shaped blank from the machined ingot. Glass, deposited on the hot ingot (~1000°) as a powder, is used as a lubricant. Before heating, the ingot is sprayed with an alcohol suspension of phosphate glass. The weight of the extruded rod is about 1200 kg. In report [602] it is stated that a rod of this weight has a length of 3.96 m and a diameter of 178 mm. However, the diameter given for the rod is apparently incorrect since according to the data on weight and length, the rod must have a diameter of 143 mm. In this case the degree of reduction during extrusion is about 90%.

As before, the calcium-thermal reduction of UF_4 is used at the Bush factory (whose technological process was described at the First Geneva Conference). The reaction apparatus and ignition devices have been developed [1252] for the production of 80 kg ingots. An experimental calcium-thermal reduction of uranium tetrafluoride [179] in ingots weighing 20 kg has also been carried out in Sweden.

In laboratory and experimental operations, a study has been made of the possibility of reducing uranium from binary fluorides of uranium and alkali metals (sodium-potassium) [1260 and 1399]. The binary fluorides are readily precipitated from solutions and may then be dehydrated well by fusion; they also give slags with a complex composition, which have a low melting point. Thus, for example, in the reduction of the binary fluoride $NaUF_5$ with magnesium, the slag melted at approximately 1000°, while in the normal reduction of UF_4 with magnesium, the slag melts at 1260°. As with the magnesium reduction of UF_4, the magnesium-thermal reduction of $NaUF_5$ was accomplished in a reactor, heated to 750° in an electric furnace.

* The numbers of the reports presented at the conference are given in brackets.

† See p. 9

‡ Abbreviation of direct ingot, i.e., directly from the ingot obtained by reduction.

POWDER METALLURGY OF URANIUM. The powder metallurgy of uranium has been studied widely in experiments and investigations, but has not been adopted in regular production. In reports [1470 and 44] and in a book* it was stated, and on the USA stand at Geneva it was shown, that the metalloceramic method produces a fine-grained, quasi-isotropic structure, which confers good stability on articles under irradiation. According to data of British [1470] and French [1162] reports, uranium powder is obtained by reduction of uranium dioxide with calcium; in the American book†, a description is given of the preparation of uranium powder by hydrogenation of normally cast uranium with subsequent dehydrogenation. Compact bodies can be formed from powder both by vacuum sintering of a freely packed powder and by hot pressing in metal dies. The powder is protected from oxidation during hot pressing by means of an argon atmosphere or the process is performed in air with preliminary moistening of the powder with kerosene, which evaporates in the die, displacing the air and protecting the powder from oxidation.

When a freely packed powder is sintered, its density reaches 18 – 18.6, i.e., ~ 2 – 5% residual porosity. A dense, practically nonporous structure is attained by hot pressing, which should be carried out‡ in the upper temperature limits of the α-region (630 – 650°) to increase the strength of the sintered article. At these temperatures a pressure of 1.85 ton/cm^2 is sufficient (instead of 5 ton/cm^2 at 500° and 3 ton/cm^2 at 600°).

However, the results of British investigations [1470] showed that a hotter pressing of powder in the region of the γ-phase is permissible: articles obtained in this way behave no worse under irradiation than those obtained by hot-pressing in the α-region. In order to create additional conditions, increasing the stability of metalloceramic articles under irradiation, use was made of methods of alloying the starting uranium powder by the combined calcium reduction of uranium dioxide with the oxides of alloying elements added [1162 and 1097]. There is also the variant of hot extrusion of long rods directly from powder with their subsequent cutting, possible thermal treatment, etc. [1470].

On the French exhibition was shown a model of a continuous vertical furnace for the reduction of dioxide to uranium powder [1162]. Briquets of a mixture of uranium dioxide powder and pulverized calcium are moved mechanically in containers along a vertical tube through a heated reaction zone filled with argon.

Metalloceramic technology, based on calcium-thermal reduction of uranium dioxide, is more economical than the standard technology, due to the exclusion of a series of operations. It is less profitable to use uranium powder obtained by hydrogenation of cast metal, since in this case the extra operations of hydrogenation and dehydrogenation are added to all the operations of the standard process.

CAST URANIUM CORES. Together with the main, most widespread processes for the production of uranium articles, combining pressure treatment of cast metal with subsequent thermal treatment, use is made of direct casting of uranium parts since this cheapens the process by cutting out pressure treatment operations [27, 1157, and 785]. Alloying the uranium with 1 – 1.5% of molybdenum is proposed [1157] for stabilizing cast articles under irradiation. Under certain casting cooling conditions, such alloying gives a homogeneous, fine-grained structure and stabilizes the uranium under thermal cycling and irradiation. Despite the quite high neutron capture cross section of molybdenum, it is possible to use natural (unenriched) uranium alloyed in this way in a gas-cooled (CO_2) reactor with magnesium-clad fuel elements, since CO_2 and magnesium absorb less neutrons than water and aluminum (in normal reactors with water cooling).

Cast uranium cores were also shown on the British stand at the exhibition. The recommended procedure for stabilization of cast cores involves alloying with small amounts of chromium (0.5 atom %) with isothermal tempering by the scheme: heating in the region of the β-phase at 760°, transfer to a bath with a temperature of 575° and soaking for conversion of the β-phase into the α-phase [27].

A description was given [44] of the preparation of cast annular cores from enriched uranium for the Dounreay reactor. Also added to this metal was 0.5 atom % of chromium (0.1 weight %). In this case, the castings were given isothermal heat treatment. A description is given of the pyrometallurgical processing of an alloy of uranium and its fission products in the fuel elements (rods of 49% enriched uranium alloy with a diameter of 2.6 mm and a length of 36 mm in a stainless steel sheath) of the EBR-II fast reactor [1782 and 541]. Regeneration is carried out by remote remelting (10 kg portions of alloy)* in a zirconium dioxide crucible in an argon chamber. Moreover, rare-earth elements go over into the slag; the ZrO_2 is only reduced to ZrO and the latter does not pass into the uranium alloy with the rest of the fission products (so-called fissium). When the rods have been cast, the following impurities, for example, (fission products) remain besides plutonium (in %): Mo – 2.5; Ru – 1.5; Pd – 0.5; Rh – 0.3; Zr – 0.2 (technetium probably remains also, but its content is not considered in the remelting). All these additives are fixed in the uranium alloy in the γ-phase, which improves the stability of the cores under irradiation.

ZIRCONIUM METALLURGY. The American exhibition showed a technological scheme for zirconium production. The main (new) points of this scheme are as follows: 1) the zirconium concentrate is fused with sodium hydroxide, the sodium silicate leached out, and the sodium zirconate dissolved in nitric acid; the previous operation of carbidization, chlorination of the carbide, etc. is eliminated; 2) instead of extraction of hafnium thiocyanate into the organic phase of methyl isobutyl ketone, the extraction of zirconium from a nitric acid solution into the organic phase of tributyl phosphate, dissolved in n-hexane, is now used.

Report [1003] noted the advantage of combining in one reactor the magnesium-thermal reduction and the vacuum distillation of magnesium and magnesium chloride from the zirconium sponge. The report described a horizontal tipping, hermetically sealed reactor with detachable heat insulation (to speed up cooling), how-

*H. H. Hausner. Powder Metallurgy in Nuclear Engineering. ASM, Cleveland, Ohio, USA, 1958.

†Same

‡Same

*See also "Casting uranium alloys under pressure" J. Atomic Energy, Vol. 5, No. 1, 84 (1958).

ever, its construction is intended for experiments and has not been tested in production. A mixture of magnesium and sodium is used instead of magnesium for the reduction of zirconium tetrachloride. The content of one of the main impurities (chlorine) in the zirconium sponge obtained is 53 millionths, instead of 350 for normal sponge obtained by the Krol method; the nitrogen content of the sponge, obtained in the combined process is 0.005%.

The exhibitions of certain countries showed zirconium ingots after arc remelting ~ 2 m long and ~ 150 mm in diameter, tubes 1.5 m long and 70 mm in diameter with a wall thickness of ~ 2 mm and zirconium ingots 1 m long and 250 mm in diameter ("Hereus " Fed. Ger. Rep.). The catalog of "Imperial Chemical Industries" (Britain) stated that zirconium ingots weighing ~ 3 tons were smelted.

NIOBIUM PRODUCTION. The properties of niobium and the technology of its production are discussed in reports [44, 305, 697, and 1274]. Examples are given [697] of the processing of euxenite concentrates (Nb_2O_5 – 27%) and niobium-containing slag from cassiterite smelting (Nb_2O_5 – 9.8%).

After removal of the bulk of iron oxide by treatment with hot hydrochloric acid, both the given products are readily stripped by chlorination (in a mixture with charcoal). The chlorination temperature was lowered to 500° by the addition of 20% NaCl to the euxenite and 20% NaF to the slag. Under these conditions, 95% of the niobium was extracted from the euxenite by chlorination and 90% from the poorer ore. Subsequent separation of tantalum from the niobium was accomplished by methyl isobutyl ketone extraction from hydrofluoric-sulfuric acid solution. The main problem of the process is the production of pure metal with the minimal oxygen content.

Methods were investigated for the reduction of potassium fluoroniobate with sodium, niobium chloride with magnesium, and niobium pentoxide with calcium or carbon in vacuum. In the description of the latter method [44], it was stated that the oxygen and carbon contents should be not higher than 0.01 – 0.02% in the finished metal. After a second vacuum sintering or vacuum remelting of the product of niobium pentoxide reduction with carbon, the carbon and oxygen contents may fall from 0.5 and 0.7% to 0.028 and 0.015%, respectively. The metal obtained contained 0.028% of nitrogen, had a Vickers hardness of 87 ± 3 and was ductile in the cold [1274]. It was stated that the addition of 0.3% of tantalum noticeably affected the mechanical properties of niobium [305].

A sintered or remelted blank is cold-rolled into a plate (sheet), then pressed into cup-shaped blanks and a tube drawn from the latter [10]. It is not practicable to extrude tubes due to the high flow pressure, which is maintained up to 800°.

During the pressure processing of niobium, intermediate annealing in vacuum is used with strict observation of the condition that the inleakage into the vacuum furnace should not exceed 0.1μliter/sec [44]. The exhibition of the firm "Hereus" showed samples of cup-shaped niobium blanks of 75 mm diameter and a thickness of ~ 4 mm for the production of tubes and the firm "Societe Industrielle des Mineurs" (France) showed samples of sintered niobium of the following composition (in %): Nb – > 99; Ta – < 0.1; Fe – 0.01; Ti – 0.001; Ni – 0.007; W – 0.003; Sb, Sn – 0.0001; Si, Al – 0.001; C – 0.013; N – 0.007; O – 0.035.

VANADIUM PRODUCTION [44, 1274]. In the development of methods of vanadium production, there are three completing reduction methods: vanadium trichloride with magnesium, vanadium pentoxide with calcium, and vanadium trioxide with carbon in vacuum. Reduction of vanadium oxides with carbon in vacuum gives worse results than the reduction of niobium [44].

Due to the lower melting point of vanadium, the temperature of the process has to be limited, which makes a long, multistage process necessary (up to 30 hours at 1700° in a vacuum of 10^{-5} mm Hg). This gives a metal containing (in %): V – > 99.6; C – 0.12; O – 0.06. In addition, the carbon reduction process is complicated by the presence in the vanadium – oxygen – carbon system of a low-melting composition (V – 96.6%; C – 2.8%; O – 0.6%) with a melting point of 1500° and this creates a risk of fusing the incompletely reduced product. The best results are achieved with calcium-thermal reduction of the pentoxide or magnesium-thermal reduction of the trichloride. Washing the regulus of calcium-reduced vanadium with 30% hydrochloric acid gave a metal that was ductile in the cold, contained (in %): V – > 99.7; O – 0.01 – 0.025; N – 0.005 – 0.015; H – < 0.005, and had a Vickers hardness of 82. Remelting in a vacuum arc furnace (10^{-3} mm Hg) gave an ingot with a Vickers hardness of 90.

Reduction of VCl_3 with magnesium gave a sponge, which, after vacuum sintering or arc remelting, also gave a metal that was ductile in the cold. The sintering was at 1800°, i.e., close to the melting point (1900°).

Electrolytic refining of vanadium from the technical metal is described in report [698]. The electrolyte consisted of NaCl and VCl_2 (2.5% vanadium concentration).

Samples of various articles made from vanadium were shown in the British and French exhibitions. The firm "Societe Industrielle des Mineurs" showed samples of cast vanadium with a Vickers hardness of 95 and sintered vanadium with the following composition (in %): V – 99.5; Fe – 0.0005; Si – 0.03; Al – 0.01; C – 0.09. Samples of fine, ductile vanadium turnings were shown and had the following composition (in %): V – 99.7; Fe – 0.025; Al – 0.02; Si – 0.04; Ca – 0.004; C – 0.07; N – 0.014; O – 0.035; H – 0.001.

BERYLLIUM TUBES FOR CLADDING FUEL ELEMENTS. The use of tubular beryllium sheaths [318] for fuel elements with UO_2 cores and carbon dioxide cooling makes it possible to raise the temperature at the sheath to 600°. The British exhibit showed extruded beryllium tubes of 10 – 20 mm diameter and 1 and 0.4 mm wall thickness. The extrusion of high-purity beryllium in the temperature ranges of greatest plasticity, 450 and 800°, is being developed and applied.*

Pure beryllium blanks [320] are made from electrolytic beryllium, refined by vacuum induction remelting in a beryllium oxide crucible with a molybdenum heater. After remelting, the metal is poured into a graphite or steel mold, lubricated with aluminum oxide. Percentages of 0.15 – 0.20 of beryllium oxide are permissible in the ingot (0.20 – 0.31% in the starting electrolytic metal). The ingot is turned and ground to a powder in a ball mill for the preparation of compact blanks and articles by a metalloceramic method. The beryllium oxide content is increased to 0.3 – 0.6% during pulver-

*The possibility of using refined magnesium-thermal beryllium from fluoride and electrolytic beryllium from chloride for these purposes is being considered.

ization. The percent of BeO in the beryllium may be decreased by decreasing the grinding time and by grinding in an atmosphere of an inert gas, as with the preceding turning. Flaky electrolytic beryllium, which is more free from metallic impurities than the magnesium-thermal one from fluoride, after firing in vacuum at 95° and removal of the chlorides, may be ground directly to a sufficiently pure powder without requiring vacuum remelting and turning [320]. This makes the process cheaper, whereas the magnesium-thermal metal from fluoride requires refining by vacuum remelting, followed by turning.

A copper lubricant, which is more convenient than a graphite one, is used in the extrusion of tubes and this lubricant is deposited on the beryllium blank (billet) from a solution (cementation). After this the copper layer is readily stripped.

Paper [320] recommends sintering of freely packed beryllium powder in vacuum at 1200 – 1220° for six hours to obtain compact blanks with a density of 97% of theoretical. It is also stated that a good quality blank may be made by hot vacuum pressing, but the plasticity depends on the purity of the beryllium.

ZIRCONIUM HYDRIDE AND ZIRCONIUM – URANIUM – HYDROGEN ALLOY FOR A HOMOGENEOUS REACTOR. Report [789] recommends zirconium hydride as a moderator. At the exhibition ("Sylvania Corning Nuclear Corporation," USA) it was shown in the forms of powder and of compact discs sintered in hydrogen. The zirconium – uranium – hydrogen alloy may be simultaneously fuel and moderator. A zirconium – uranium – hydrogen alloy containing ~ 8 weight % of uranium with a 20% enrichment and atomic ratios of Zr : U : H = ~ 100 : 3 : 100 was chosen for a low-power experimental homogeneous reactor [789]. The hydrogen in this alloy is held by the zirconium and acts as moderator. The hydrogen concentration in unit volume of zirconium hydride is greater than that in water.

Being the basis of the alloy, zirconium imparts to it a high melting point, transparency to slow neutrons, and good heat conductivity. The technological scheme for the production of the zirconium – uranium – hydrogen alloy is as follows: 1) zirconium sponge is melted with 8 weight % of uranium pieces in an arc furnace with a water-cooled copper crucible; 2) blanks with a diameter of ~ 150 mm diameter are hot extruded to give rods of 35.5 mm diameter, which are cut to a length of 355 mm; 3) the pieces are heated in a vacuum furnace to 750°; 4) the amount of pure hydrogen required for the alloy (about 1 weight %) is slowly introduced into the furnace; and 5) the hydrogen is shut off and the alloy cooled slowly with the furnace (operations 3, 4, and 5 take several hours).

The hydrogenated alloy in the shape of a rod of the dimensions given above is placed in a cellular aluminum sheath. Aluminum discs with samarium oxide pressed into them are placed directly at the ends of the rod. Graphite plugs, ~ 102 mm high, are placed in the ends of the tubes, the fuel elements filled with helium, the tube ends with the aluminum plugs sealed and the sealing of the whole tested with a mass spectograph. This alloy has a negative reactivity coefficient. In testing a similar alloy (with 90% enriched uranium) irradiated in MTR (flux 10^{13} neutr./cm^2·sec) to a burn-up of 1.5 to 2.5%, no changes at all were found in its size, weight, structure, and hydrogen content. The possibilities of this alloy and, in particular, the temperature limits of its possible use require study. One of these problems is the determination of the temperature limits for the stable retention of hydrogen in the alloy when irradiated.

Received November 5, 1958

REFRACTORY FUELS AND HIGH-TEMPERATURE FUEL ELEMENTS

G. A. Meerson

On the basis of foreign material presented at the Second International Conference on the Peaceful Uses of Atomic Energy (Geneva, 1958), we consider aspects of the production and use of fuel elements (FE) with uranium dioxide cores in tubular and laminar sheaths and also aspects of the use of uranium and thorium carbides and oxides for FE of high-temperature (up to 1000°) reactors with gas cooling and the use of thorium metal for FE.

Due to the change in form and dimensions under irradiation and the gas swelling at 550 – 600° of FE cores of uranium and its alloys and the need for raising the FE temperature of power reactors, a great deal of attention has been payed to the use of refractory uranium compounds.

URANIUM DIOXIDE. The use of uranium dioxide for FE was described in reports* [142], [182], [192], [193], [318], [784], [1165], [2368], [2380], and [2404] and demonstrated in the exhibitions of various countries. In order to stabilize the shrinkage process during dioxide sintering (for the preparation of articles with exact forms and dimensions), all the processes affecting the particle form and dimensions of the original UO_2 powder have been studied and standardized: these include precipitation of diuranate or some other starting uranium salt, its firing, the reduction to UO_2, etc.

The structural requirements of UO_2 powder intended for the sintering of articles from it are different from those of UO_2 powder intended for the production of uranium tetrafluoride. Therefore, when UO_2 is produced, for example, by reduction in a standardized continuous furnace [1165], the reduction temperature for the production of UO_2 for sintering is higher than that for the production of UO_2 to be used for UF_4 preparation.

American production technology for uranium dioxide sintered briquets, presented in report [2380] and on the exhibition stand on FE for the PWR reactor at Shippingport, involves mixing of the prepared powder with binding agents (polyvinyl alcohol and Sterotex) and pressing in dies with the die and stamp made from hard carbide alloys. (These dies work without noticeable wear on automatic hydraulic presses under a pressure of ~ 20 ton/cm^2). The briquets are fired in hydrogen at ~ 1700° for eight hours until the density is 93 – 95% of theoretical. The sintered briquets are ground with a tolerance of ± 0.01 mm.

There is a report [318] on the possibility of lowering the sintering temperature of the briquets to 1450° by the use of nonstoichiometric dioxide (for example, the composition $UO_{2.18} - UO_{2.2}$ or the introduction of oxygen, steam, or other oxidants into the sintering furnace atmosphere. However, briquets from nonstoichiometric uranium dioxide behave worse in a reactor: a high temperature is developed in the center of the briquet and the excess oxygen subslimes in the form of UO_3, while dissociation of UO_3 leads to the transfer of oxygen and the oxidation of new amounts of UO_2, etc. As a result, a fused region, which sometimes forms in the center of a briquet, grows in size as a result of oxygen migration, while it is much more stable in stoichimetric uranium dioxide. To avoid these complications, it is recommended that a briquet of nonstoichiometric uranium dioxide is reduced in hydrogen after sintering in an argon atmosphere. Briquets obtained in this way are more stable [318] than those obtained by direct sintering of UO_2 at 1700°.

Among other methods of promoting uranium dioxide sintering, the addition of other oxides, for example TiO_2, to it should be mentioned [784].

FUEL ELEMENTS FROM UO_2 BRIQUETS IN TUBULAR SHEATHS OF ZIRCALLOY-2 (FOR THE HIGH-PRESSURE WATER-COOLED REACTOR AT SHIPPINGPORT [2380]). For the production of a tubular sheath from a zircalloy-2 ingot, ~ 310 mm in diameter, a blank of diameter ~ 46 x 170 mm^2 is prepared by hot extrusion with subsequent machining and drilling out of the hole. The tube is then extruded at 840°. In report [2380], it was indicated that the extrusion was carried out in steel or copper sheaths to avoid possible oxidation of the zirconium during hot extrusion and also to produce "metallic lubrication." However, on the exhibition stand devoted to this process, the zircalloy-2 blank was shown as being extruded in two concentric sheaths, a steel sheath directly on the blank and a copper one above it.

The intermediate steel sheath serves to prevent interdiffusion of copper and zircalloy-2 during hot extrusion. The sheaths are stripped with nitric acid from the extruded tube of diameter 63.5 x 51 mm^2 and the surface trimmed on a lathe: the tube is then cold-drawn, subjected to intermediate vacuum annealing and again drawn down in size: the external diameter is 10.7 mm and the wall thickness, 0.7 mm. Such a tube with a welded plug at one end is loaded with 26 sintered UO_2 briquets, the tube filled with helium from the other end and a zircalloy plug welded on. The total length of this element is 260 mm. An assembly of 120 tubes is spaced with zircalloy end plates with holes and placed in an over-all zircalloy casing with a cross-section of ~ 140 x 140 mm^2 and a length of ~ 2.75 m.

FUEL ELEMENTS FROM LAMINAR UO_2 BRIQUETS IN A ZIRCALLOY-2 SHEATH (RECONSTRUCTED SHIPPINGPORT REACTOR [2380]). The tubular FE described are to be replaced by laminar ones (with a greater specific surface for heat transfer), which consist of pressed and sintered UO_2 plates with a density ~ 96% of theoretical. The sintered plates do not require grinding since in the pressing and sintering it is possible to maintain the thickness tolerance within the limits of ± 0.05 mm. There are no rigid requirements as regards the length and width of the sintered plates since it is desirable to have 5% free space between the core and the sheath of the FE. The dimensions of the UO_2 plates have not been determined finally [2380]. This report presented photographs of UO_2 plates measuring 1.75 x 6.5 x 88 mm. They were packed in the pockets of a zircalloy-2 collector plate (for example, 15 plates in one assemblage in three rows).

*The numbers of the reports presented at the conference are given in brackets.

The two sides of the collector plate with UO_2 plates in it are covered with zircalloy sheaths 0.64 mm thick. The whole assemblage has a thickness of 3 mm. The adhesion of the sheaths and the collector plate is effected by means of the "eutectic diffusion methods." For this purpose, a layer of copper (nickel or iron) ~0.05 mm thick is deposited on the zircalloy plates by cementation from a solution of a copper (nickel or iron) salt. The final choice of solder-metal has not been made. Then the washed and dried plate-sheaths are layed onto the collector plate and the whole assembly fixed by welding at the corners and heated for 1/2 hour in a horizontal tubular furnace at 1000°. A slight excess pressure of an inert gas is maintained in the furnace. The Cu - Zr (885°) (or Fe - Zr = 934° or Ni - Zr = 961°) eutectic melts and the copper (nickel or iron) diffuses into the zirconium, the liquid disappears and a sound, gas-tight diffusion joint is formed between the zircalloy plates.

SEED FUEL ELEMENTS OF THE PWR REACTOR (SHIPPINGPORT [787]). The cores of these FE consist of plates of an alloy of zircalloy-2 with 6.7% of enriched uranium ~ 0.6 mm thick, enclosed in a zircalloy-2 sheath, 0.4 mm thick. The uranium is approximately 3% enriched. At elevated temperatures, the alloy forms a monophase solid solution of β-zirconium and γ-uranium with a solidus point of ~ 1650°.

Uranium is fused in an arc furnace with zircalloy-2 in an inert atmosphere. The ingot is forged, rolled into a strip, and cut into pieces, which are remelted. This ingot is used to fabricate a rod, 63.5 mm in diameter, which is used as the consumable electrode in a third arc fusion. The homogeneous ingot obtained is forged and rolled into a plate~3 mm thick. The plate, pressed between two zircalloy sheets, is inserted into a steel sheath to prevent oxidation and rolled at approximately 785°. During the rolling, the zircalloy sheets are welded to the core alloy.

OTHER VARIATIONS IN THE TECHNOLOGY OF FABRICATING TUBULAR FUEL ELEMENTS FROM SOLID UO_2 WITH METALLIC SHEATHS. The exhibitions also showed examples of tubes of stainless steel, zirconium, and aluminum with consolidated uranium dioxide powder, obtained by forging tubes together with UO_2 on rotating forging machines. The ends of the tubes were welded up in an inert atmosphere. By means of rotation forging, the density of the core may be brought up to 75 - 94% of theoretical, depending on the type of the UO_2 powder and the properties of the material of the sheath, whose thickness may be reduced to 0.6 mm. The deficiency of the method consists of the fact that it is more than usually difficult to attain the standard core density and sheath thickness.

URANIUM MONOCARBIDE AND THE URANIUM MONOCARBIDE - URANIUM CERMET. Reports [318, 1162, 964, and 1443] described the preparation and properties of uranium monocarbide (melting point 2250°) and the cermet (metalloceramic alloy) of the monocarbide with small amounts of uranium. Uranium monocarbide has about four times the heat conductivity of UO_2, contains more uranium per unit volume, is wet by molten uranium and fuses with it to form a cermet, whose heat conductivity is similar to that of uranium and whose strength is several times greater than that of the monocarbide or uranium dioxide.

The formation of a dense and strong cermet requires a relatively small amount of uranium. Its structure consists of firmly sintered, refractory grains of monocarbide with the spaces between the grains filled with cementing and consolidating uranium.

It is also possible to prepare sintered articles from monocarbide alone, which does not undergo conversion right up to the melting point. However, pure UC is more brittle than the UC + U cermet. Uranium carbide is decomposed by water and therefore it is not suitable for use in fuel elements for water-cooled reactors. On the other hand, it is more stable than UO_2 towards liquid sodium. The molding conditions for making articles from UC or a UC + U cermet can be eased by preliminary pressing or extrusion (for example, with preheating to 800°) of a mixture of uranium and graphite powders and then sintering of the blank with simultaneous carbidization at a temperature of~1000°.

It was reported [1162] that the stability of the cermet can be improved if the uranium powder is replaced by a powder of uranium alloy, for example, with molybdenum (obtained by coreduction of the oxides), etc. In general, a small amount of an alloying additive produces a noticeable concentration of it in the uranium part of the cermet, especially if the alloying element, for example molybdenum, has a lower affinity for carbon than uranium.

The exhibition of the firm "Degussa" (Fed. Ger. Rep.) showed sintered rods (for the cores of high-temperature FE) from UC and UO_2, 5 - 12 mm in diameter and 20 - 30 mm in length. However, despite certain advantages in the properties of UC and the UC + U cermet, the possibilities and conditions of their use in high-temperature FE still require further investigation.

FUEL ELEMENTS AT 1000° FROM Th - U CARBIDES WITH GRAPHITE SHEATHS FOR A GAS-COOLED (NITROGEN OR HELIUM) REACTOR [314]. A further increase in the FE temperature to 1000° on the sheath was planned [314] in a reactor with FE on a graphite base. A mixture of thorium and U^{235} oxides (U : Th=5-12%) is first dispersed in graphite and then by subsequent heating and finally, during the initial use of the FE, the oxides are converted into carbides. Dispersion of the uranium and thorium in graphite eliminates the danger of distortion or destruction of the heat producing cores of the FE and improves the heat conductivity. The graphite contains about ~ 0.66 weight% of uranium-235. It is also planned to use U^{235} first and then replace it either partially or completely by U^{233} (complete replacement will be possible if a breeding ratio equal to or greater than 1 is achieved in operating the reactor).

The cladding material chosen is consolidated (impregnated) graphite, which must be impermeable to gases (fission products) at high temperatures. To guarantee this, besides an improvement in graphite production technology, a stream of cooling gas is passed inside the sheath and a lower pressure maintained than outside the sheath. The FE consists of:

1) a central rod of about ~23 mm diameter of normal graphite and 1.8 m long;

2) the rod is surrounded with graphite rings (external diameter ~ 36 mm, height ~ 1.5 m) with particles of carbide embedded in it and placed in

3) a tubular, hexahedral sheath beneath a 50 mm seal of "impregnated" graphite with a round inner channel.

In the middle of each external face of the hexahedron is a small longitudinal ridge, which acts as a spacer for the gap through which the cooling gas flows.

The height of the fuel element is 2.4 m. Cooling gas is fed into the sheath through a porous plug in the upper end of the element and this carries radioactive gases into an absorber filled with activated charcoal, from which the gas passes through a purifying system (to remove O_2, CO_2, CO, and N_2O) and back into circulation. The gas pressure in the system is up to 20 atm. Irradiated FE cores are combusted to give a mixture of uranium and thorium oxides, which require further chemical processing. The possibility of leaching carbides from graphite with acids followed by chemical processing of the solution is being studied. The technology of graphite production for reactors is being improved.

The firm "Degussa" (Fed. Ger. Rep.) exhibited samples with a density of 2.08. However, they did not attain the same gas impermeability as achieved by the British firms "General Electric" and "Hawker Siddeley Nuclear Power." "General Electric" demonstrated an apparatus with a graphite tube (with steel tubes firmly bonded to it), electrically heated to 600°, filled with carbon dioxide and contained in a vessel in which a vacuum was maintained when the pump was turned off.

Together with the methods being developed for the production of gas-impermeable graphite, which require reorganization of graphite production technology, a method is being developed for sealing the pores of normally prepared graphite by its impregnation in vacuum with concentrated aqueous solutions of high-molecular organic compounds (furfuryl alcohol), though the method does not give the same gas impermeability at 1000° as in the experiment of 600°, described above.

When heated to 1100 – 1200°, furfuryl alcohol decomposes with the liberation of a disperse carbon deposit, blocking up the pores of the graphite. Articles from this graphite have a smooth, lustrous, nongreasy surface and outstanding strength and elasticity (for example, balls of this graphite bounce on a stone floor).

The industrial exhibition of the firm "Degussa" showed [1005] graphite balls of ~ 50 – 60 mm diameter with inclusions of uranium and thorium carbides (the larger balls) for FE of the "Brown-Joverin" reactor in Switzerland. Uranium carbide (20% enriched) mixed with carbon is introduced into channels drilled in the graphite balls. The channels are sealed with plugs. The surface temperature of the balls during reactor operation is up to 1100°.

The advantage of the balls [1005] consists of an increased mechanical and thermal strength, radiation stability, and ease of loading and unloading from the reactor. They do not have sheaths. Solid carbide-forming fission products are retained in the graphite. Gases (fission products) are removed by circulation of an inert cooling gas, which is passed through an adsorber with activated charcoal (at -190°).

FUEL ELEMENTS FROM A ThO_2 - UO_2 MIXTURE. It is possible to use a mixture of the oxides ThO_2 + UO_2 instead of the carbides [314]. Beryllium oxide (instead of graphite) possesses certain advantages as a moderator and, possibly, as a base for FE cores of the disperse type, since it absorbs neutrons less. It is also convenient for cooling with oxidizing gases. However, beryllium oxide is less heat stable than graphite. A combination of ThO_2+UO_2 with a BeO base is being investigated for a high-temperature reactor together with a reactor with FE of graphite and carbides.

The British exhibition showed a model of an experimental FE with a graphite sheath, not loaded with carbides but with glazed, gas-impermeable tablets of Al_2O_3 with inclusions of enriched uranium oxides and thorium oxide tablets. These tablets are interchangeable and their ratio and also the ratio to graphite tablets can be varied. This facilitates experimental work with model FEs with various ratios of ThO_2, UO_2, and graphite.

FUEL ELEMENTS BASED ON METALLIC THORIUM WITH THE ADDITION OF 3 – 7% OF U^{235}. In thorium – uranium alloys, the uranium is present as isolated inclusions in a thorium base (the solubility of uranium in thorium at 20° is less than 1 weight % and at 1000°, about ~1.5 weight %). With a 3% uranium content, the strength of thorium at 500° is increased by 50% [706].

The USA is constructing two thorium-base reactors, one by "Consolidated Edison" with high-parameter water cooling (stand in USA exhibition) and SRE with sodium cooling [785] for testing FE at high temperatures to a high burn-up factor and for studying the behavior of the thorium – uranium alloy.

The FE of the SRE reactor consists of seven tubes, 2.4 m long, made from stainless steel, 0.25 mm thick. Each tube is filled with 12 cores, 19 mm in diameter and 152 mm long, made from an alloy of thorium with 7.6% of highly enriched U^{235}. A gap of 0.25 mm between the cores and the sheath is filled with a sodium – potassium alloy.

The thorium – uranium alloy is prepared by induction fusion in vacuum (1700 – 1750°) in beryllium oxide crucibles or graphite crucibles, lined with beryllium oxide, and cast in graphite molds, coated with magnesium zirconate.

In order to cheapen the process and raise the yield of the finished product, the alloy is directly molded into a bar with almost the finished dimensions. The processes of vacuum induction melting with stationary molding or centrifugal molding are compared. The bar is swaged to the required diameter on a rotary machine and cut off to the required length on a lathe. With an improvement in casting, additional rotary swaging may become unnecessary [785]. The smelting technology, casting in the preparation of alloy bars, may be combined with a pyrometallurgical method of processing hot bars, similar to that described in report [541] on FE for the EBR-II reactor.

It was also reported [1705] that the high plasticity of thorium and its good sintering properties make it convenient and practicable to fabricate articles from thorium by the metalloceramic method, i.e., pressing and sintering of powders (eliminating melting and molding processes).

Thorium is refractory, does not undergo phase changes up to 1400° and has a cubic lattice, which is radiation-stable [785], but in the first experimental reactors, the temperature in the center of a core based on metallic thorium will not exceed 650°. A further increase in temperature is hindered by gas swelling and to counteract this it is necessary to investigate the possibility of strengthening thorium by alloying or of replacing a metallic system by an oxide or a carbide one.

Received November 5, 1958

A CONTRIBUTION ON THE MECHANISM OF PLUTONIUM NITRATE EXTRACTION BY MONO- AND DIBUTYL PHOSPHATES

V. B. Shevchenko and V. S. Smelov

In a previous communication [1] we examined the effect of monobutyl phosphate (MBP) and dibutyl phosphate (DBP) on the extraction of plutonium nitrate by tributyl phosphate (TBP).

In the present work the mechanism of plutonium extraction by MBP and DBP is elucidated. An investigation was made of the mechanism of plutonium nitrate extraction by MBP and DBP with an ionic strength equal to 6. It was shown that plutonium is extracted in the form of PuK_4, where K is $[(C_4H_9)_2PO_4]^-$ or $[C_4H_9HPO_4]^-$. It was calculated that the equilibrium constant for the reaction of plutonium nitrate with MBP equals $(1.5 \pm 0.25) \cdot 10^3$ and with DBP, $(6.15 \pm 0.85) \cdot 10^3$.

GENERAL COMMENTS AND EXPERIMENTAL PROCEDURE. The experimental procedure and treatment of results are partly derived from the work [2], in which a study was made of the mechanism of zirconium extraction by thenoyltrifluoroacetone. For elucidation of the extraction mechanism, three series of experiments were performed in which a study was made of the dependence of the plutonium distribution coefficient (E) on the concentration of MBP and DBP, H^+ ions and NO_3^- ions. Instead of the thermodynamic activities of the extractant and the H^+ ions, we used the concentrations and the activity coefficients were kept constant by means of the ionic strength, equal to 6. The high value of the ionic strength made it possible to vary the concentrations of H^+ and NO_3^- ions over a wide range. Chemically pure lithium nitrate was used to keep the ionic strength constant. The change in the activity of water in the transition from 6 M HNO_3 to 6 M $LiNO_3$ was not considered. For studying the effect of NO_3^- ion concentration, the ionic strength was kept constant with a mixture of nitric and perchloric acids.

The nitric and perchloric acid were purified by additional distillation. The water was doubly distilled. Benzene (thiophene-free), purified by distillation, was used as diluent for MBP and DBP. The transfer of plutonium into benzene was not considered ($E \approx 10^{-3}$). The extractions were performed in glass separating funnels with a shaking period of 30 minutes. The volumes of the phases were 10 ml. The temperature varied over the range 20 – 22°.

So as to keep the composition of the aqueous phase constant, the benzene was first saturated with a solution similar in composition to the one investigated.

Average data from several experiments are presented in Tables 1 – 4. The plutonium was present in the tetravalent state with an initial concentration of 50 mg/liter.

ANALYSIS PROCEDURE. After standing for a day or centrifuging, the phases were separated and their plutonium contents determined from the α-count. Self-absorption was considered for solutions with a high $LiNO_3$ content. The deviations in the results from determinations on two parallel samples were 5 – 7%. MBP and DBP were determined by methods described in paper [1] and also by precipitation of the binary phosphates of magnesium and ammonium [3]. The error in the MBP and DBP determinations was 7 – 12%. The change in the phase volumes during extraction was allowed for in the calculations.

Table 1. Distribution of DBP Between Organic and Aqueous Phases

Composition of aqueous phase, mole/liter			Distribution coefficient, E	
HNO_3	$LiNO_3$	$HClO_4$	Initial concentration* 0.1 mole/liter	Initial concentration, 0.01 mole/liter
1	5	—	99,0	80,1
2	4	—	99,9	85,2
3	3	—	123,3	98,7
4	2	—	146,3	105,6
5	1	—	178,5	143,8
6	—	—	228,1	178,5
1	—	5	222,5	181,9
3	—	3	233,8	190,0
5	—	1	240,0	186,1

*Here and later, the initial and equilibrium concentrations of DBP and MBP refer to their concentrations in the organic phase.

DISTRIBUTION OF MBP AND DBP BETWEEN ORGANIC AND AQUEOUS PHASES.* The mathematical interpretation of the experimental results required accurate data on the concentration of the extractant in the organic phase. As we established previously, MBP has a tendency to pass into the aqueous solution. Therefore, the equilibrium concentrations of MBP and DBP were first established. For this purpose, solutions of MBP and DBP in benzene were shaken with aqueous solutions containing various amounts of HNO_3 and $LiNO_3$, HNO_3 and $HClO_4$.

Table 1 shows that DBP passes into the aqueous phase to an insignificant extent and therefore the initial and equilibrium concentrations of DBP will be equated in subsequent calculations.

Table 2 shows that a considerable fraction of MBP from the starting concentration passes into a solution containing lithium nitrate and nitric acid. The distribution of MBP between the organic and aqueous phases is expressed well by the equation (for the given aqueous phase composition)

$$\frac{C_{org}^{0.882}}{C_{aq}} = 2.52, \qquad (1)$$

where C_{org} is the concentration of MBP in the organic phase and C_{aq}, that in the aqueous phase. Increasing the aqueous-phase acid concentration increases the MBP distribution coefficient (Table 3).

*The MBP and DBP concentrations are expressed in mole/liter.

Table 2. Distribution of MBP Between Organic and Aqueous Phases
(Composition of aqueous phase: HNO_3 and $LiNO_3$, 3 mole/liter each)

Initial concentration, mole/liter	0,001	0,003	0,005	0,008	0,01	0,03	0,05	0,08	0,1
Distribution coefficient, E	1,22	1,32	1,38	1,47	1,56	1,78	1,90	2,03	2,12

Table 3. Distribution of MBP Between Organic and Aqueous Phases
(Initial MBP concentration: 0.01 mole/liter)

Composition of aqueous phase, mole/liter			Distribution coefficient E
HNO_3	$LiNO_3$	$HClO_4$	
1	5	—	1,41
2	4	—	1,48
3	3	—	1,56
4	2	—	1,61
5	1	—	1,69
6	—	—	1,76
1	—	5	1,77
3	—	3	1,75
5	—	1	1,77

Table 4. Dependence of Distribution Constants on Nitric Acid Concentration

Nitric acid concentration, mole/liter	Equilibrium constants, K_e			
	equilibrium concentration of DBP, mole/liter		equilibrium concentration of MBP, mole/liter	
	0,01	0,001	0,01	0,001
1	$5,12 \cdot 10^3$	$5,37 \cdot 10^3$	$1,38 \cdot 10^3$	$1,74 \cdot 10^3$
2	$5,64 \cdot 10^3$	$6,1 \cdot 10^3$	$1,29 \cdot 10^3$	$1,59 \cdot 10^3$
3	$6,2 \cdot 10^3$	$6,15 \cdot 10^3$	$1,29 \cdot 10^3$	$1,47 \cdot 10^3$
4	$5,76 \cdot 10^3$	$6,32 \cdot 10^3$	$1,26 \cdot 10^3$	$1,46 \cdot 10^3$
5	$6,1 \cdot 10^3$	$6,6 \cdot 10^3$	$1,31 \cdot 10^3$	$1,41 \cdot 10^3$
6	$6,12 \cdot 10^3$	$7,08 \cdot 10^3$	$1,26 \cdot 10^3$	$1,32 \cdot 10^3$

On the basis of data presented in Tables 2 and 3, allowance was made for its transference into the aqueous phase in further experiments with MBP.

EFFECT OF MBP AND DBP CONCENTRATION ON PLUTONIUM DISTRIBUTION COEFFICIENT. Figures 1 and 2 illustrate data on the effect of MBP and DBP concentration on the plutonium distribution coefficient.

In range of DBP equilibrium concentrations from 0.0001 – 0.01 mole/liter, the slope of the plot of $\lg E$ against $\lg C_{DBP}$ was 0.98 for plutonium extraction from a solution containing 1 mole/liter of HNO_3 and 5 mole/liter of $LiNO_3$, 0.98 for a solution containing 3 mole/liter of HNO_3, 3 mole/liter of $LiNO_3$, and 0.94 for a solution containing 6 mole/liter of HNO_3. For MBP, the slopes of curves of $\lg E$ against $\lg C_{MBP}$ for the extraction of plutonium from solutions containing 1, 3, and 6 mole/liter of HNO_3 and also 5, 3, and 0 mole/liter of $LiNO_3$, respectively, were 0.96, 0.91, and 0.90.

DEPENDENCE OF PLUTONIUM DISTRIBUTION COEFFICIENT ON H^+ ION CONCENTRATION. For this series of experiments, the concentrations of MBP and DBP were kept constant. With DBP, the initial concentration could be taken as the equilibrium one, as was stated above. For MBP, the plutonium distribution coefficients were calculated for each separate experiment on the determined equilibrium concentration, which was not difficult to do as long as the MBP distribution coefficient between organic and aqueous phases of different composition was known.

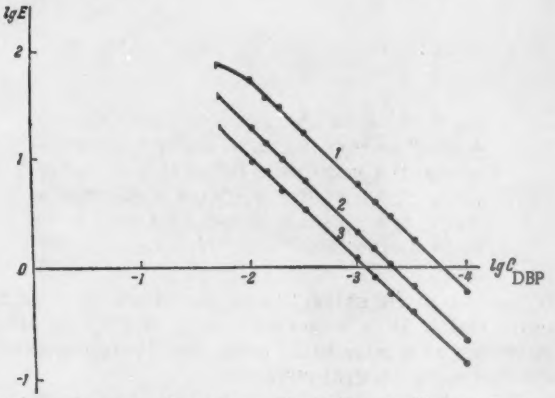

Fig. 1. Relation of plutonium distribution coefficient, E, to DBP concentration. Initial aqueous solution contained: 1) 1 mole/liter of HNO_3 + 5 mole/liter of $LiNO_3$; 2) 3 mole/liter of HNO_3 + 3 mole/liter of $LiNO_3$; 3) 6 mole/liter of HNO_3.

Over the DBP equilibrium concentration range studied (0.0003 – 0.01 mole/liter), the slopes of curves of $\lg E$ against $\lg [H^+]$ equalled 0.9 (Fig. 3). For MBP, the observed slope of the curve was 0.95 – 1.1 over the MBP concentration range 0.001 – 0.10 mole/liter (Fig. 4).

DEPENDENCE OF PLUTONIUM DISTRIBUTION COEFFICIENT ON NO_3^- ION CONCENTRATION. In this series of experiments, the ionic strength was kept constant with a mixture of nitric and perchloric acids. The data presented in Figure 5 shows that the plutonium distribution coefficient hardly depends on the concentration of NO_3^- ions for the region of MBP and DBP contents studied. As regards the slight decrease in the distribution coefficient, observed in the change from a solution containing 1 mole/liter of HNO_3 and 5 mole/liter of $HClO_4$ to a 6 M solution of HNO_3, this decrease is apparently connected with a change in the activity of water.

CALCULATION OF THE EQUILIBRIUM CONSTANTS OF PLUTONIUM NITRATE EXTRACTION BY MBP AND DBP. The equilibrium constants for the reaction of plutonium nitrate with MBP and DBP are presented in Table 4. Over the range of nitric acid concentrations studied, the average value of the equilibrium constant was $(6.15 \pm 0.85) \cdot 10^3$ for DBP and $(1.5 \pm 0.25) \cdot 10^3$ for MBP.

DISCUSSION OF RESULTS. At the present time it is impossible to give a strict interpretation of the data we obtained on the mechanism of plutonium extraction by mono- and dibutyl phosphates and therefore a series of assumptions has to be made. The process

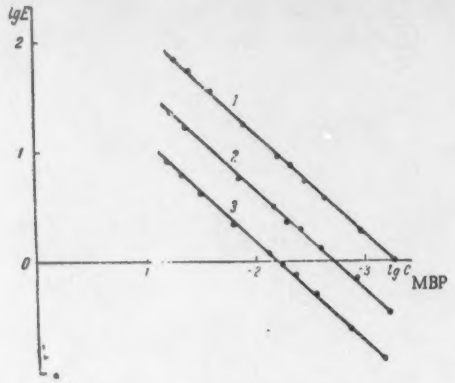

Fig. 2. Relation of plutonium distribution coefficient, E, to MBP concentration. Initial aqueous solution contained: 1) 1 mole/liter of HNO_3 + 5 mole/liter of $LiNO_3$; 2) 3 mole/liter of HNO_3 + 3 mole/liter of $LiNO_3$; 3) 6 mole/liter of HNO_3. lg$E$ refers to the equilibrium concentration of MBP.

occurring in the extraction of plutonium by an extractant, which is a monobasic acid (MBP can also be regarded as a monobasic acid) may be represented by the following general equation:

$$[PuR_n]^{4-n}_{aq} + [4-n]HR \rightleftarrows PuR_4{}_{org} + (4-n)H^+_{aq}, \quad (2)$$

where

$$R = [H(C_4H_9)PO_4]' \text{ or } [(C_4H_9)_2PO_4]'$$

(n may have the value 1, 2, 3, or 4)

Since the equilibrium concentration of plutonium in the aqueous solution was less than 2.10^{-4} mole/liter, the possibility of complex formation of plutonium with formation may be neglected.

The equilibrium constant of this reaction may be written thus:

$$K_p = \frac{C_{PuR_4} \cdot C^{4-n}_{H^+}}{C^{4-n}_{PuR_n} \cdot C^{4-n}_{HR}}. \quad (3)$$

The indexes denoting the phase are omitted. The observed plutonium distribution coefficients were determined by the expression

$$E = \frac{C_{PuR_4}}{C^{4-n}_{PuR_n}}. \quad (4)$$

Since the effect of NO_3^- ions on the plutonium distribution coefficient is insignificant, we may neglect the possibility of complex formation of plutonium with NO_3^- ions and also the existence of mixed complexes either with R' and $[NO_3]'$ ions or with R' and $[OH]'$ ions.

It was shown previously that the logarithmic relation of the plutonium distribution coefficient to the concentrations of MBP, DBP, and H^+ ions is expressed by a straight line with a slope equal to unity. Consequently, equation (2) may be written thus:

$$PuR_3^+ + HR \rightleftarrows PuR_4 + H^+. \quad (5)$$

Hence the experimental data leads to the conclusion that the extractant is simultaneously a complex former in the aqueous phase.

Received May 7, 1958

Literature

1. V.B. Shevchenko and V.S. Smelov, J. Atomic Energy 5, 5, 542 (1958) [USSR].
2. R.E. Coonnick, W.H. Mcvey, J. Amer. Chem. Soc. 71, 3182 (1949).
3. I.M. Kilthoff and E.B. Sandell, Quantitative Analysis [Russian translation] (Moscow, 1948) p. 406.

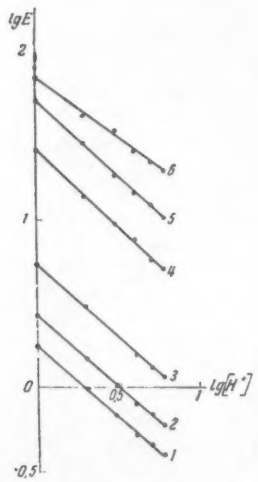

Fig. 3. Relation of plutonium distribution coefficient, E, to H^+ ion concentration. Equilibrium concentrations of DBP (in mole/liter): 1) 0.0003; 2) 0.0005; 3) 0.001; 4) 0.005; 5) 0.01; 6) 0.02.

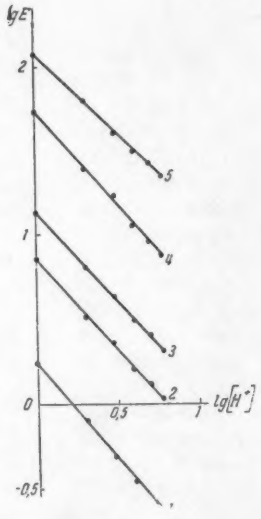

Fig. 4. Relation of plutonium distribution coefficient, E, to H^+ ion concentration. Equilibrium concentration of MBP (in mole/liter): 1) 0.001; 2) 0.005; 3) 0.01; 4) 0.05; 5) 0.1.

Fig. 5. Relation of plutonium distribution coefficient, E, to NO_3^- ion concentration. Equilibrium concentration of MBP (in mole/liter): 1) 0.01; 3) 0.1; Equilibrium concentration of DBP (in mole/liter) 2) 0.1; 4) 0.1.

RADIOCHEMICAL STUDIES OF NUCLEAR REACTIONS LEADING TO THE FORMATION OF π MESONS

A. K. Lavrukhina, I. M. Grechishcheva, and B. A. Khotin

A study of nuclear reactions leading to the formation of π-mesons is of value for understanding nuclear forces. A radiochemical method is used for detecting such reactions and this makes it possible to determine the cross section of reactions of very low probability.

Reactions of the type $(p,\pi^{\pm})$ and $(p,p\pi^{+})$ have been studied with the nuclei of elements of average atomic weight. It was found that their cross section equals $\sim 10^{-30}$ cm^2/nucl. at proton energies of 480 – 660 Mev. A noticeable increase in the cross section was observed in the range of energies 110 – 480 Mev. Such reactions could not be detected for nuclei of heavy elements. The products of the $(p,2\pi^{+})$ reaction with copper could not be identified.

The possibility of a $(p,\pi^{\pm})$ reaction in the interaction of a particle with a complex of nucleons in a nucleus is discussed. The information obtained gives a fuller understanding of the processes occurring when high-energy particles react with complex nuclei than can be obtained from the theory of nucleon-nucleon collisions.

The possibility of using a radiochemical method for detecting reactions forming π-mesons was first demonstrated in paper [1] on the example of the reaction Cu^{65} $(p,p\pi^{+})$ Ni^{65} copper was bombarded with protons with energies up to 420 Mev). This method was then used for detecting the $Si^{30}(p,\pi^{+})Si^{31}$ reaction [2].

The present paper presents the results of radiochemical investigations on some nuclear reactions leading to the formation of π-mesons. The greatest attention was paid to the $(p,p\pi^{+})$ reaction, studied on various nuclei and the $Cu^{65}(p,\pi^{-})Ga^{66}$ reaction and the possibility of detecting the twin formation of mesons on the example of the $Cu^{65}(p,2\pi^{+})Ni^{66}$ reaction was investigated.

The experiments were carried out with protons of 110 to 660 Mev, accelerated on the synchrocyclotron of the Nuclear Problems Laboratory of the OIYaI (Joint Institute for Nuclear Research). For this purpose targets were irradiated at various radii of the circulating proton beam for 1 $^1/_2$ to 2 hours. An aluminum monitor determined the intensity of the proton beam. The cross section of the Al^{27} $(p, 3pn)Na^{24}$ reaction was assumed to be 10 m – barns. The procedure used for identifying the radioisotopes and determining the values of their formation cross sections was similar to that described previously [3].

Study of the $(p,p\pi^{+})$ Reaction on Various Nuclei

Reactions of the $(p,p\pi^{+})$ type were studied, as in paper [1], on the example of the $Cu^{65}(p,p\pi^{+})Ni^{65}$ reaction, but with a greater range of energies, which made an unequivocal interpretation of the results possible. In addition, we attempted to detect such reactions with nuclei of heavy elements, which, as a result of fission, form a large number of radioactive isotopes. In connection with this, the detection of the $(p,p\pi^{+})$, reaction, which proceeds with a considerably smaller yield than the $(p, 2pxn)$, reaction, is quite difficult. For the investigation we chose the $La^{139}(p,p\pi^{+})Ba^{139}$ and $Au^{197}(p,p\pi^{+})$ Pt^{197} reactions.

Spectrally pure copper plates, 25 x 7 x 0.5 mm^3, 50 – 200 mg of La_2O_3 and 400 – 800 mg of gold were used as targets and were dissolved in 50% HNO_3 solution, 2N HNO_3 and aqua regia, respectively, after proton irradiation. From solutions of isotopic carriers we isolated the following radioisotopes: nickel from copper, barium from lanthanum, and platinum from gold.

THE $Cu^{65}(p,p\pi^{+})Ni^{65}$ REACTION. Nickel was isolated in the form of nickel dimethylglyoximate after preliminary separation of the hydroxides using a suspension of ZnO (this operation was performed twice). The precipitate was extracted with chloroform. Precipitation of the nickel with dimethylglyoxime and its extraction with chloroform were performed three times. The nickel dimethylglyoximate precipitate obtained was dried at 110 – 120° for 30 min and then weighed. The chemical yield of nickel was 60%. The activity of an aliquot part of this preparation was measured on a standard end-window counter. On analyzing the nickel decay curve (in the irradiation of copper with 200 – 660 Mev protons), two half-lives (T) were found, 2.5 and 38 hours. On irradiating with protons with 110-Mev energy, the component corresponding to $T = 2\,^1/_2$ hours was missing. The energy of the β-radiation was 0.9 Mev. These data make it possible to identify the radioisotopes as Ni^{65} with $T = 2.56$ hours and Ni^{57} with $T = 36$ hours and $E_\beta = 0.845$ Mev [4]. The values of the Ni^{65} formation cross section at different proton energies were given in Table 1 and Figure 1.

Table 1

Formation Cross Section of Some Isotopes at Different Proton Energies

Proton energies	Cross section, 10^{-27} cm^2		
	Ni^{65}	barium isotope with T = 2 hours	platinum isotope with T = 8 hours
110—120	Not detected	10.0	44.2
200—220	0.018	31.3	46.9
340	0.024	—	36.0
480	0.12	22.6	15.8
660	0.22	—	17.6

These data show that the cross section of the $Cu^{65}(p,p\pi^{+})Ni^{65}$ reaction increases by a factor of 6.6 in energy range 220 – 480 Mev. The cross section of this reaction increases little (by a factor of less than 2) with a further increase in energy to 660 Mev. The curve in Figure 1 in the energy region 110 – 480 Mev is similar to the relation of the π^{+}-meson formation cross section in carbon to proton energy over the same range of energies (Figure 2) [1].

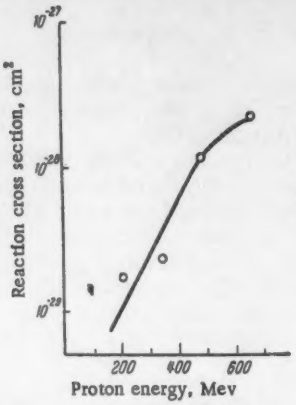

Fig. 1. Relation of Ni^{65} formation cross section to proton energy.

The slowing down in the growth of the $(p,p\pi^+)$ reaction cross section in the energy range 480 – 660 Mev may be explained by an increase in the probability of competing $(p,p\pi^+xn)$ reactions with an increase in the energy of the bombarding protons. It was also established that at proton energies of 2 Bev, the formation cross section of π-mesons is small [5]. It is possible that a certain number of the mesons formed even at an energy of ~ 700 Mev are absorbed by the nuclei in which they are formed.

THE La^{139} $(p,p\pi^+)$ Ba^{139} REACTION. The barium was isolated as the sulfate after preliminary precipitation of barium nitrate (several reprecipitations) and separation of Sb_2S_3 from a tartaric acid solution with hydrogen sulfide and $Fe(OH)_3$ with ammonia. The barium sulfate precipitate was fired and weighed. The chemical yield of barium was 60%.

Figure 3 gives the barium decay curve and the following half-lives were found on analyzing it: 2.48 hours and 11 days. The energies of the β-radiation were 0.2 – 0.3 and 2.8 – 3.1 Mev. The half-lives of the β^+- and β^--radiations were determined by measurement of a magnetic analyzer. These were 2 hours and 2.5 days for the β^+-radiation and 2 and 34 hours for β^--radiation. The energy distribution curve of the electrons formed a narrow peak in the low energy region. This made it possible to identify the barium isotopes: Ba^{133m} (i.c.)* with T = 38 hours and Ba^{131} (K)† with T = 2.4 days whose daughter product, Cs^{128} with T = 3.8 min, has a radiation energy of 3 Mev.

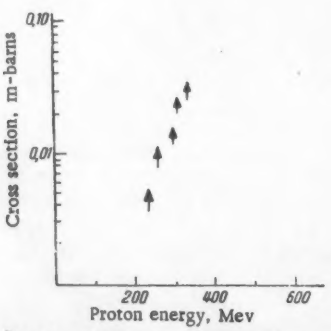

Fig. 2. Relation of π^+-meson formation cross section in carbon to proton energy.

*i.c. – isomeric conversion.

Electrons with this energy were detected in the barium radiation spectrum. A half-life of two hours was found for both the electron and positron radiation of barium. It may therefore belong to the isotopes Ba^{129} (β^+) with T = 2 hours and Ba^{139} (β^-) with T = 1.5 hours. Examination of the data on the energy of the β-radiation and the total radiation revealed no electrons with E = 2.3 Mev, but soft electrons with energies of 0.2 – 0.3 Mev were found and these correspond to the conversion electrons of Cs^{129} with T = 31 hours. The isotope Cs^{129} is a daughter nucleus of Ba^{129} and causes all the electron radiation in barium, which has an activity with T = 34 hours.

We calculated the values of the formation cross section of the barium isotope with T = 2 hours. Table 1 shows that the formation cross section of the barium isotope with T = 2 hours changes insignificantly in the energy range of 110 – 480 Mev.

However, quite a difference was observed in the formation cross sections of Ni^{65} and the barium isotope with T = 2 hours. For example, at a proton energy of 480 Mev, the ratio $\sigma Ni^{65}/\sigma Ba$ with T = 2 hours = 0.005 and with a decrease in proton energy, the ratio decreased considerably. All this indicated that the bulk of the activity with T = 2 hours did not belong to Ba^{139}, which could have been formed by the $La^{139}(p,p\pi^+)$ reaction. Thus, it was impossible to establish this reaction radiochemically.

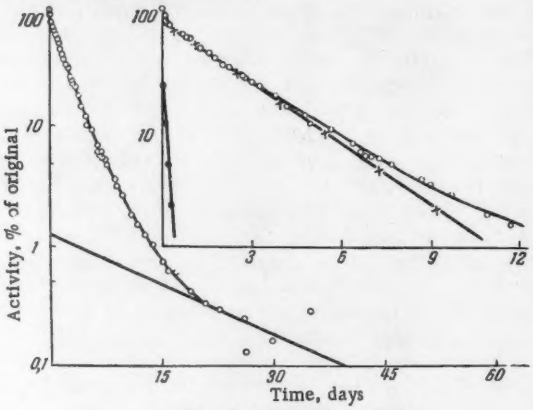

Fig. 3. Barium decay curve.

THE Au^{197} $(p,p\pi^+)$ Pt^{197} REACTION. The platinum was isolated with formic acid after preliminary precipitation of gold with SO_2 from a 40% hydrochloric acid solution. The platinum precipitate was dissolved in aqua regia and precipitated as platinum dimethylgloximatic and then as ammonium chloroplatinate. In the last operation the platinum was again precipitated with formic acid. The precipitate was fired and weighed. The chemical yield of platinum was 15%.

Analysis of the decay curve of the total platinum radiation (Fig. 4) showed the following half-lives: 8 hours and 3.9 and 10 days. The β-radiation energies were found to be 0.2 – 0.3 and 0.7 – 0.9 Mev. These data were obtained for the bombarding proton energy range of 120 – 660 Mev. This makes it possible to identify the platinum isotopes: Pt^{188} (K) with T = 10.5 days, total Pt^{191} isotopes (K) with T - 3 days, Pt^{193m} (i.c.) with T = 4.3 – 4.6 days and Pt^{195} (i.c.) with

†K – K-capture.

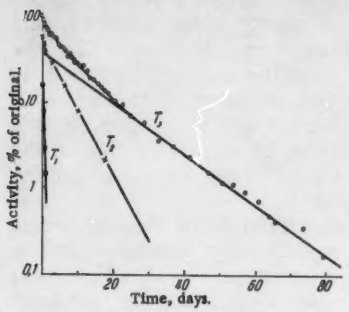

Fig. 4. Platinum Decay Curve; $T_1 = 8$ hours; $T_2 = 3.9$ days; $T_3 = 10$ days.

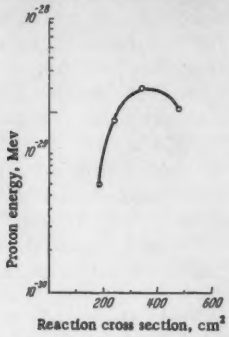

Fig. 5. Relation of the cross section of the $Cu^{65}(p,\pi^-)Ga^{66}$ reaction to proton energy.

$T = 3.5$ — 4.4 days. The energies found for the β-radiation belong to the daughter of Pt^{188}, Ir^{188} with $T = 41.5$ hours, which emits conversion electrons (with energies of 0.2 and 0.9 Mev). The half-life of eight hours probably belonged to a new platinum isotope. In any case, it could not belong to the isotope Pt^{197} with $T = 18$ hours, which must be formed by the Au^{197} $(p,p\pi^+)$ reaction. The value of the formation cross section of the isotope with $T = 8$ hours (see Table 1) is very great in comparison with the Ni formation cross section and did not increase with an increase in the energy of the bombarding particles, a phenomenon characteristic of reactions forming π^--mesons. Thus it was impossible to detect the Pt^{137} isotope and consequently, to establish the reaction of π^--mesons formation.

A Study of the $Cu^{65}(p,\pi^-)Ga^{66}$ Reaction

After proton irradiation, one gram of spectrally pure copper was dissolved with heating in a 50% solution of HNO_3. Gallium was isolated as the basic acetate. Gallium hydroxide was first precipitated with ammonia and iron hydroxide with excess NaOH (each twice), then the gallium chloride was extracted with diethyl ether, saturated with 6 *N* HCl. The basic gallium acetate precipitate was fired to Ga_2O_3 and weighed. The chemical yield of gallium was 50%.

The gallium decay curve had one component corresponding to $T = 10$ hours. The energy of the β-radiation was 3.7 Mev. These data make it possible to identify the isotope Ga^{66}.

The values of the formation cross sections of gallium at different bombarding proton energies are given in Table 2.

A considerable increase in the yield of the Ga^{66} isotope in the proton energy range 130 — 350 Mev (by a factor of about 3.5) and a certain decrease in the yield when the energy was increased up to 480 Mev was observed. Such a change in Ga^{66} yield can hardly be explained by only a secondary reaction with α-particles, $Cu^{65}(\alpha, 3n)$, as we had done previously [6,7]. The cross section of this reaction cannot increase with an increase in proton energy to the extent that we observed in our experiments. Thus, according to the data in [8], the cross section of star formation per atom of Ilford G-5 type photoemulsion with >2 rays in the star, increases only by a factor of 1.3 with an increase in proton energy from 110 — 340 Mev. The number of secondary α-particles would increase to the same extent as on the average, one α-particle is formed per fission. From this point of view, the decrease in Ga^{66} yield at a proton energy of 480 Mev is also incomprehensible.

It would be more correct to assume that when copper is bombarded with protons, Ga^{66} is formed in two ways: by the $Cu^{65}(\alpha, 3n)Ga^{66}$ reaction and the $Cu^{65}(p,\pi^-)Ga^{66}$ reaction, which are accompanied by π^--meson emission. In the latter case, the Ga^{66} yield would change very radically with an increase in proton energy. At an energy of 130 Mev, the Ga^{66} yield would be zero as the threshold of meson formation for nuclei of average atomic weight is about 200 Mev. The yield of this isotope is greatest at a proton energy of about 300 Mev and then it again decreases with an increase in proton energy. This is explained by the fact that at proton energies above 350 Mev, the emergent proton must have a high kinetic energy (~200 Mev). The probability of the formation of mesons with an energy of ~ 200 Mev, when the bombarding particles have an energy of over 350 Mev [9] is very small. In this case, the probability of reaction (p,π^-xn) increases.

The curve in Figure 5, plotted according to data in Table 2 and showing the difference in the values of the cross sections of Ga^{66} formation and of the $Cu^{65}(\alpha, 3n)$ Ga^{66} reaction, reflects a phenomenon analogous to the one described above. The cross section of the second reaction is taken to be that of Ga^{66} formation at a proton energy of 110 Mev. One may assume that the data given in Table 2 characterize the cross section of the (p,π^-) reaction on copper.

Attempt to Detect the $Cu^{65}(p,2\pi^+)Ni^{65}$ Reaction

In order detect the reaction corresponding to the double emission of π^+-mesons, we measured repeatedly the activities of nickel samples, separated by S. Sekerskii from copper, irradiated with protons

Table 2. Gallium Formation Cross Section in Relation to Proton Energy

Proton energy, Mev	Cross section, 10^{-29} cm²	
	Ga^{66}	$Cu^{65}(p,\pi^-)Ga^{66}$
130	1.3±0.15	—
190	2.0±0.2	0.6
250	3.1±0.2	1.8
350	4.4±0.25	3.1
480	3.5±0.2	2.2

Table 3

Cross Sections of Reactions Accompanied by π^--Meson Emission Under the Action of 480 and 660 Mev Protons

Type of reaction	Reactions investigated	Cross section, 10^{-30} cm²/nucl.	
		E_p=480 Mev	E_p=660 Mev
(p,π^+)	$Si^{30}(p,\pi^+)Si^{31}$	2.2	4.0
(p,π^-)	$Cu^{63}(p,\pi^-)Ga^{66}$	0.34	—
$(p,p\pi^+)$	$Cu^{65}(p,p\pi^-)Ni^{63}$	2.0	3.4
$(p,p\pi^+)$	$La^{139}(p,p\pi^+)Ba^{139}$	Not detected	
$(p,p\pi^+)$	$Au^{197}(p,p\pi^+)Pt^{197}$	»	»
$(p,2\pi^+)$	$Cu^{65}(p,2\pi^+)Ni^{66}$	»	»

of 480 and 660 Mev. The activity measurement was begun several days after target irradiation, when the Ni^{65} isotope with $T=2.5$ hours had decayed completely, and was continued for six months. The decay curves obtained contained only one component, corresponding in activity to $T=36$ hours, which belongs to Ni^{57}. The Ni^{66} activity with $T=56$ hours could not be detected.

Discussion of Results

To compare the results of this work with those in paper [2], we give Table 3, which contains the cross sections of various reactions which are accompanied by π-meson emission under the action of protons with energies of 480 and 660 Mev. Certain conclusions can be drawn from the data in the table on some of the reactions of meson formation:

1) the cross section of the (p,π^+) reaction with complex nuclei is of the order of 10^{-30} cm^2/nucl. and the emission of π^+-mesons is more probable than that of π^--mesons. The ratio $\frac{\sigma(p,\pi^+)}{\sigma(p,\pi^-)}=6.5$;

2) the $(p,p\pi^+)$ reaction is more probable than the (p,π^-) reaction, which agrees with the concepts on the nature of nuclear reactions induced by high-energy particles. Apparently, the relatively high cross section of the (p,π^+) reaction on silicon [2] may be explained by some contribution from the competing (d,p) reaction;

3) a retardation in the growth of the cross sections of the $(p,p\pi^+)$ and (p,π^+) reactions is observed with an increase in the proton energy from 480 to 660 Mev.

The $(p,2\pi^+)$ reaction could not be detected radiochemically as its cross section is considerably smaller than that of the $(p,p\pi^+)$ reaction. Also the (p,π^+) and $(p,p\pi^+)$ reactions with heavy nuclei could not be identified by this method as the number and cross section of the reactions, accompanied by neutron emission is in this case considerably higher than with light nuclei.

We should note especially that the $(p,\pi^\pm)$ reactions contradict nucleon-nucleon reactions in nuclei, (p,n) and (p,p), in which mesons and secondary high energy nucleons are formed. To explain the emission of mesons only, one must assume the existence of interaction between the incident fast proton and a nucleon complex in the nucleus, which results in the formation of high energy π-mesons, with the rest of the energy of the bombarding particle emitted as γ-quanta. Such reactions, of course, should occur with very low probability, which decreases with an increase in the energy of the bombarding particles. The results we obtained show that the cross section of the (p,π^+) reaction is a factor $3\cdot10^3$ smaller than the cross section of the $p+p\rightarrow\pi^++n$, reaction, which, according to data in [10], is $(10.9\pm1.1)\times10^{-27}$ cm^2 at a proton energy of 660 Mev*. The decrease in cross section of such a reaction with an increase in proton energy is especially noticeable, as exemplified by the $Cu^{65}(p,\pi^-)Ga^{66}$ reaction.

It was pointed out previously [11] that it was possible to explain the emission of the nuclei of light elements as the result of the exchange of mesons, arising during the collision of a bombarding particle with a nucleus, simultaneously between several nucleons. The nucleons are thus bound into one complex, possessing a high energy, and are therefore capable of leaving the nucleus. In some cases (probably very rare ones) such conditions could arise where one of the mesons formed could have a high energy, while the nucleonic fragment, on the contrary, has a low one. Then the π-meson would escape from the nucleus, leaving it in a deactivated state. Such an explanation is confirmed by the cross section of the (p,π^-) reaction being a factor of 180 smaller than the cross section of the escape of C^{11} nuclei [6, 7] from copper under the action of 480-Mev protons.

At the present time, experimental facts exist, which indicate interaction between fast particles and a nucleon complex in a nucleus [12 – 15]. However, a final theory on this phenomenon has not yet been postulated [16] and therefore, if further experiments should confirm our data on $(p,\pi^\pm)$ reactions, they could contribute to a better understanding of the nature of the reaction of fast particles with complex nuclei than could be derived from the theory of nucleon-nucleon collisions.

Received July 14, 1957

Literature

1. Si. C. Fung and A. Turkevich, Phys. Rev., 95, 176 (1954).
2. S. Sekerskii and A. K. Lavrukhina, Doklady Akad. Nauk SSSR 117, 61 (1957).
3. A. P. Vinogradov, I. P. Alimarin, V. I. Baranov, A.K. Lavrukhina, T.V. Baranova, F.I. Pavlotskaya, A.A. Bragina, and Yu. V. Yakovlev, Session of Acad. Sci. USSR on Peaceful Uses of Atomic Energy, June 1–5, 1955 (Meeting of the Div. Chem. Sci.) [in Russian]. (Moscow: Acad. Sci. USSR Press, 1955) p. 97.
4. G. Seaborg, I. Perlman, and D. Hollander, Table of Isotopes [Russian translation]. (Moscow: Foreign Lit. Press, 1956) pp. 57, 58.
5. J. Miller and G. Friedlander, Bull. Am. Phys. Soc. 28, 3, UA4 (1953).
6. A. P. Vinogradov, I. P. Alimarin, V. I. Baranov, A. K. Lavrukhina, T. V. Baranova, and F. I. Pavlotskaya, Session of Acad. Sci. USSR on Peaceful Uses of Atomic Energy, July 1–5, 1955 (Meeting of Div. Chem. Sci.) [in Russian]. (Moscow: Acad. Sci. USSR Press, 1955) p. 132.
7. A. K. Lavrukhina, Doctor's Dissertation [in Russian]. (Moscow: GEOKhI Acad. Sci. USSR, 1955).
8. G. Germain, Phys. Rev. 82, 526 (1951).
9. Annual Rev. Nuclear Sci. 1, 1 (1952).
10. B. S. Neganov and O. V. Savchenko, J. Exptl.-Theoret. Phys. (USSR) 32, 1265 (1957).
11. V. I. Veksler, Doklady Akad. Nauk SSSR 82, 865 (1952).
12. L. S. Azhgirei, I. K. Vzorov, V. P. Zrelov, M. G. Meshcheryakov, B. S. Neganov, and A. F. Shabudin, J. Exptl.-Theoret. Phys. (USSR) 33, 1185 (1957).
13. O. V. Lozhkin, J. Exptl.-Theoret. Phys. (USSR) 33, 354 (1957).
14. N. T. Porile and N. Sugarman, Phys. Rev. 107, 1422 (1957).
15. V.B. Kurchatov, V.N. Mechedov, L.V. Chistyakov, M. Ya. Kuznetsova, N. I. Berisova, and V. G. Solov'ev, J. Exptl.-Theoret. Phys. (USSR) 35, 56 (1958).
16. D. I. Blokhintsev, Uspekhi Fiz. Nauk 61, 137 (1957).

* It is also interesting to note that the bulk of the mesons formed in the latter reaction are in the high-energy section of the spectrum.

THE SCATTERING OF NEUTRONS IN PARA- AND ORTHOHYDROGEN

Ē. A. Chistova and S. I. Drozdov

The present paper contains calculations of the characteristics of neutron scattering in hydrogen, which are of importance for calculating the slow-neutron spectrum in a moderating medium. The total cross section, the mean asymmetry of the scattering, and the mean energy loss per collision are found for the gas of para- and orthohydrogen functions of the neutron energy and the temperature of the moderating medium. The results are presented in the form of formulas and of curves obtained with the electronic computer of the Computing Center of the Academy of Sciences of the USSR. The treatment given is for the range of energies above the temperature of the gas, for which one can neglect the thermal motion of the molecules. Account is taken of the rotational levels and the zero-point vibrations of the nuclei in the molecule.

1. Statement of the Problem

It is well known that the slowing down of neutrons of energy much higher than the binding energy of the atoms of the medium is well described by the simplest model of the collisions of elastic spheres. In this case such characteristics of the process as the average energy loss in one collision and the average asymmetry of the scattering do not depend on the energy of the neutron and the temperature of the moderating medium. When, however, the neutron energy becomes comparable with the binding energy of the atoms, the properties of the binding begin to play an important part in the slowing-down process. In this case the characteristics mentioned above are in general functions both of the energy and also of the temperature. An attempt is made in the present paper to calculate as functions of the neutron energy and the temperature the total cross section and the mean asymmetry of the scattering, and also the mean energy loss per collision, for the simplest medium: a gas of para- and orthohydrogen.

2. The Fundamental Relations

The problem reduces to the calculation of average values. The averaging in question is carried out in several stages. First, in calculating the energy loss and the asymmetry of the scattering one finds the mathematical expectations of these quantities by using the quantum-mechanical distribution that characterizes the process of scattering of a neutron by the H_2 molecule. This distribution consists of the differential cross section for elastic or inelastic scattering [1]. Second, the quantities in question are averaged over the Maxwell and Boltzmann statistical distributions for the translational and internal degrees of freedom for the state of the molecule before the scattering. For example, according to reference [2] one can represent the averaging of the scattering cross section over the Maxwell distribution in the form

$$\sigma(E,\theta)=\frac{2}{\sqrt{\pi}}\frac{\exp(-x_0^2)}{x_0^2}\times \\ \times\int_0^\infty \sigma\left(\frac{\theta x^2}{A}\right)x^2\exp(-x^2)\,\mathrm{sh}(2xx_0)\,dx, \qquad (1)$$

where E is the energy of the neutron; θ is the temperature of the medium; A is the ratio of the mass of the molecule to that of the neutron; $x_0^2=\frac{AE}{\theta}$. The function $\sigma(E')$ to be averaged depends on the energy of the neutron in the laboratory coordinate system, $E'=\frac{\theta x^2}{A}$.

Assuming that $\sigma\left(\frac{\theta x^2}{A}\right)$ varies more slowly than the exponential function in Eq. (1), one can show without difficulty by calculating the integral (1) by the method of steepest descent that for

$$x_0^2=\frac{AE}{\theta}\gg 1 \qquad (2)$$

the quantity $\sigma(E,\theta)\approx\sigma\left(\frac{\theta x_0^2}{A}\right)=\sigma(E)$ does not depend on the temperature θ, i. e., in this case the averaging operation (1) is unnecessary. Hereafter we shall neglect the thermal motion of the molecules, assuming that the condition (2) is satisfied.

Let us go on to the averaging over the scattering cross section. In being slowed down the neutron loses part of its energy in the excitation of vibrational and rotational levels of the molecule [1]:

$$\varepsilon_{nl}=\frac{\hbar^2}{mR^2}l(l+1)+n\hbar\omega;\quad \frac{\hbar^2}{mR^2}=0{,}00736\ \text{ev} \\ \hbar\omega=0{,}546\ \text{ev} \\ n,\ l=0,1\ldots, \qquad (3)$$

where m is the mass of the proton and R is the equilibrium distance between the nuclei. We confine ourselves to the range of energies below the threshold of excitation of the first vibrational level, so that the energy of the neutron in the laboratory system is $E<\frac{3}{2}\hbar\omega$. In this case the vibrational levels are not excited, but the zero-point vibrations of the nuclei in the molecule can have an important effect. According to reference [3], the total cross section for elastic or inelastic scattering of a neutron by a H_2 molecule, with the molecule changing its rotational energy ($l'\to l$), but staying in the lowest vibrational state ($n=0$), has the form

$$\sigma_{l'l}(E)=\frac{\pi 2^5}{9}\frac{2l+1}{(k_0R)^2}c_{s's} \\ \times\sum_{L=|l'-l|}^{l'+l}(C^{L0}_{l'0l0})^2\,I_{1L}(k_{l'l}); \qquad (4)$$

$$I_{mL}(k_{l'l})=\int_{\frac{1}{2}R|k_0-k_{l'l}|}^{\frac{1}{2}R(k_0+k_{l'l})}x^m j_L^2(x)\,e^{-dx^2}\,dx, \qquad (5)$$

where the Clebsch-Gordan coefficients are given by

$$(C^{L0}_{l'0l0})^2=(2L+1)\left(\frac{g!}{(g-l')!\,(g-l)!\,(g-L)}\right)^2 \\ \times\frac{(l'+l-L)!\,(l+L-l')!\,(l'+L-l)!}{(l'+l+L+1)!},$$

if $l'+l+L=2g$ is even, and $C^{L0}_{l'0l0}=0$ if $l'+l+L$ is odd; $j_L(x)=\sqrt{\frac{\pi}{2x}}\cdot J_{L+\frac{1}{2}}(x)$ – is the spherical Bessel function; and the coefficient $\alpha=\frac{\hbar^2}{mR^2}\cdot\frac{1}{\hbar\omega}=1.35\cdot10^{-2}$ allows for the existence of the zero-point vibrations. For $\alpha=0$ ($\hbar\omega\to\infty$) Eqs. (4) and (5) describe the scattering by a rigid molecule that has only rotational levels [4]. The quantities k_0, $k_{l'l}$ are the wave numbers of the incident and scattered neutrons, and according to Eq. (3)

$$k_0R=11\sqrt{E};$$
$$k_{l'l}R=11\sqrt{E+0{,}011\,[l'(l'+1)-l(l+1)]},$$

where E is the energy of the incident neutron in the laboratory reference system, in electron volts. The coefficients $c_{s's}$, which depend on the spins of the molecule before and after the scattering (s' and s, respectively are given in terms of the amplitudes of the n, p scattering in the triplet and singlet states (a_1 and a_0) respectively) by well-known formulas [4]:

$$c_{s's}=(3a_1+a_0)^2+s(s+1)(a_1-a_0)^2;\ s'=s;$$
$$c_{s's}=(3-2s')(a_1-a_0)^2;\ s'\neq s; \qquad (6)$$
$$a_1=-0{,}52\cdot10^{-12}\ \text{см};\ a_0=2{,}34\cdot10^{-12}\ \text{см}.$$

Since s', $s=0$ or 1, we get from this the results, in barns:

$$c_{00}=0{,}60;\ c_{01}=24{,}60;\ c_{10}=8{,}20;\ c_{11}=17{,}00. \qquad (6)$$

For given l', l the values of s' and s are chosen in accordance with the Pauli principle from the condition that the parities of the numbers l' and s', l' and s must be the same respectively.

The average value of the cosine of the scattering angle in the center-of-mass system, i. e., the mean asymmetry in the scattering, with transition of the molecule from one rotational state to another ($l'\to l$) is defined by the expression

$$\mu_{l'l}(E)=\frac{\int\cos\vartheta\cdot\sigma_{l'l}(E,\vartheta)\,d\Omega}{\sigma_{l'l}(E)}. \qquad (7)$$

Substituting here the known expression for the differential scattering cross section in the center-of-mass system, $\sigma_{l'l}(E,\vartheta)$ [3], one gets without difficulty the following formula:

$$\mu_{l'l}(E)=\frac{k_0^2+k_{l'l}^2}{2k_0k_{l'l}}-\frac{2}{R^2k_0k_{l'l}}\cdot\frac{\sum_L(C^{L0}_{l'0l0})^2I_{3L}(k_{l'l})}{\sum_L(C^{L0}_{l'0l0})^2I_{1L}(k_{l'l})}, \qquad (8)$$

where the quantities $I_{mL}(k_{l'l})$, $m=1.3$ are defined by the integral (5). Using Eqs. (7) and (5), it is not hard to show that near the threshold of inelastic scattering, where $k_{l'l}\to0$,

$$\lim_{k_{l'l}\to0}\mu_{l'l}(E)=0. \qquad (9)$$

This result corresponds to the fact that in the center-of-mass system inelastic scattering near threshold occurs isotropically. The mean asymmetry of the scattering by a molecule that before the scattering was in the state l is obviously characterized by the function

$$\mu_{l'}(E)=\frac{\sum_l\sigma_{l'l}(E)\mu_{l'l}(E)}{\sum_l\sigma_{l'l}(E)}. \qquad (10)$$

Finally, the mean asymmetry of the scattering in H_2 gas at temperature Θ, for cases in which the condition (2) holds, is obtained by averaging the quantity $\mu_{l'}(E)$ over the Boltzmann distribution [5]:

$$\mu(E,\Theta)=\frac{\sum_{l=0,2,\ldots}\mu_l(E)(2l+1)\exp-\frac{\varepsilon_l}{\Theta}+3\sum_{l=1,3,\ldots}(2l+1)\mu_l(E)\exp-\frac{\varepsilon_l}{\Theta}}{\sum_{l=0,2\ldots}(2l+1)\exp-\frac{\varepsilon_l}{\Theta}+3\sum_{l=1,3\ldots}(2l+1)\exp-\frac{\varepsilon_l}{\Theta}}, \qquad (11)$$

where $\varepsilon_l=\varepsilon_{0l}$ [Eq. (3)]. The temperature of the gas is assumed so low that we can neglect the thermal excitation of the vibrational levels of the molecule.

In analogy with Eq. (11) one calculates the statistical average $\sigma(E,\Theta)$ of the total scattering cross section

$$\sigma_{l'}(E)=\sum_l\sigma_{l'l}(E).$$

Let us turn now to the calculation of the mean energy loss per collision. If the scattering in the center-of-mass system is through an angle ϑ and the energy of the molecule changes by the amount $\Delta\varepsilon_{l'l}=\varepsilon_l-\varepsilon_{l'}$ ($l'\to l$), then, using the laws of conservation of momentum and energy, we can get the following expression for the fractional energy loss in the laboratory coordinate system:

$$\frac{\Delta E_{l'l}}{E}=\frac{2A}{(A+1)^2}(1+\Delta_{l'l}(E,\vartheta));\ \Delta_{l'l}(E,\vartheta)=$$
$$\frac{A+1}{2}\cdot\frac{\Delta\varepsilon_{l'l}}{E}-\left(1-\frac{A+1}{A}\frac{\Delta\varepsilon_{l'l}}{E}\right)^{1/2}\cos\vartheta. \qquad (12)$$

Calculating the mathematical expectation of this quantity by the use of the differential scattering cross section $\sigma_{l'l}(E,\vartheta)$, we find the mean energy loss in scattering by a molecule in the state l' ($A=2$

$$\frac{\Delta E_{l'}}{E}=\frac{4}{9}(1+\Delta_{l'}(E));$$

$$\Delta_{l'}(E)=\frac{\sum_l\left[\frac{3}{2}\frac{\Delta\varepsilon_{l'l}}{E}\sigma_{\ l}(E)-\left(1-\frac{3}{2}\frac{\Delta\varepsilon_{l'l}}{E}\right)^{1/2}\sigma_{l'l}(E)\mu_{l'l}(E)\right]}{\sum_l\sigma_{l'l}(E)}. \qquad (13)$$

Finally, the mean fractional energy loss per collision in the gas at temperature Θ is

$$\overline{\frac{\Delta E}{E}}(E,\Theta)=\frac{4}{9}(1+\Delta(E,\Theta)), \qquad (14)$$

where the function $\Delta(E,\Theta)$ is obtained by averaging the quantities $\Delta_{l'}(E)$ [Eq. (13)] over the Boltzmann distribution of Eq. (11).

3. Asymptotic Formulas

Let us consider the scattering of neutrons by a diatomic molecule at relatively high energy, for which the wavelength is small in comparison with the dimensions of the molecule. We shall neglect spin and assume that the molecule is a rigid rotator possessing only rotational levels. Under the condition $k_0R\gg1$ the differential scattering cross section does not depend on the initial state of the molecule and can be put in the form [6]

$$\sigma(\mathcal{E},\vartheta)=\int_{-E}^{0}\sigma(\mathcal{E},z,\vartheta)\,dz; \qquad (15)$$
$$\sigma(\mathcal{E},\ ,\vartheta)=\left(\frac{\mu}{m}\right)^2\sum_\nu\alpha_\nu^2\frac{k}{k_0}\int_0^1\delta\left(\varepsilon+\frac{(\hbar q)^2}{2M}(1-x^2)\right)dx.$$

Here $\mathcal{E}=\frac{A}{A+1}E-$ is the total energy in the reference system of the common center of mass; $\mu=\frac{mA}{A+1}-$ is the reduced mass for the nuclei and molecule; $M-$ $\varepsilon=\frac{\hbar^2}{2\mu}(k^2-k_0^2)$; and $\vec{q}=\vec{k}-\vec{k}_0$; $a_\nu=\frac{A_\nu+1}{A_\nu}a_\nu$, where $a_\nu-$ is the amplitude for scattering of a neutron by a free nucleus of atomic weight A_ν. The function $\sigma(\mathcal{E},\varepsilon,\vartheta)$ gives the distribution of the scattered neutrons in energy and angle.

We find the energy spectrum of the neutrons scattered in different directions by integrating the expression (15) over all angles (in doing this one must make the change of variables $d\Omega=\frac{\pi\,dq^2}{kk_0}$). We confine ourselves to the case of light molecules, for which we have the condition $\left|\frac{\mu-M}{\mu+M}\right|^2\ll 1$ (scattering for the case $\frac{\mu}{M}\ll 1$ is considered in reference 7). Then

$$\sigma(\mathcal{E},\varepsilon)=\frac{M}{\mu}\left(\frac{\mu}{m}\right)^2\frac{1}{2\mathcal{E}}\ln\left[\frac{1+x(z)}{1-x(z)}\right]\cdot\sum_\nu\pi a_\nu^2;$$

$$x(z)=\frac{\left(1+\frac{M}{\mu}\right)z+1+\sqrt{1+2z}}{z+1\sqrt{1+2z}};\quad z=\frac{\varepsilon}{2\mathcal{E}},$$

and for $z\ll 1$ (16)

$$\sigma(\mathcal{E},\varepsilon)\approx\frac{M}{\mu}\left(\frac{\mu}{m}\right)^2\frac{1}{2\mathcal{E}}\left[\frac{Mz}{8\mu}+\ln\left(-\frac{8\mu}{Mz}\right)\right]\sum_\nu\pi a_\nu^2.$$

To find an asymptotic expression for the elastic scattering cross section it is convenient to use Eqs. (4) and (5), setting $k_0R\gg 1$ and $l'=l=0$. For H_2 molecules with spin effects included we have

$$\sigma_{00}(\mathcal{E})=\frac{\pi 2^4}{9}\frac{c_{00}}{(k_0R)^2}\ln(2\gamma k_0R);\quad \ln\gamma=0{,}577\ldots. \tag{17}$$

Thus the cross sections for the individual processes of elastic and inelastic scattering fall off essentially in inverse proportion to the energy of the incident neutron. Integrating the function $\sigma(\mathcal{E},\varepsilon)$ with respect to ε, we easily see that the total cross section for scattering by the rotator does not depend on the energy

$$\sigma=\sum_\nu\pi a_\nu^2\cdot\frac{M}{\mu}\left(\frac{\mu}{m}\right)^2\int_{-\frac{1}{2}}^{0}\ln\frac{1+x(z)}{1-x(z)}\,dz. \tag{18}$$

Since it is assumed that the nuclei in the molecule are rigidly bound, the cross section so obtained does not in general agree with the cross section for scattering by the free nuclei, $\sigma_f=4\pi\sum_\nu a_\nu^2$. In fact, for the H_2 molecule the calculation by Eq. (18) gives $\sigma=\frac{4}{9}\sigma_f$. In the case of scattering by a rotator with large reduced mass the two cross sections are approximately equal, since $\sigma\approx\sigma_f\left(1-\frac{4\mu}{3M}\right)$ for $\frac{\mu}{M}\ll 1$ [6].

The asymmetry of the scattering with the molecule going into an excited state of energy $|\varepsilon|$, and the mean asymmetry, are given by the respective expressions

$$\mu(\mathcal{E},\varepsilon)=\frac{\int\cos\vartheta\cdot\sigma(\mathcal{E},\varepsilon,\vartheta)\,d\Omega}{\sigma(\mathcal{E},\varepsilon)};$$

$$\bar{\mu}=\frac{\int_{-\mathcal{E}}^{0}\int\cos\vartheta\cdot\sigma(\mathcal{E},\varepsilon,\vartheta)\,d\varepsilon\,d\Omega}{\sigma}.$$

Using Eqs. (15) and (16), we get from this the following relation

$$\mu(\mathcal{E},\varepsilon)=\frac{1+z}{\sqrt{1+2z}}+\frac{M}{\mu}\frac{z}{\sqrt{1+2z}}\left[\frac{1}{2}+\frac{x(z)}{(1-x^2(z))\ln\frac{1+x(z)}{1-x(z)}}\right],$$

and for $z=\frac{\varepsilon}{2\mathcal{E}}\ll 1$

$$\mu(\mathcal{E},\varepsilon)\approx 1+\frac{Mz}{2\mu}-\frac{2}{\ln\left(-\frac{8\mu}{Mz}\right)}\times$$

$$\times\left[1-z\left(1-\frac{M}{4\mu}+\frac{M}{8\mu}\frac{1}{\ln\left(-\frac{8\mu}{Mz}\right)}\right)\right]. \tag{19}$$

The asymmetry of the elastic scattering ($\varepsilon=0$) can be calculated conveniently by direct use of Eqs. (5) and (8), if we set $k_0R\gg 1$ and $l'=l=0$. For the H_2 molecule we have

$$\mu_{00}(\mathcal{E})=1-\frac{1}{\ln(2\gamma k_0R)}. \tag{20}$$

The mean asymmetry of the scattering, like the total cross section σ, does not depend on the energy:

$$\bar{\mu}=\frac{\int_{-\frac{1}{2}}^{0}\left[\frac{1+z}{\sqrt{1+2z}}\int_0^{x(z)}\frac{dx}{1-x^2}+\frac{M}{\mu}\frac{z}{\sqrt{1+2z}}\times\int_0^{x(z)}\frac{dx}{(1-x^2)^2}\right]dz}{\int_{-\frac{1}{2}}^{0}dz\int_0^{x(z)}\frac{dx}{1-x^2}}. \tag{21}$$

Thus, unlike the s-scattering of neutrons by free nuclei, the scattering by the rotator involves a transfer of angular momentum by the neutron, and therefore in general the mean asymmetry of the scattering is different from zero.

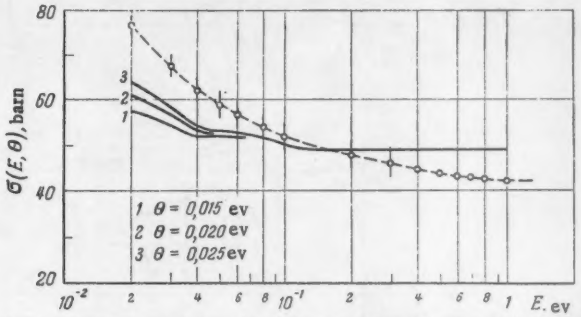

Fig. 2. Total cross section $\sigma(E,\theta)$ for scattering of neutrons in H_2 gas at temperatures $\theta\neq 0$. The vibrations of the nuclei are not taken into account. The dashed curve shows experimental values of the total cross section [7] for $\theta=0{,}025$ ev. (The case $\theta=0$, for which $\sigma(E,0)=\sigma_0(E)$, is shown in Fig. 1 (1).) The smaller theoretical value of the total cross section as compared with the experimental value at low energies ($E<0.1$ ev) is explained by the neglect of the thermal motion of the molecules. For $E>0.1$ ev the total cross section $\sigma(E,\theta)$ ceases to depend on E and θ and agrees with the cross section $\sigma_{ll'}(E)$ (Fig. 1), since in this case the latter does not depend on E and l'. The deviation from the experimental values in this range of energies is explained by the use of the rigid-rotator model.

The formulas (19) and (20) show that with increase of the energy E the asymmetry of the elastic and inelastic scattering approaches unity rather slowly (logarithmically), i. e., at high energies the elastic or inelastic scattering is mainly forward. But before the quantities $\mu(\mathcal{E},\varepsilon)$ and $\mu_{00}(\mathcal{E})$ reach their limiting values the cross sections $\sigma(\mathcal{E},\varepsilon)$ and $\sigma_{00}(\mathcal{E})$ of the corresponding quantities become very small, since they fall off in inverse proportion to the energy. Therefore the mean asymmetry $\bar{\mu}$ is considerably smaller than unity.

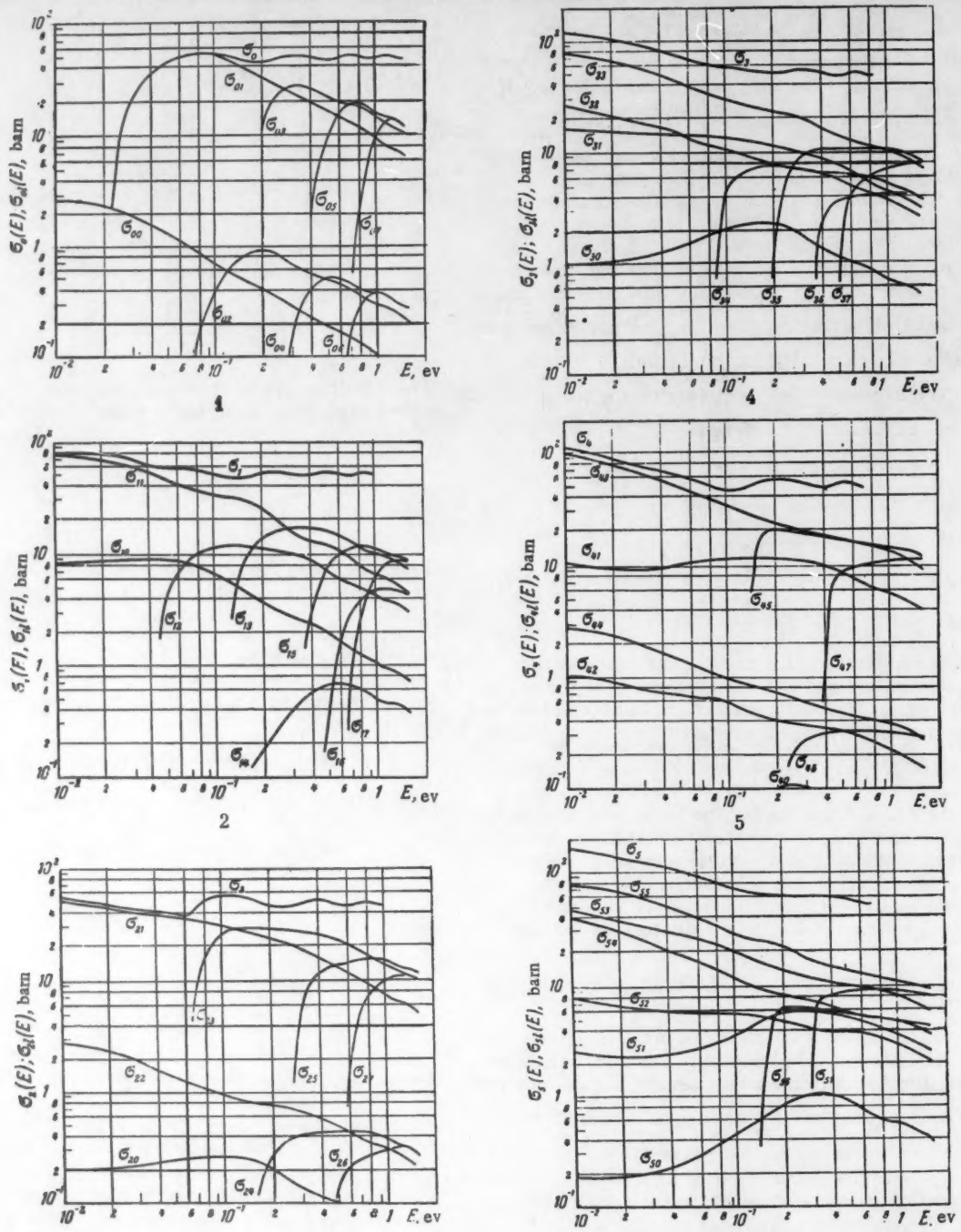

Fig. 1. Cross sections $\sigma_{l'l}$ for elastic and inelastic scattering by a H_2 molecule, and total cross section $\sigma_{l'} = \sum_l \sigma_{l'l}$, as functions of the neutron energy in the laboratory coordinate system, for $l' \leq 5$ and $l \leq l'$. The vibrations of the nuclei in the molecule are not taken into account. In agreement with the asymptotic formulas (1), (14)—(16) the cross sections of the individual processes fall off rapidly with increasing energy, and the total cross sections approach a constant limit that does not depend on E, l'. The limiting value of the total cross section (49 barns) corresponds to the scattering by a rigid rotator and is fairly close to the cross section for scattering by free protons (41 barns).

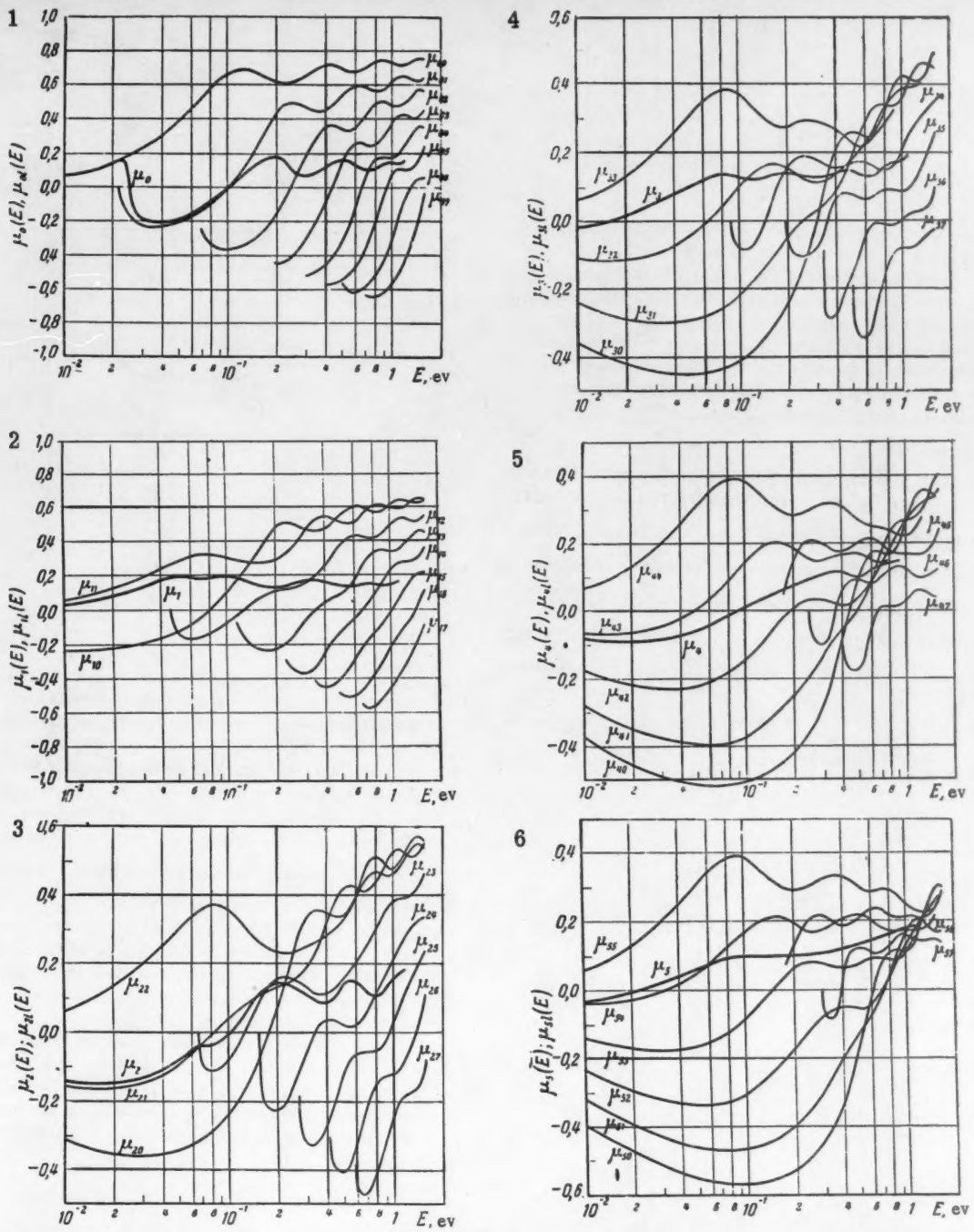

Fig. 3. Asymmetry $\mu_{l'l}$ of the elastic and inelastic scattering of neutrons by a H_2 molecule, and mean asymmetry $\mu_{l'}$, as functions of the neutron energy E in the laboratory coordinate system, for $l' \leqslant 5$ and $l \leqslant 7$. The vibrations of the nuclei are not taken into account. The asymmetry is positive for the elastic scattering ($l'=l$), since in this case forward scattering predominates. At low energies ($E < 0.1$ ev) the asymmetry of the inelastic scattering is negative, which corresponds to backward scattering. Near the threshold of inelastic scattering ($l'<l$) the asymmetry goes to zero, in accordance with Eqs. (1) and (7) the scattering is isotropic. With an increase of the energy the asymmetry of the inelastic scattering becomes positive, since in this case the fractional change in the neutron's energy is smaller and the process becomes nearly elastic in its character. At sufficiently high energies the asymmetry of the elastic and inelastic scattering slowly increases, in agreement with the asymptotic formulas (17) and (18). The mean asymmetry $\mu_{l'}$ of the scattering is small in comparison with the asymmetries $\mu_{l'l}$ of the individual processes. With increase of the energy, as predicted by the asymptotic formula (19), $\mu_{l'}(E)$ practically ceases to depend on E, and l', and does not go to zero. Since, however, in the scattering of a neutron of sufficiently high energy the nuclei in an actual molecule can be regarded as free, actually the asymmetry $\mu_{l'}$ of the scattering must become equal to zero. Thus the rigid-rotator model leads to an incorrect limiting value of $\mu_{l'}$.

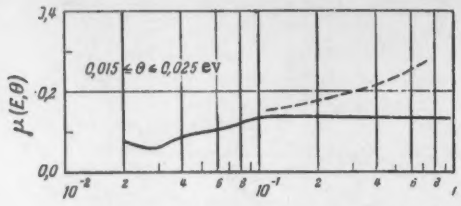

Fig. 4. Mean asymmetry $\mu(E, \Theta)$ of the scattering of neutrons in H_2 gas at temperature $\Theta \neq 0$. (The case $\Theta=0$, for which $\mu(E, 0)=\mu_0(E)$, is shown in Fig. 3 (1).) The dashed curve is obtained by including effects of the zero-point vibrations of the nuclei in the molecule ($\Theta=0.025$ ev). The mean asymmetry is small and depends only weakly on the temperature. Near the threshold for excitation of the first vibrational level (0.82 ev) the zero-point vibrations of the nuclei appreciably increase the asymmetry of the scattering.

In fact, for the H_2 molecule we have approximately, from Eq. (21), $\bar{\mu} \approx 0{,}3$, and with increase of the ratio $\frac{M}{\mu}$ the asymmetry of the scattering decreases. A heavy molecule scatters neutrons practically isotropically, since according to reference [6] $\mu \approx \frac{4}{9}\frac{\mu}{M}$ for $\frac{\mu}{M} \ll 1$.

The mean energy loss $\frac{\Delta E}{E}(\mathcal{E}, \varepsilon)$ in a collision in which the molecule goes into a state with energy $|\varepsilon|$, is given by the formula

$$\frac{\Delta E}{E}(\mathcal{E}, \varepsilon) = \frac{1}{\sigma(E, \varepsilon)} \int \frac{\Delta E}{E}(\mathcal{E}, \varepsilon, \vartheta)\, \sigma(\mathcal{E}, \varepsilon, \vartheta)\, d\Omega,$$

where in accordance with Eq. (12)

$$\frac{\Delta E}{E}(\mathcal{E}, \varepsilon, \vartheta) = -\frac{2}{A}\left(\frac{\mu}{m}\right)^2 \left[1 + Az - \cos\vartheta \sqrt{1+2z}\right].$$

From this, using Eqs. (15) and (16) we find

$$\frac{\Delta E}{E}(\mathcal{E}, \varepsilon) = -\frac{2}{A}\left(\frac{\mu}{m}\right)^2 z \times \left[1 + A + \frac{M}{2\mu} + \frac{M}{\mu}\frac{x(z)}{(1-x^2(z))\ln\frac{1+x(z)}{1-x(z)}}\right],$$

and for $z = \frac{\varepsilon}{2\mathcal{E}} \ll 1$

$$\frac{\Delta E}{E}(\mathcal{E}, \varepsilon) \approx -\frac{2}{A}\left(\frac{\mu}{m}\right)^2 \left\{z\left(1 + A + \frac{M}{2\mu}\right) - \frac{2}{\ln\left(-\frac{8\mu}{Mz}\right)}\left[1 + z\frac{M}{4\mu}\left(1 - \frac{1}{2\ln\left(-\frac{8\mu}{Mz}\right)}\right)\right]\right\}. \quad (22)$$

From these formulas it follows that the energy loss is positive, and for a fixed neutron energy E it increases slowly with increase of the excitation energy of the molecule. On the other hand, with increase of the neutron energy the fractional energy loss associated with the excitation of a definite molecular level approaches zero logarithmically. The mean fractional energy loss, averaged over the various final states of the molecule, does not depend on the energy E:

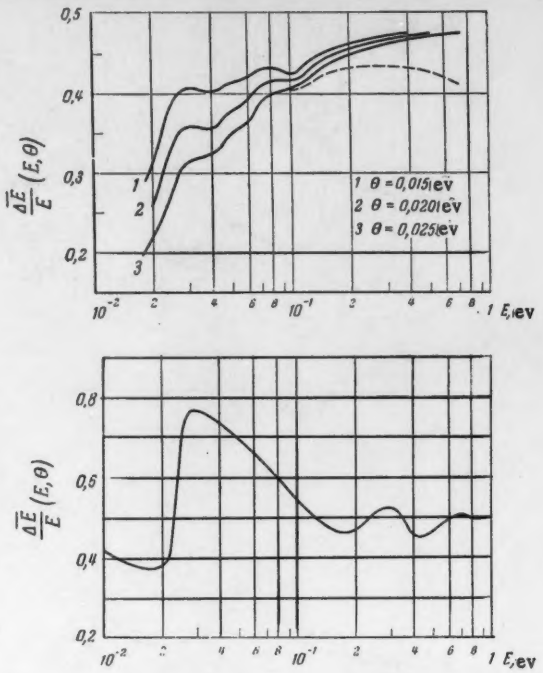

Fig. 5. Mean fractional energy loss $\frac{\overline{\Delta E}}{E}(E, \Theta)$ of a neutron per collison in H_2 gas at temperature $\Theta \neq 0$ (1) and $\Theta=0$ (2) (energy loss defined in laboratory coordinate system). The dashed curve is obtained by taking into account the zero-point vibrations of the nuclei in the molecule ($\Theta = 0.025$ ev). Near the threshold for excitation of the first rotational level (0.222 ev) there is a decided increase in the energy loss. If we neglect the vibrations of the nuclei, then at energies $E > 0.1$ ev, corresponding to the excitation of many levels, the quantity $\frac{\overline{\Delta E}}{E}$ increases monotonically with the energy ($\Theta \neq 0$), and in accordance with Eq. (23) approaches the constant value $\frac{\overline{\Delta E}}{E} = \frac{1}{2}$, which agrees with the energy loss in a collision with a free proton. If we take the zero-point vibrations of the nuclei into account, the energy loss near the threshold for the excitation of the first vibrational level (0.82 ev) is reduced by 10 to 15 percent. This effect is due to the fact, which can be seen from Eqs. (4) and (5), that the zero-point vibrations reduce the cross sections for excitation of the rotational levels, and thus reduce the energy losses. With increase of the temperature the mean loss decreases, since there is an increase in the part played by molecules in excited states; in collision with such molecules the neutron may gain as well as lose energy.

$$\frac{\overline{\Delta E}}{E} = -\frac{2}{A}\left(\frac{\mu}{m}\right)^2 \int_{-\frac{1}{2}}^{0} \left[(1+A)\int_0^{x(z)} \frac{dx}{1-x^2} + \frac{M}{\mu}\int_0^{x(z)} \frac{dx}{(1-x^2)^2}\right] z\, dz \Big/ \int_{-\frac{1}{2}}^{0} dz \int_0^{x(z)} \frac{dx}{1-x^2}. \quad (23)$$

From this formula we have for the H_2 molecule approximately $\frac{\overline{\Delta E}}{E} \approx 0{,}5$, which agrees with the value of the fractional energy loss in collisions of neutrons with free protons.

4. Results of the Calculations

The formulas given in Section 2 were used by E. A. Chistova to calculate with the machine at the Computing Center of the Academy of Sciences of the USSR the cross sections $\sigma_{ll'}(E)$, $\sigma_{l'}(E)$, $\sigma(E, \Theta)$ and the scattering asymmetries $\mu_{ll'}(E)$, $\mu_{l'}(E)$, $\mu(E, \Theta)$, and also the fractional energy loss per collision $\frac{\overline{\Delta E}}{E}(E, \Theta)$ as functions of the neutron energy E in the laboratory coordinate system and the temperature T of the gas, for the range of energies 0.01 ev $< E <$ 1 ev and the temperatures $\Theta = 0, 0.015$, 0.020, and 0.025 ev. For these values of the energy and temperature one could take as the initial and final states of the H_2 molecule the rotational levels with $l \leqslant 5$ and $l \leqslant 7$, respectively. The main body of the calculations was made without taking into account the vibrations of the nuclei in the molecule; this is justified only for $E \ll \hbar\omega$, i. e., in our case say for $E \leqslant 0.1$ ev. Therefore the zero-point vibrations were taken into account in the calculations of $\frac{\Delta E}{E}(E, \Theta)$ and $\mu(E, \Theta)$ in the range 0.1 ev $< E <$ 1 ev.

The results of the calculations are shown in Figs. 1–5. They show in particular that the mean energy loss and the total scattering cross section reach their limiting values, corresponding to the scattering by free nuclei, already at neutron energies comparable with the energies of the first rotational levels of the molecule.

Received September 4, 1958.

Literature

1. A.M.L. Messiah, Phys. Rev. 84, No. 2, 204 (1951).
2. M. Hamermesh, J. Schwinger, Phys. Rev. 69, 5, 145 (1946).
3. S.I. Drozdov, J. Atomic Energy 1, No. 3, 50 (1956)
4. J. Schwinger, E. Teller, Phys. Rev. 52, No. 4, 286 (1937).
5. L. Landau and E. Lifshits, Statistical Physics [in Russian], (Gostekhizdat, 1951).
6. A.C. Zemach, R.J. Glauber, Phys. Rev. 101, No. 7, 118 (1956).
7. E. Melkonian, Phys. Rev. 76, No. 12, 1750 (1949).

PERTURBATION THEORY FORMULAS FOR THE EFFECT OF THE DIMENSIONS ON THE CRITICAL MASS IN A FAST REACTOR

S. B. Shikhov

This paper deals with a method for calculating the critical mass of a reactor provided with a sufficiently thick reflector as a function of the composition of the core and its dimensions.

The working formula is obtained by an application of the theory of similarity to the usual first-approximation scheme of perturbation theory. For the calculation of the coefficients of the formula it is necessary to have the spatial and energy spectra of the neutron fluxes and values calculated numerically for some fixed volume of the reactor with a sufficiently thick reflector. By means of the coefficients so obtained for the formula it is possible to predict the critical mass over a wide range of variation of the dimensions of the core (over a change by about a factor two).

If the size of the core goes beyond the limits of the interval thus accessible, one has to calculate the coefficients for a new range of the dimensions, and this requires a new numerical computation of the spectra.

In this paper we give a formula containing coefficients calculated for a certain typical spectrum of a fast reactor for a number of isotopes contained in the core. The formula is checked by a nine-group calculation for volumes of the core ranging from 200 to 1000 cubic decimeters. The constants for the nine-group calculation were obtained from Soviet and foreign material published up to 1955.

Introduction

The calculation of the critical mass of a fast reactor involves cumbersome computations, even in relatively simple cases in which the reactor consists only of the core and a single-layer reflector. The calculation involves the determination of the spatial distribution of the neutrons of the fission spectrum, as softened by the effects of inelastic and elastic scattering by the heavy nuclei contained in the core and the screen.

If the dimensions of the reactor exceed several mean free paths of the fast neutrons, the calculation reduces to the solution of a system of multigroup diffusion equations with boundary conditions. In the case of design calculations for a small reactor one has to solve a multigroup system of gas-kinetic equations with the corresponding boundary conditions.

The calculations are complicated by the presence of inelastic transitions from each energy group into all the lower groups, and by the necessity of applying iteration methods for the determination of the k_{eff} of the system. The critical charge is determined by "sending" k_{eff} to unity. All of these computations can be carried out only by numerical methods by the use of high-speed computing machines. Under such conditions it is extremely useful to possess a formula providing a sufficiently reliable estimate of the critical charge without the solution of spatial-energetic boundary-value problems.

Theory

In its general form, useful for the computation of any reactor, the formula can be derived from the exact satationary gas-kinetic equation for the balance of additions and removals from the number of neutrons possessing lethargy U and having their velocities directed along the unit vector $\vec{\Omega}$:*

$$0 = -\vec{\Omega}\nabla\varphi(\vec{r}, u, \vec{\Omega}) - \Sigma(\vec{r}, u)\varphi(\vec{r}, u, \vec{\Omega}) + \int\int_{-\infty}^{u} \varphi(\vec{r}, u', \vec{\Omega}')\, du'\, d\Omega'\, \Sigma_{si}(\vec{r}, u', U, \mu_0) + \frac{\chi(u)}{4\pi}\cdot\frac{Q(\vec{r})}{k_{\text{eff}}}. \quad (1)$$

*Cf. e. g., reference 1, pp. 280, 281.

Here the notations are those adopted in [4], and

$$\Sigma_{si}(\vec{r}, u', U, \mu_0) = \Sigma_s(\vec{r}, u', U, \mu_0) + \Sigma_{\phi}(\vec{r}, u', U, \mu_0)$$

is the macroscopic differential cross section for elastic and inelastic scattering with transition of a neutron from the state $(u', \vec{n}')$ into the state $(u, \vec{n})$, and $U = u - u'$ characterizes the change of the lethargy in the transition.

In accordance with the definition of the total cross section in terms of the differential cross section we have

$$\int_0^{\infty}\int \Sigma_{si}(\vec{r}, u', U, \mu_0)\, dU\, d\Omega = \Sigma_{si}(\vec{r}, u') = \Sigma_s(\vec{r}, u') + \Sigma_i(\vec{r}, u').$$

The quantity

$$Q(\vec{r}) = \int\int_{-\infty}^{\infty} \nu_f(\vec{r}, u)\Sigma_f(\vec{r}, u)\varphi(\vec{r}, u, \vec{n})\, du\, d\Omega \quad (2)$$

gives the total number of fission neutrons produced in 1 cm^3 in 1 sec at the point with the coordinates $\vec{r}$.

The quantity $\chi(u)$ gives the spectrum of the fission neutrons normalized to unit lethargy range; for simplicity it is assumed that the angular distribution of the fission neutrons is isotropic and that the energy spectrum of the neutrons does not depend on the energy of the incident neutron.

It is convenient to write Eq. 1 in the abbreviated form

$$\hat{L}\varphi = \hat{\omega}\varphi - \Sigma_i\varphi + \frac{\chi(u)}{4\pi}\cdot\frac{Q(\vec{r})}{k_{\text{эфф}}} = 0, \quad (1')$$

where the linear integro-differential operator $\hat{\omega}$ is defined by the expression

$$\hat{\omega}\varphi = -\vec{\Omega}\nabla\psi(\vec{r}, u, \vec{\Omega}) + \int\int_{-\infty}^{u} \varphi(\vec{r}, u', \vec{\Omega}')\, du'\, d\Omega' \cdot \Sigma_{si}(\vec{r}, u', U, \mu_0).$$

The general perturbation theory is developed by the use of the adjoint equation

$$\hat{L}^+\varphi^+ = \hat{\omega}^+\varphi^+ + \frac{\nu_f(\vec{r}, u)}{k_{\text{eff}}}\Sigma_f(\vec{r}, u)\,Q^+(\vec{r}). \tag{3}$$

Here the operator $\hat{\omega}^+$ adjoint to the operator $\hat{\omega}$ is defined by the expression

$$\hat{\omega}^+\varphi^+(\vec{r}, u', \vec{\Omega}') = \vec{\Omega}'\nabla\varphi^+(\vec{r}, u', \vec{\Omega}') + \int_{u'}^{\infty}\int \Sigma_{si}(\vec{r}, u', U, \vec{\Omega}_0)\,dU\,d\Omega\,\varphi^+(\vec{r}, u, -\vec{\Omega}).$$

The adjoint function $\varphi^+ = \varphi^+(\vec{r}, u, \vec{\Omega})$ has the physical significance of the importance function for a neutron having the coordinates r, the lethargy U, and the direction of motion given by the unit vector $\vec{\Omega}$*.

Then $Q^+(r)$ has the physical meaning of the importance of a fission neutron, and is given by

$$Q^+(\vec{r}) = \int_{-\infty}^{\infty}\int \frac{\chi(u)}{4\pi}\varphi^+(\vec{r}, u, -\vec{\Omega})\,du\,d\Omega. \tag{4}$$

The fact that Eq. 3 is adjoint to Eq. 1 is obvious. As is well known, the Eqs. 1 and 3 determine the same value of k_{eff}. Let us rewrite these equations in dimensionless form. For this purpose we introduce the dimensionless coordinates.

$$\vec{r}_0 = \frac{\vec{r}}{l},$$

where l is some characteristic dimension of the system. For this dimension we take the largest linear dimension of the core. The gradient operator is now expressed in the form

$$\nabla = \frac{\partial}{\partial\vec{r}} = \frac{1}{l}\cdot\frac{\partial}{\partial\vec{r}_0} = \frac{1}{l}\nabla_0.$$

After substituting this expression in Eqs. 1 and 3 we multiply these two equations by l. Then all of the macroscopic cross sections take the dimensionless form

$$l\Sigma = \Sigma_0 \tag{5}$$

(hereafter we shall use the index zero for all operators expressed in terms of dimensionless coordinates and cross sections).

The balance equations for the density and the importance function now take the form

$$0 = \hat{\omega}_0\varphi - \Sigma_{t_0}\varphi + \frac{\chi(u)}{4\pi}\cdot\frac{Q_0}{k_{\text{eff}}} = \hat{L}_0\varphi, \tag{6}$$

$$0 = \hat{\omega}_0^+\varphi^+ - \Sigma_{t_0}\varphi^+ + \frac{\nu_f\Sigma_{f_0}}{k_{\text{eff}}}Q^+ = \hat{L}_0^+\varphi^+. \tag{7}$$

Obviously, corresponding to similar forms and identical values of the dimensionless macroscopic cross sections Σ_0 one has identical energy and spatial distributions of the neutrons and importance functions, and also identical values of k_{eff}.

The values of the macroscopic cross sections will be preserved if the nuclear densities ρ of all isotopes occuring in the composition of the reactor are changed in inverse proportion to the change of the linear dimensions of the system, i.e., if we set

$$\rho \sim \frac{1}{l}. \tag{8}$$

* We here use the definition of the importance of a neutron given in reference 2.

Since the critical mass P of the reactor is proportional to the product of the nuclear density by the volume V_c of the core, from the condition (8) we get the following dependence of the critical mass P on the linear dimension:

$$P \sim V\rho \sim \frac{l^3}{l} = l^2. \tag{9}$$

The relation (9) has reasonably good accuracy for the evaluation of the critical mass over a certain limited range of variation of the dimensions. An improvement of the relation (9) can be obtained on the basis of the first approximation of perturbation theory. In developing the theory we shall use the scheme proposed by L. N. Usachev. Suppose that there is some change of the macroscopic dimensionless cross sections for the system:

$$\Sigma_0 \to \Sigma_0'.$$

Then there are also changes of the operators $\hat{L}$ and $\hat{\omega}$. Since these operators are linear functions of the macroscopic cross sections, we have

$$\hat{L}_0 \to \hat{L}_0', \quad \hat{\omega}_0 \to \hat{\omega}_0'.$$

Let us denote the variations of these operators by the symbol δ

$$\delta\Sigma_0 = \Sigma_0' - \Sigma_0, \quad \delta\hat{L}_0 = \hat{L}_0' - \hat{L}_0, \quad \delta\hat{\omega}_0 = \hat{\omega}_0' - \hat{\omega}_0.$$

Obviously, $\delta\hat{L}_0$ and $\delta\hat{\omega}_0$ are linear functions of $\delta\Sigma_0$. The change of the macroscopic cross sections is accompanied by a change of the spatial and energy distribution of the neutrons. The perturbed neutron fluxes now satisfy the equation

$$\hat{L}_0'\varphi' = 0. \tag{10}$$

We form the scalar product of Eq. 7 by φ', and that of Eq. 10 by φ^+, and subtract one result from the other. Then we get the identity

$$(\varphi^+, \hat{L}_0'\varphi') - (\hat{L}_0^+\varphi^+, \varphi') = 0,$$

where the brackets denote the triple integral over the entire volume of the reactor, over the lethargy, and over the solid angle. By means of a property of adjoint operators this identity can be brought into the following form

$$(\varphi^+, \hat{L}_0'\varphi') - (\varphi^+, \hat{L}_0\varphi') \equiv 0.$$

From this it follows that

$$\begin{aligned}(\varphi^+, (\hat{L}_0' - \hat{L}_0)\varphi') &\equiv 0,\\ (\varphi^+, \delta\hat{L}_0\varphi') &\equiv 0.\end{aligned} \tag{11}$$

If in the identity (11) we replace the perturbed fluxes by their unperturbed values, we get the first approximation of perturbation theory

$$(\varphi^+, \delta\hat{L}_0\varphi) = 0. \tag{12}$$

The symbolic product in this equation is linear in the quantities

$$\delta\Sigma_0, \quad \frac{1}{k_{\text{eff}}}, \quad \frac{1}{k_{\text{eff}}},$$

and from it one can directly calculate the difference

$$\delta\left(\frac{1}{k_{\text{eff}}}\right) = \frac{1'}{k_{\text{eff}}} - \frac{1}{k_{\text{eff}}} \simeq \frac{\delta k}{k_{\text{eff}}},$$

which gives the change of the reactivity caused by the perturbation of the dimensionless cross sections.

If we require that the perturbed system be critical, then we must set $k'_{\text{eff}} = 1$ in Eq. 12 and calculate the corresponding change of the critical mass. The calculations will be accurate enough if the replacement of φ' by φ in the passage from the identity (11) to Eq. 12 does not bring with it much change in the value of the symbolic product, i.e., if the spatial and energy perturbations of the neutron fluxes are small.

If in Eq. 12 we substitute the expression (1') for $\hat{L}\varphi$ and if we then use the definition (4) of the importance function of a fission neutron, we get

$$(\varphi^+, \delta\hat{L}_0\varphi) = -(\varphi^+, \delta\Sigma_{t_0}\varphi) + (\varphi^+, \delta\hat{\omega}_0\varphi) + \\ + \frac{1}{k_{\text{eff}}}\int Q^+Q'_0\,dV - \frac{1}{k_{\text{eff}}}\int Q^+Q_0\,dV = 0, \tag{13}$$

where

$$Q'_0 = \int\int_{-\infty}^{\infty} \nu_f\Sigma'_{f_0}\varphi\,du\,d\Omega, \tag{14}$$

$$Q_0 = \int\int_{-\infty}^{\infty} \nu_f\Sigma_{f_0}\varphi\,du\,d\Omega. \tag{15}$$

If we set

$$\delta Q_0 = \int\int_{-\infty}^{\infty} \nu_f\delta\Sigma_{f_0}\varphi\,du\,d\Omega,$$

$$Q'_0 = \delta Q_0 + Q_0,$$

$$\frac{1}{k_{\text{eff}}} = \delta\left(\frac{1}{k_{\text{eff}}}\right) + \frac{1}{k_{\text{eff}}}$$

and neglect the product

$$\delta\left(\frac{1}{k_{\text{eff}}}\right)\delta Q_0$$

as a higher-order quantity, we get as the result the expression

$$-(\varphi^+, \delta\Sigma_{t_0}\varphi) + (N^+, \delta\hat{\omega}_0\varphi) + \\ + \frac{1}{k_{\text{eff}}}\int Q^+\delta Q_0\,dV + \delta\left(\frac{1}{k_{\text{eff}}}\right)\int Q^+Q_0\,dV, \tag{16}$$

which is convenient for the determination of $\delta\left(\frac{1}{k_{\text{eff}}}\right)$.

Equation 13 gives in explicit form the relation between the dimensions of the system and the volume fractions of the isotopes of which it is composed. Let the reactor be divided into separate zones, the nth zone having the volume V_n. Then any dimensionless macroscopic cross section of the nth zone can be represented in the form

$$\Sigma_0^{(n)} = l\sum_m \varepsilon_m^{(n)}\sigma_{m}\rho_m,$$

where ρ_m is the nuclear density of the mth isotope, which has microscopic cross section σ_m and volume fraction ε_m. The left member of Eq. 12 can now be written as a linear function of the volume fractions

$$\sum_{n,\,m}(l'\varepsilon_m^{(n)\prime} - l\varepsilon_m^{(n)})A_m^{(n)} + \\ + \sum_{n,\,m}\left(\frac{l'\varepsilon_m^{(n)\prime}}{k_{\text{eff}}} - \frac{l\varepsilon_m^{(n)}}{k_{\text{eff}}}\right)B_m^{(n)} = 0. \tag{17}$$

It is not hard to verify that the coefficients $A_m^{(n)}$ and $B_m^{(n)}$ can be expressed as follows:

$$A_m^{(n)} = \rho_m\int_{V_n} dV\int d\Omega\int_{-\infty}^{\infty} du\Big[-\sigma_m N + \\ + \int d\Omega'\int_{-\infty}^{u}\varphi(\vec{r}, u', \vec{n}')\,\sigma_{si,\,m}(u', U, \mu_0)\,du'\Big]; \tag{18}$$

$$B_m^{(n)} = \rho_m\int_{V_n} dV\,Q^+\int d\Omega\times \\ \times\int_{-\infty}^{\infty}\nu_{fm}(u)\,\sigma_{fm}(u)\,\varphi(\vec{r}, u, \vec{n}). \tag{19}$$

Equation 17 gives the desired relation between the reactivity of the system, its linear dimensions, and the volume fractions of the elements contained in it.

If one uses the age-diffusion approximation, the expressions for the coefficients $A_m^{(n)}$ and $B_m^{(n)}$ take the following forms:

$$A_m^{(n)} = \rho_m\int_{V_n} dV\int_{-\infty}^{\infty} du\Big\{\Phi^+(\vec{r}, u)\times \\ \times\Big[-\sigma_{cfi,\,m}\Phi(\vec{r}, u) + \int_{-\infty}^{u}\Phi(\vec{r}, u')\,du'\,\sigma_{in,\,m}\times \\ \times(u', v) - \xi_m(u)\frac{\partial\sigma_{s,\,m}(u)\,\Phi(\vec{r}, u)}{\partial u}\Big] + \\ + 3\sigma_{tr}(\vec{r}, u)\,\vec{i}^+(\vec{r}, u)\,\vec{i}(\vec{r}, u)\Big\}; \tag{20}$$

$$B_m^{(n)} = \rho_m\int_{V_n} dV\,Q^+(\vec{r})\times \\ \times\int_{-\infty}^{\infty}\nu_{fm}(u)\,\sigma_{fm}(u)\,\Phi(\vec{r}, u). \tag{21}$$

In the diffusion approximation the relations between the neutron flux $\Phi(\vec{r}, u)$ and importance function $\Phi^+(\vec{r}, u)$ and the spatial, angular, and energy distributions of the neutron flux and importance is given by the well-known relations:*

$$\varphi(\vec{r}, u, \vec{n}) \cong \frac{\Phi(\vec{r}, u)}{4\pi} + \frac{3}{4\pi}\vec{i}(\vec{r}, u)\cdot\vec{\Omega},$$

$$\varphi^+(\vec{r}, u, -\vec{n}) \cong \frac{\Phi^+(\vec{r}, u)}{4\pi} - \frac{3}{4\pi}\vec{i}^+(\vec{r}, u)\cdot\vec{\Omega},$$

which contain the first two terms of the expansions of φ and φ^+ in series of spherical harmonics. Furthermore

$$\sigma_{tr}(u) = \sigma_t(u) - \bar{\mu}_0(u)\,\sigma_s(u),$$

$$\vec{i}(\vec{r}, u) = -\frac{1}{3\Sigma_{tr}(\vec{r}, u)}\nabla\Phi(\vec{r}, u), \tag{22}$$

$$\vec{i}^+(\vec{r}, u) = -\frac{1}{3\Sigma_{tr}(\vec{r}, u)}\nabla\Phi^+(\vec{r}, u), \tag{23}$$

$$Q^+(\vec{r}) = \int_{-\infty}^{\infty}\chi(u)\,\Phi^+\,du, \quad Q(\vec{r}) = \int_{-\infty}^{\infty}\nu_f\Sigma_f\Phi\,du. \tag{24}$$

The quantity $\xi_m(u)$, appearing in the expression (20) is the mean logarithmic energy loss in an elastic collision; if there is anisotropy in the center-of-mass system this quantity depends on the energy.

*Cf. e. g., reference 3.

In the multigroup approximation the integrals over the lethargy that appear in the expressions (22) and (21) are represented as finite sums over all the p-groups

$$A_m^{(n)} = \rho_m \int_{V_n} dV \sum_{k=1}^{p} \left\{ \Phi_k^+(\vec{r}) \cdot \left[-\sigma_{cf,\,\text{yB},\,m}^{(k)} \Phi_k(\vec{r}) + \right. \right.$$

$$\left. \left. + \sum_{j=1}^{k-1} \sigma_{\text{re},\,m}^{kj} \Phi_j(\vec{r}) \right] + 3\sigma_{tr,\,m}^{(k)} \vec{i}_k^+(\vec{r}) \vec{i}_k(\vec{r}) \right\}; \qquad (25)$$

$$B_m^{(n)} = \rho_m \int_{V_n} dV \cdot Q^+(\vec{r}) \sum_{k=1}^{p} (\nu_f \sigma_f)_k \Phi_k(\vec{r}). \qquad (26)$$

The multigroup microscopic cross sections appearing in these expressions are averaged over the neutron spectrum of the given reactor, as is recommended, for example, in reference 4, or over the neutron spectrum and the importance spectrum (reference 1, Section 62), which latter procedure seems better justified.

The removal cross section σ_{re}^{kj} takes account of both elastic and inelastic scattering with passage of a neutron from group j to group k. The main practical importance of the formula (17) is in the solution of the problem of two zones, i.e., the problem of a reactor consisting only of the core (zone $n = 1$) and an infinitely thick reflector (zone $n = 2$). If, however, the porosity of a uranium screen does not exceed 30 percent, then if the thickness is larger than 20 cm it can be regarded as practically infinite in the calculation of the reactivity.

In such cases one can confidently use the formula (17) with the coefficients A_m^{∞} and B_m^{∞} calculated for an infinite screen.

Test of the Formula and Discussion of Results

The formula (17) has been tested by means of nine-group calculations in the age-diffusion approximation for spherical geometry. Calculations were carried out for two spherical reactors of volumes 205 and 930 cubic decimeters. We shall call them "system I" and "system II", respectively. The thickness of the reflector in terms of the extrapolated boundary was taken the same for both systems—50 cm. The volume fractions of U^{238}(ε'_8), iron (ε_{Fe}) and sodium (ε_{Na}) making up the reflector were also taken to be the same in both systems, with the values $\varepsilon_8 = 0.7$; $\varepsilon_{Fe} = 0.1$; $\varepsilon_{Na} = 0.2$.

It was assumed that the core consists of fuel alloy with volume fraction ε_{fuel}, iron with volume fraction ε_{Fe}, and sodium with volume fraction ε_{Na}. The values of the volume fractions of the core materials are not the same for systems I and II; they are given in Table 1. The table also gives the values of R, the radius of the spherical core. The fuel alloy assumed was plutonium diluted with some other substance. The calculations were made for each system with five types of alloys, containing U^{238}, Ba, Zr, Fe, and Mo with the plutonium. For all the elements making up the active zone a nine-group system of constants was constructed, based on the experimental data published up to 1955.

Table 1. Comparative Characteristics of Systems I and II

	ϵ_{fuel}	ε_{Na}	ε_{Fe}	R, cm
System I	0.33	0.50	0.17	36.5
System II	0.36	0.53	0.11	60.3

The determinations of the critical mass and the calculations of the neutron spectra and of the spatial distributions of the neutron fluxes and importance functions were made by solving a system of multigroup diffusion equations for the neutron density and importance function. The quantity k_{eff} was determined by the method of iteration of the sources. The computations were carried out by the method of finite-difference factorization explained in the book by G.I. Marchuk [4], and were done under his direction. A study of the spectra obtained with different alloying materials in systems I and II showed that in general they have the same character. The results of the solution of the critical problem for systems I and II are presented in Table 2, where ε_9 denotes the volume fraction of the main fissionable isotope, plutonium. The spectra obtained for each modification of system I were used to construct the coefficients of the formula (17) according to Eqs. 25, 26. System I was regarded as an unperturbed system. The quantities k_{eff} and k'_{eff} for each modification were taken in accordance with Table 2.

Table 2. Results of the Calculations for Systems I and II

Composition of fuel alloy	System I		System II	
	ε_9	k_{eff}	ε_9	k_{eff}
Pu+U^{238}	0.050	0.97	0.034	1.02
Pu+Zr	0.052	1.05	0.023	1.01
Pu+Mo	0.050	0.99	0.033	1.02
Pu+Fe	0.052	0.99	0.031	1.07
Pu+Ba	0.055	0.98	0.032	1.07

For each modification with the different alloying elements the value of ε'_9 for system II was found from the formula (17), with the coefficients $A_m^{(n)}$ and $B_m^{(n)}$ computed from the calculated spectrum for the same modification of system I. The error in the calculation of ε'_9 did not exceed 10 percent. This made it possible to take as a basis a certain typical spectrum for a fast reactor and calculate from it a set of universal coefficients for the formula (17). The spectrum adopted for this purpose was that of system I with U^{238} as the alloying element.

Table 3 shows the results of calculations of the quantity ε'_9 by Eq. 17 with the coefficients computed from this spectrum. The table also shows the comparison with the computed value of ε'_9. Table 4 gives the coefficients $A_m^{(n)}$ and $B_m^{(n)}$ for the types of materials for which the results are listed in Table 3.* The nuclear densities are taken under normal conditions. The coefficients relating to the screen are given only for U^{238}, Na, and Fe.

* The calculations of coefficients and the check of the formula (17) were carried out by Engineers A. P. Karbaeva and V. A. Kuz'micheva.

Table 3

Comparison of the Results of Calculations of ϵ'_3 by the Formula (17) With Those of Diffusion Calculations

Composition of fuel alloy	System I			System II		
	Eq. (17)	computed values	error, percent	Eq. (17)	computed values	error, percent
Pu+U^{238}	—	0.050	—	0.030	0.0340	10
Pu+Zr	0.051	0.052	2	0.024	0.0230	3
Pu+Mo	0.052	0.050	4	0.032	0.0330	3
Pu+Fe	0.051	0.052	2	0.032	0.0312	2
Pu+Ba	0.049	0.055	10	0.031	0.032	3

Table 4. Coefficients for Formula (17)

Element	$A_m^{(1)}$	$B_m^{(1)}$	$A_m^{(2)}$	$B_m^{(2)}$
U^{238}	−0.2651	0.2524	−0.0006	0.0235
Pu^{239}	−1.9925	6.3167	—	—
Zr	0.0665	0	—	0
Mo	−0.0297	0	—	0
Na	0.0187	0	0.0097	0
Fe	−0.0025	0	0.0264	0

Conclusions

The check of the formula (17) by the solution of nine-group age-diffusion equations has shown the applicability of the formula for an increase of the dimensions of a system by a factor of two, or possibly more than two. The errors in the calculations of the constants shown in Table 3 for the different alloying elements and for spherical volumes from 200 to 1000 cubic decimeters do not exceed 10 percent. The possibility of application to other fissionable isotopes and alloying elements and to other ranges of volumes of the core, on the basis of the neutron spectra and importance spectra adopted here, still needs to be specially checked by calculations of the spectra in the new ranges of sizes.

For the alloying elements considered here and in the range of dimensions indicated, the coefficients given in Table 4 can be accepted, subject to the condition that the screen can be regarded as infinite.

In conclusion the writer thanks Active Member of the Academy of Sciences of the Ukrainian SSR A.I. Leipunskii, G.I. Marchuk, and L.N. Usachev for a discussion of the work.

Received June 21, 1958

Literature

1. G.I. Marchuk, Supplement No. 3-4 to J. Atomic Energy (1958) [USSR].
2. L.N. Usachev, "Reactor Construction and the Theory of Reactors", Reports of the Soviet Delegation at the International Conference on the Peaceful Uses of Atomic Energy [in Russian] (Geneva, AN SSSR Press, 1955) p. 251.
3. A.I. Akhiezer and I. Ya. Pomeranchuk, Some Problems of Nuclear Theory (in Russian) (GITTL, 1950).
4. R. Erlich and H. Hurwitz "Multigroup Methods for Neutron Diffusion Problems." Nucleonics 12, 2, 23 (1954).

THE CORRELATION OF THE EXPERIMENTAL DATA ON CRITICAL HEAT LOADS IN FORCED FLOW OF WATER HEATED BELOW THE BOILING TEMPERATURE

B. A. Zenkevich

At low pressures, theory predicts a simplification of the similarity-parameter equation proposed by the writer [2] on the basis of a correlation of the experimental data on critical thermal loads in forced flow of water not heated to boiling, in the pressure range 100--210 atmos.

It is shown that it is possible to apply the previously proposed similarity-parameter equation over a wider range of pressures, namely 35--210 atmos.

Furthermore an analysis of the published experimental data on q_{cr} at low pressures confirms the theoretical conclusion about a degeneration of the functional connections between the parameter to be determined and the two determining parameters at water pressures close to atmospheric pressure, owing to which the similarity-parameter equation for this case takes a considerably simpler form. A computational formula obtained on the basis of this equation is recommended for the pressure range 1--15 atmos.

The conditions of mechanical, thermal, and material interaction of the vapor and liquid phases at their interface in film vaporization which correspond to a crisis in the boiling in forced flow of water heated below the boiling temperature are described by a system of equations that includes: *

a) the equation of equilibrium of the mechanical forces

$$\frac{W_x\gamma}{g}(W_x'' - W_x) = \sigma\left(\frac{1}{R_1}+\frac{1}{R_2}\right) + \mu\left(2\frac{\partial W_x}{\partial x}+\frac{\partial W_x}{\partial y}+\frac{\partial W_x}{\partial z}\right); \quad (1)$$

b) the equation of heat balance

$$(q_{cr})_x = W_x''\gamma''r + c_\mu \Delta t_{II} W_x\gamma; \quad (2)$$

c) the equation of material balance

$$W_x''\gamma'' = W_x\gamma. \quad (3)$$

In these equations the signs of integrations for the summational-statistical treatment of the equilibrium of the interface have been omitted.

Using Eq. 3, we can bring Eq. 1 into the form

$$\frac{W_x''^2\gamma''}{g} - \frac{W_x^2\gamma}{g} = \sigma\left(\frac{1}{R_1}+\frac{1}{R_2}\right) + \mu\left(2\frac{\partial W_x}{\partial x}+\frac{\partial W_x}{\partial y}+\frac{\partial W_x}{\partial z}\right) \quad (4)$$

or, what is the same thing,

$$\frac{W_x''^2\gamma''}{g} - \frac{\gamma''}{\gamma}\cdot\frac{W_x''^2\gamma''}{g} = \sigma\left(\frac{1}{R_1}+\frac{1}{R_2}\right) + \mu\left(2\frac{\partial W_x}{\partial x}+\frac{\partial W_x}{\partial y}+\frac{\partial W_x}{\partial z}\right). \quad (5)$$

As has been shown in reference 2, the experimental data on critical heat loads in forced motion of water not heated to boiling are satisfactorily correlated in the pressure range 100 – 210 atmos in terms of the following similarity parameters obtained from Eqs. 1 – 3 or 2 – 4:

$$K = \frac{q_{cr}}{r}\sqrt{\frac{\nu}{\sigma g W_0}}; \quad K_1 = \frac{\gamma''}{\gamma_{II}}; \quad K_2 = \frac{i_s - i_{II}}{r}; \quad R = \frac{W_0\sqrt{\frac{\sigma}{\gamma'-\gamma''}}}{\gamma_{II}\nu}. \quad (6)$$

*The notations used are those introduced in reference 2.

It follows from Eq. 5 that at very small values of the ratio $\frac{\gamma''}{\gamma}$* (i.e., at pressures close to atmospheric pressure) the second term in Eq. 5 or Eq. 4 can be neglected. Then for the critical condition of the boiling the equation of the equilibrium of the mechanical forces at the interface between the phases can be written in the form

$$\frac{W_x''^2\gamma''}{g} = \sigma\left(\frac{1}{R_1}+\frac{1}{R_2}\right) + \mu\left(2\frac{\partial W_x}{\partial x}+\frac{\partial W_x}{\partial y}+\frac{\partial W_x}{\partial z}\right). \quad (7)$$

The physical meaning of the neglect of the second term of Eq. 5 or Eq. 4 is that at low pressure, i.e., for small values of $\frac{\gamma''}{\gamma}$, the reaction force arising at the interface owing to the phase transition is practically completely determined by the momentum of the vapor-phase flow, and the momentum of the liquid-phase flow is very small in comparison with it.

When analyzed by the methods of similarity theory Eqs. 7, 2, and 3 give the following primary similarity parameters:

$$\left\{\frac{W''^2\gamma''l}{g\sigma};\ \frac{\mu W}{\sigma};\ \frac{q_{cr}}{rW''\gamma''};\ \frac{c_p\Delta t_{II}W\gamma}{rW''\gamma''};\ \frac{W''\gamma''}{W\gamma}\right\}. \quad (8)$$

The system of parameters (8) can be transformed to the form

$$\left\{\frac{W''^2\gamma''l}{g\sigma};\ \frac{q_{cr}}{rW''\gamma''};\ \frac{W''\gamma''}{W\gamma};\ \frac{q_{cr}}{r}\sqrt{\frac{\nu}{\sigma g W_0}};\ \frac{c_p\Delta t_{II}}{r}\right\}. \quad (9)$$

In this system only the last parameter is composed of quantities that can be prescribed, and therefore it is a determining or independent parameter. All the other parameters of the system (9) are determinable parameters. Omitting from consideration the first

*The size of the ratio $\frac{\gamma''}{\gamma}$ shows what the momentum of the liquid-phase flow amounts to as a fraction of the momentum of the vapor-phase flow.

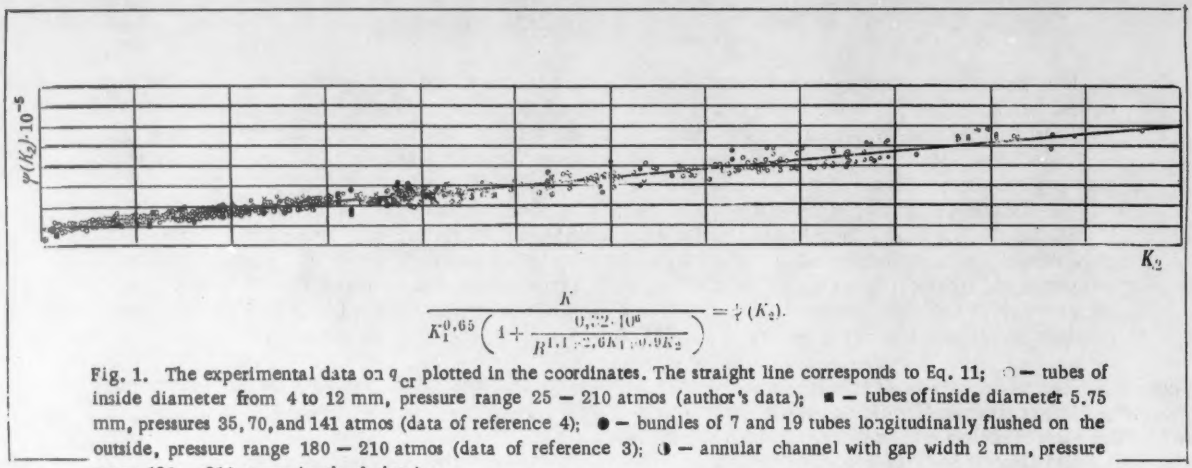

Fig. 1. The experimental data on q_{cr} plotted in the coordinates. The straight line corresponds to Eq. 11; ○ — tubes of inside diameter from 4 to 12 mm, pressure range 25 — 210 atmos (author's data); ■ — tubes of inside diameter 5.75 mm, pressures 35, 70, and 141 atmos (data of reference 4); ● — bundles of 7 and 19 tubes longitudinally flushed on the outside, pressure range 180 — 210 atmos (data of reference 3); ◑ — annular channel with gap width 2 mm, pressure range 120 — 210 atmos (author's data).

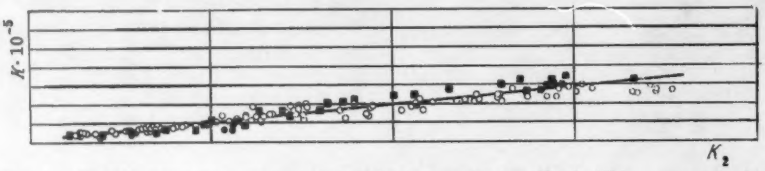

Fig. 2. Experimental data on q_{cr} plotted in the coordinates $K=\psi_1(K_2)$. ● — annular channel with gap 6.6 mm, pressure range 2.1-6.3 atmos (data of reference 5); ■ — channel of rectangular cross section 12.5 x 5 mm with ribbon heater in the center, pressure range 1 — 11.5 atmos (data of reference 6); ○ — annular channel with gap from 2 to 5.6 mm, range 1 — 22 atmos (data of reference 7); ◐ — graphite plates spaced along the axis of the working tube, pressure 1 atmos (data of reference 8).

three parameters, on the basis of the third theorem of the Kirpichev-Gukhman theory of similarity we can write the equation

$$\frac{q_{cr}}{r}\sqrt{\frac{\nu}{\sigma g W_0}}=\Psi_1\left(\frac{c_p\Delta t_н}{r}\right). \qquad (10)$$

From what has been said it follows that as the pressure is lowered the functional connections between the determinable parameter K and the determining parameters K_1 and R must degenerate, and on the basis of the relation (10) it must be possible to correlate the data on critical heat loads in forced flow of water not heated to boiling by means of the parameters K and K_2, the former of which is a determinable parameter.

To establish the pressure ranges in which the experimental data can be correlated either by means of the parameters of the system (6) or the parameters of the relation (10), the relevant experimental data have been subjected to analysis.

Figure 1 shows a plot in terms of the parametric equation

$$K=K_1^{0,65}(95+420\,K_2)\left(1+\frac{0,32\cdot 10^6}{R^{1,1+2,6K_1+0,9K_2}}\right)\times \times 10^{-5} \qquad (11)$$

over the pressure range 25 — 210 atmos of the experimental data on q_{cr} obtained for the motion of water in channels with various geometries* (over 1400 experimental points were used in plotting this diagram). As can be seen from the diagram, the experimental data in the pressure range in question are satisfactorily correlated by means of the parameters of the system (6).

An analysis of the experimental data on q_{cr} for the pressure range from 1 to 22 atmos, taken from the work of various authors, has shown that these data are not at all well described by the parametric equation 11. They are, however, satisfactorily correlated by means of the parameters of the relation (10), as is shown graphically in Figure 2. The straight line that gives an average for the experimental points corresponds to the equation

$$K=(2,5+184\,K_2)\cdot 10^{-5}. \qquad (12)$$

The dimensional form of Eq. 12 has the form

$$q_{cr}=r\sqrt{\frac{\sigma g W_0}{\nu}}(2,5+184\,K_2)\cdot 10^{-5}\ \frac{\text{kcal}}{\text{m}^2\cdot\text{hr}}. \qquad (13)$$

The results of the analysis of the experimental data as shown in Figure 2 confirm to a first approximation the theoretical conclusion that at low pressures there is degeneration of the functional connections between the parameter to be determined, K, and the determining parameters K_1 and R.

It must be kept in mind that no sharp boundary can be drawn between the ranges of applicability of Eqs. 11 and 12. The analysis (the comparison of the computed and experimental values of q_{cr}) has shown that Eq. 11 can be applied in the pressure range from about 35 to

*The writer's experiments for $p<100$ atmos were performed with the same tubes and by the same method as described in reference 1.

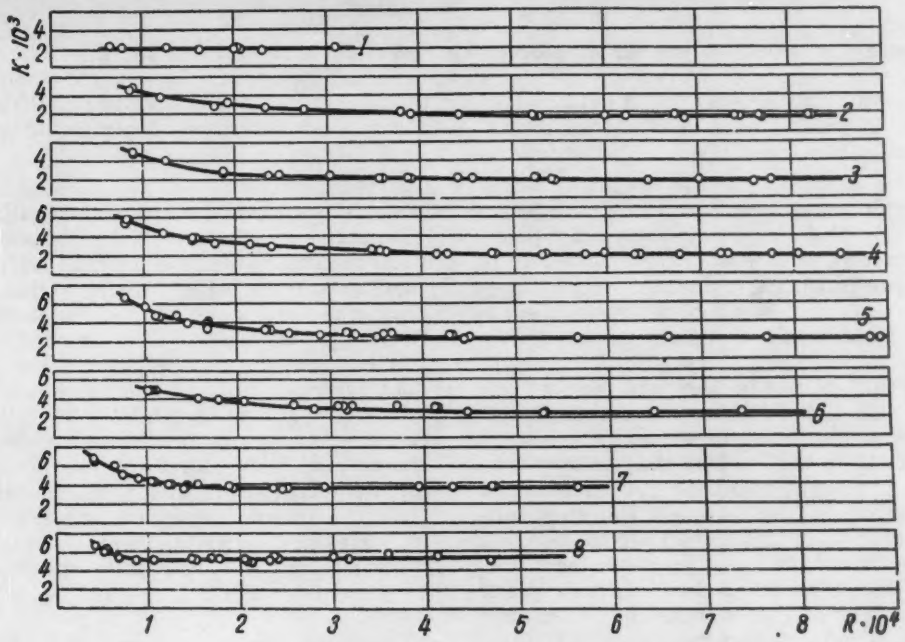

Fig. 3. The relation $K = \varphi(R)$ for the mean parameters:

1 — p=1 atmos; Δt_α=54.4° C; K_1=5.91·10⁻⁴; K_2=0.1 [6], [7][1];
2 — p=30 atmos; Δt_α=37.2° C; K_1=0.017; K_2=0.096;
3 — p=40 atmos; Δt_α=37° C; ; K_1=0.023; K_2=0.100;
4 — p=60 atmos; Δt_α=31.6° C; K_1=0.037; K_2=0.100;
5 — p=80 atmos; Δt_α=27.7° C; K_1=0.0537; K_2=0.100;
6 — p=100 atmos; Δt_α=24.8° C; K_1=0.0788; K_2=0.105;
7 — p=140 atmos; Δt_α=15.3° C; K_1=0.126; K_2=0.100;
8 — p=180 atmos. Δt_α=9.1° C. K_1=0.214. K_2=0.108.

[1]The experimental points obtained for working sections with gap $\delta \geq 2.3$ mm are taken from reference 7.

210 atmos, and Eq. 12 in the pressure range from about 1 to 15 atmos. The range $15 < p$ atmos must be regarded as a transition region.

It follows from the analysis of Eq. (13) that a change of the pressure of the water in the range about 1 -- 20 atmos, with other conditions kept constant, should have almost no effect on the quantity q_{cr}, since the effects of the changes of the physical parameters r, σ, and of the water approximately cancel each other in this range of pressures. The absence of an effect of the pressure has been noted by McAdams [5] (p = 2.1 -- 6.3 atmos) and by Gunther [6] (p = 1 -- 11.5 atmos). Also in the experiments of Chirkin and Yukin [7] (p = 1 -- 22 atmos) practically no effect of the pressure was observed.

A point worthy of attention is the extremely complex character of the connection between the parameters K and R, which arises when the pressure is varied over a wide range. As has been noted in reference 2, the extent of the effect of R on K has an inverse dependence on the numerical values of the parameters K_1 and K_2. At very small values of K_1, however, as follows from the above statements, the effect of R on K disappears almost completely.

Figure 3 gives a graphic representation of the dependence $K = \varphi(R)$ for various pressures (i.e., various values of K_1) with values K_2 0.1 that are practically constant for each series of experimental points. It can be seen from these curves that as the pressure is lowered from 180 to 80 atmos the effect of R on K becomes stronger, that it becomes weaker for $p <$ 60 atmos, and that it can be no longer be perceived at p = 1 atmos.

O. L. Peskov, N. D. Sergeev, Z. F. Deryugin, and N. A. Gushchina took part in the taking of the measurements and the analysis of the data.

Received June 18, 1958

Literature

1. B.A. Zenkevich and V.I. Subbotin, J. Atomic Energy 3, 149 (1957) [USSR].
2. B.A. Zenkevich, J. Atomic Energy 4, 74 (1958) [USSR].
3. B.A. Zenkevich, V.I. Subbotin, and M.F. Troyanov, J. Atomic Energy 4, 370 (1958).
4. H.F. Buchberg et al., Studies in Boiling Heat Transfer, [Russian Translation] (AEC USA NAT-11-1-Gen-9, March 1951).
5. W.H. McAdams et al., Ind. and Eng. Chem. 41, 1945 (1949).
6. F.C. Günther, Trans. ASME 73, 115 (1951).
7. V.S. Chirkin and V.P. Yukin, J. Tech. Phys. (USSR) 22, 1542 (1956)*.
8. S.S. Kutateladze and V.M. Borishanskii, Énergomashinostroenie, 2, 10 (1957).

*Soviet Physics-Technical Physics, p. 1503.

ELECTROSTATIC CHARGED-PARTICLE ACCELERATORS

V. N. Glazanov

A survey is given of studies on electrostatic particle accelerators. The main attention is given to problems of increasing the energy of the accelerated particles and the beam power in electrostatic generators. A comparison of the different methods of voltage stabilization is made. In conclusion a brief discussion is given of cascade generators designed for the production of high-power beams.

The electrostatic machine was the first electric machine. As early as a century ago it produced potentials of the order of hundreds of thousands of volts. The possibility of producing high alternating voltages by means of transformers and of rectifying them by mechanical and electronic rectifiers put a stop for some decades to research work with electrostatic generators (ESG). Interest in them was renewed only in the 1930's (work of A. F. Ioffe and of van de Graaff) [1, 2] in connection with the necessity of producing constant potentials of hundreds of thousands of volts and of millions of volts at relatively low currents, for the acceleration of charged particles. For such voltages it was found to be more difficult to develop a high-voltage rectifier than an electrostatic generator.

The present ESG reproduces the main principle of the first electrostatic machines, but differs from them in its construction and in the way the charge is applied. Figure 1 shows: the influence machine; the rotor machine of A. F. Ioffe [1]; the disk machine of Kossel [3]; and the belt machine of van de Graaff. Diagrams of the charge-transfer process are presented in Fig. 2 [1]. At the point A the capacity of an element of the rotor or belt is C_1 and its charge is q_1 (Fig. 2, a, b). The element is disconnected from the source at potential U_1. The capacity of this element relative to the charging plate (earth) decreases with the motion of the rotor; the charge remains constant, and the potential rises to the value U_3. The curve AB is an equilateral hyperbola ($UC = q = \text{const}$). At the point B the potential of the rotor element is U_3. When this element is connected to the collector the potential falls to the value U_2; the capacity meanwhile remains constant at C_2, and the charge $q_1 - q_2$ is removed and transferred to the collector. Beginning at the point C, the element moves in the direction toward the charging device, its capacity increases to C_1, and its potential falls to U_4, the charge q_2 remaining constant. Finally, the rotor element has its potential raised to U_1 and receives the charge $q_1 - q_2$.

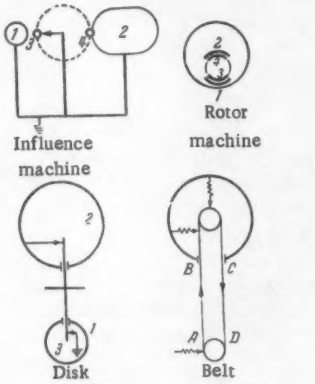

Fig. 1. Schemes of electrostatic machines

Thereafter the process repeats itself, and is reminiscent of the Carnot cycle. After several revolutions the potentials U_2 and U_3 become approximately equal (Fig. 2, c).

In each cycle the rotor element transfers to the collector at potential U_2 a certain quantity $q_1 - q_2$ of electricity from the source at potential U_1. The area $ABCD$ (Fig. 2, b) represents the mechanical work W; $ADEF$ represents the electric energy W_2 received from the source; and $BCEF$ represents the energy W_1 received by the collector ($W = W_1 - W_2$). It is assumed, of course, that the efficiency of the machine is equal to unity and that all of the mechanical work is converted into electric energy. The ratio $\frac{W_2}{W_1} = \frac{U_2}{U_1}$ is the transformation coefficient. Despite the fact that in its general scheme and principle of operation the belt generator does not differ from the simplest electrostatic machines, its detailed construction has a number of special features that make it possible to increase the potential produced by the generator by at least an order of magnitude, and reach 1 Mv. Persistent research and development work has been required, however, for further increases of the voltage. It took

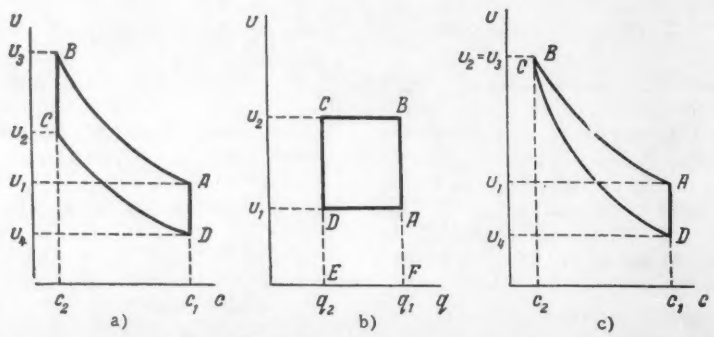

Fig. 2. Diagrams of the operation of the ESG.

The generator voltage varies because of nonuniform motion of the belt (slow fluctuations), lack of constancy of the load current, and mechanical vibrations of the column (rapid oscillations).

Measurements of the generator voltage can be made by means of a potentiometer (accuracy of measurement several percent), a generating voltmeter (accuracy down to 0.5 percent), the value of a magnetic field deflecting the beam, or the potential difference on the deflecting plates of an electrostatic analyzer. By the last two methods accuracy to 0.01—0.03 percent can be assured. Analyzers are almost exclusively used to check the energy in ESG's, since they fulfill three functions: they measure the voltage, provide a sensing device for the voltage-stabilization system, and eliminate particles with energies outside a prescribed range.

An analyzer is a complicated device using stabilized magnetic or electric fields. The use of electrostatic analyzers is clear from the diagrams shown in Figs. 5 and 6. A magnet first deflects the beam by 10 to 15 degrees; this makes the construction of the electrostatic analyzer easier. The entry of the beam into and its exit from the vacuum chamber are limited by insulated jaws forming slits. The radius of curvature of the beam in the electric field of the analyzer depends on the charge and mass of the particles and the strength of the field; one tries to keep this last factor strictly constant. At its emergence from the electric field the beam executes oscillations synchronous with the variations of the generator voltage, and consequently also synchronous with the variations of the energy of the accelerated ions. A certain part of the beam strikes the slit jaws, and the middle part, which is more homogeneous in energy, reaches the target. The current coming to one of the jaws of the slit gives a signal showing increase of the particle energy, and that to the other a signal for decrease of the energy; these are also signals of increase or decrease of the generator voltage relative to the prescribed value. By means of an electronic circuit these signals keep the generator voltage constant.

The relation that holds for an electrostatic analyzer is $U_0 = \frac{r}{2d} U_d$, where U_0 is the voltage on the collector, r is the mean radius of the gap between the plates, d is the width of the gap, and U_d is the voltage across the plates. Therefore the accuracy of the measurement of the accelerating voltage is determined by the precision with which the plates are shaped and the radius is measured, the precision of the location of the gap between the plates, and the accuracy with which the voltage across the plates is maintained and measured.

In operating installations the energy of the protons (deuterons) is kept constant to accuracy 0.01—0.03 percent, but under these conditions the current emerging from the electrostatic analyzer is very small (a few percent of the value of the current at the entrance to the analyzer). It is possible to achieve still higher accuracy by reducing the separation of the jaws of the slits (input and output). Naturally, this leads to a further decrease of the useful proton current.

A number of ESG's have two tubes: one is used for the voltage stabilization with an electrostatic analyzer, and the current in the other goes to the target (Fig. 5).

The high accuracy with which the particle energy can be measured and held constant, which can be achieved by means of the electrostatic analyzer, has made it possible to determine the thresholds of reactions: $Li_3^7(p, \gamma)$—440 kev, $F_9^{19}(p, \gamma)$ —873.5 kev, $Al_{13}^{27}(p,\gamma)$ — 993.3 kev, $Li_3^7(p,n)$—1887 kev; these are useful reference points for checking the voltage of an ESG.

In the construction of the vacuum chamber of an electrostatic analyzer, high accuracy must be attained in determining the radius of curvature of the plates (about 0.1 mm for a radius of 150 cm) and finishing the gap between them (3 to 5 microns for a 5 mm gap). These difficulties have led to the disuse of the electrostatic analyzer and the utilization of magnetic analyzers, which give a markedly larger current output together with a comparatively small increase of the spread in energy. For example, in one generator [6] voltage stability better than 0.025 percent has been achieved with a current of 30 μ a to the target.

The generator voltage U_0, the magnetic field strength H, the radius r of the trajectory of the ions, and the charge e and the mass m of an accelerated ion are connected by the relation

$$U_0 = \frac{e(Hr)^2}{2c^2m}.$$

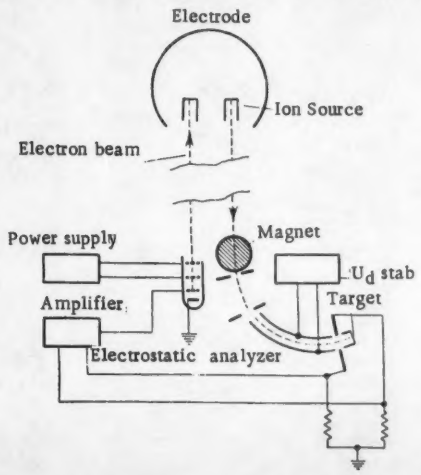

Fig. 5. System for automatic voltage regulation of an ESG by the electron-beam method.

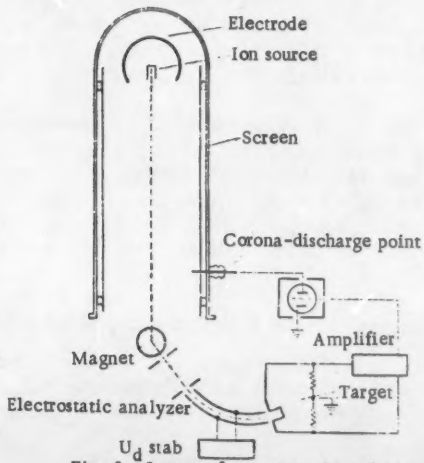

Fig. 6. System for automatic voltage regulation of an ESG by the methods of corona discharge and capacity screen.

For a constant magnetic field matched to the value of U_0 the ion beam passes through the analyzer. When there is a change in the voltage U_0 the beam is deflected from the center of the slit. The constancy of the energy of the accelerated particles is fixed by the constancy of the magnetic field strength in the analyzer. Owing to hysteresis and temperature deformations of the magnet yoke, high particle-energy stability cannot be assured in systems that make use of current-stabilizers to control the excitation current of an electromagnet. Recently a system has come into use that is based on continuous measurement of the magnetic field by means of the resonance absorption of high-frequency energy in a paramagnetic (proton-containing) substance, for example – water.

With a magnetic analyzer, as with the electrostatic system, a signal from the jaws of the slit is fed to a device that acts on the value of the potential of the high-voltage electrode. Three main methods for affecting the fast oscillations of the voltage are used [7]:

1) regulation of the voltage of a metal screen around the ESG, which is insulated from the tank, to a potential of some tens of kilovolts (Fig. 6);

2) production of a corona load inside the tank (Fig. 6);

3) production of an electron load in a tube (Fig. 5).

If, in the first case, a certain potential relative to earth* is applied to the screen, the potential of the high-voltage electrode relative to earth is increased. The potential of the screen is regulated by means of the signal coming from the analyzer.

The method of regulating the load current with a corona current is simple, but its sensitivity is not very high. When a magnetic analyzer is used with this method the monochromaticity of the beam is maintained within 0.1–0.2 percent. Further increase of the accuracy can be obtained by narrowing the slits (at the expense of reducing the target current), or by using for the stabilization ions of another mass present in the beam, sending them into a separate chamber. In this last case the entire proton beam falls on the target.

Voltage stabilization by means of an electron beam sent upward from below (cf., Fig. 5) has high accuracy, but produces an electronic load which reduces the breakdown voltage of the tube. When the electron-gun filament burns out, the vacuum system of the generator must be opened up. Furthermore, the electronic load increases the x-radiation in the upper part of the tube and produces ionization of the gas in the tank, thus increasing the possibility of breakdown. The x-radiation is also undesirable from the point of view of safe operation.

The stabilization systems that have been described act on the fast oscillations of the voltage. The slow variations of the voltage are eliminated by controlling the system for "spraying" the charge onto the belt. The degree of voltage stabilization of an accelerator by the first and third methods can be estimated at $2-3 \cdot 10^{-4}$.

The Energy of the Electrostatic Generator

The first belt ESG designed for nuclear research, with a potential of about a million volts, appeared in 1931 [2]. The use of a compressed gas as the medium surrounding the generator made it possible to raise the potential of such a generator to 2.5 Mv, with a height only half of that of the generator set up in the open air. Further increase of the voltage was prevented by breakdowns (flashovers) along the column and the belt.

About 1940, it was proposed that the potential distribution along the belt and column could be evened out by the insertion of conducting plates with rings (Fig. 4). The desired potential distribution on them was assured by an ohmic voltage divider placed inside the column. This made possible another marked increase; in 1949 a generator under pressure, but without a tube, produced a potential of 5 Mv [8], but with a tube the potential did not go above 2 Mv. It became clear that the weak link of the generator with compressed gas and uniform potential distribution is the tube.

Numerous studies in the U.S.A. on the construction of individual tube components made it possible in 1947 to increase the potential of a generator with a tube to 3 Mv [9], and in the U.S.S.R. in 1949, 2.5 Mv was reached. In 1953 the American company "High Voltage Engineering" began serial production of generators for 2 and 5 Mv.

Further increase of the voltage came to a halt. In 1948 the Massachusetts Institute of Technology announced a project for a 12-Mv generator [10], and according to incomplete data, particle energies of about 8 Mev were achieved with this generator in 1955; there is no further communication about this accelerator.

In the U.S.S.R., the first equipment for electrostatic particle acceleration was set up in the laboratories of B. M. Gokhberg (Moscow) and A. K. Val'ter (Khar'kov). Now industrial ESG's of energies 2.5 and 5 Mev have been developed in the Scientific Research Institute of Electro-physical Apparatus. Serial production of these devices has been started.

The maximum breakdown potential gradient in a uniform field in open air is 30 kv/cm, but at potentials of about 1 Mv and at larger distances from the electrode to the walls this value goes down by almost a factor of 10. At potentials of about 3 Mv, increasing the distance no longer does any good. At potentials of about 3 Mv the unevennesses that cannot be avoided in the construction

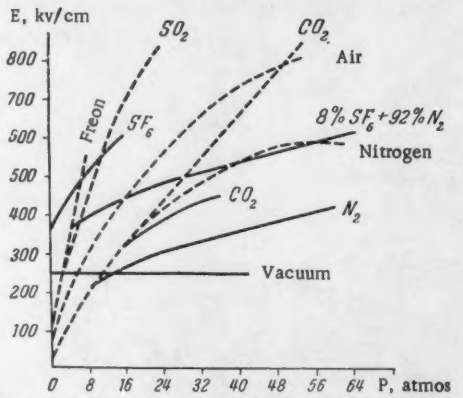

Fig. 7. Pressure dependence of the breakdown voltage in various gases:

————: uniform field between plane electrodes (diameter 15 cm, gap 12.7 mm); – – – –: weakly nonuniform field between spheres of diameter 6.3cm (gap 2.5 mm)

*The system for applying the potential is just the same as for the use of a corona-discharge point.

almost a quarter of a century to raise the voltage from 1 to 6 Mv, whereas the energy of particles from linear accelerators increased in the same time from 1 to 600 Mev (Fig. 3) [4].

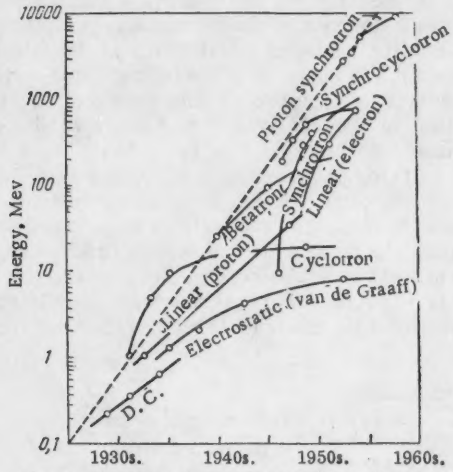

Fig. 3. Increase of the energy of accelerators (from Livingston's book).

In fifteen countries there are in use and under construction 110 electrostatic and 37 cascade generators; Potentials of 3 Mv or more are produced by 33 of them; potentials of 5 Mv or more are produced by 13 of them [5]. A diagram of one of these generators with its discharge tube is shown in Fig. 4. Two belts* transfer charge to the high-voltage electrode, inside which are located devices for taking off the charge, and an ion source and the electric generator to operate it. The high-voltage electrode rests on a column of insulators. In order to improve the potential distribution along the column, metal equipotential surfaces are spaced along it. Inside the column there is the vacuum tube in which the ions produced by the source are accelerated.

Very severe requirements are placed on an ESG, and only their fulfillment has enabled this accelerator to take a secure place among the other accelerators, despite the fact that the energy of the particles from the ESG is smaller by a factor 1500 than that from the proton synchrotron ("synchrophasotron"). What are these requirements

The potential difference produced must be not less than 1.5 Mv (one of the reactions most often used to produce monochromatic neutrons, the reaction $H^3(p,n)He^3$, has its threshold at proton energy 1.019 Mev). Smooth variation of the energy of the accelerated particles must be provided for. The absolute value of the energy of the accelerated particles must be measured with high accuracy, and the monochromaticity of the beam must be strictly maintained. The amount of proton (or deuteron) current must be adequate for physical researches.

The electrostatic generator can be used for the study of the excitation levels of light and intermediate nuclei, for the study of nuclear reactions (particularly those involving light nuclei), and to produce beams of monochromatic neutrons (by the acceleration of deuterons and protons). Electrostatic generators in which electrons are accelerated are of great importance in the study of chemical reactions. Finally, ESG's serve as injectors for other accelerators.

*Generators with one belt are certainly more commonly used.

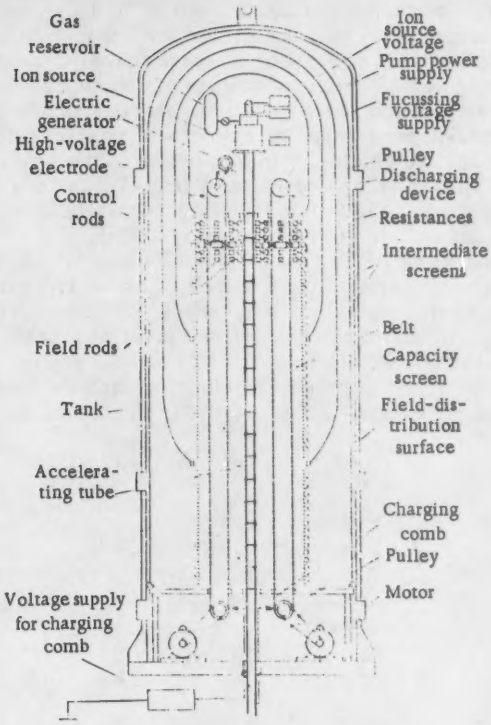

Fig. 4. Section of a 3-Mv electrostatic generator.

Voltage Stabilization of the ESG

The operation of the ESG is characterized by three features that are very important for physical researches:

1) the possibility of regulating the energy of the accelerated particles, beginning at 15 to 20 percent of the nominal value;

2) maintenance of constancy of this energy to accuracy 10^{-4};

3) the possibility of determining the value of the particle energy to this same precision.

These features are achieved by regulation of the potential of the high-voltage electrode over a wide range to accuracy ~ 0.01 percent, and by insertion into the path of the beam of charged particles of a filter (monochromator) that "cuts out" all particles with energies larger or smaller than the prescribed value. The monochromator is at the same time the sensing device for the voltage-stabilization system.

The voltage spread of the beam of particles at the output of the accelerating tube can arise from instability of the voltage on the collector (the high-voltage electrode) and from inequalities in energy of the ions coming from the source. In high-frequency sources, which are often used in electrostatic accelerators (60 out of the 110 ESG's have high-frequency sources) the excitation voltage of the discharge is small and the spread of energies of the ions does not exceed 20-30 ev, i. e., less than 0.001 percent of the nominal value of the accelerator energy. This inhomogeneity can be neglected.

of large electrodes become centers of local corona discharges (unterminated discharges). In installations of relatively low power, corona losses have led to sharp lowering of the generator voltage or to breakdown.

In compressed gases (nitrogen, air, carbon dioxide) the breakdown voltage in uniform or nearly uniform fields increases almost in proportion to the pressure as it is taken up to 8 or 9 atmos (Fig. 7), and reaches values around 250 kv/cm [10]. Beyond this the increase of the breakdown voltage becomes slower.

In operating ESG's, the calculated potential gradient is chosen considerably smaller than in laboratory experiments, and does not exceed 120 kv/cm, in a mixture of nitrogen and carbon dioxide at a pressure of 16 to 20 atmos (see table). In many generators the breakdown gap between the electrode and the tank is divided up by two or three screens to smooth out the field.

Table

Characteristics of Some Electrostatic Generators

	Year of completion	Operating potential, Mv	Gas	Pressure, atmos	Height of an element of the accelerating tube, cm	Field strengths, kv/cm	
						in the gas space	along the column
U.S.S.R.	1956	4—5	N_2+CO_2	20.0	2.5	95	12
	1953	3.0	N_2+CO_2	8.0	3	120	10
	1953	1.7	$N_2+CO_2+SF_6$	8.0	3	140	14
U.S.A	1956	5.5	N_2+CO_2	16.0	—	120	14.8
	1956	3.0	N_2+CO_2	20.0	—	110	17.3
	1955	2.0	N_2+CO_2	24.5	—	—	24.4
France	1952	5.0	N_2	10.0	—	—	13.3
	1955	5.0	$N_2+CCl_2F_2$	20.0	7,5	140	13.5
England	1956	3.8	$N_2+CCl_2F_6$	10.0	6,7	150	13.8
Canada	1951	4.0		28.0	—	—	14.6

Such a decided difference between the maximum field strengths produced under laboratory conditions (true, for electrode separations not exceeding 15 cm) and the operating field strengths in actual equipment is explained by contamination of the electrodes, for example by the dust which is very easily formed in belt ESG's.

The addition of a small amount of sulfur hexafluoride (SF_6) considerably increases the breakdown field strength (see Fig. 7). The distance between the high-voltage electrode and the tank for a 5-Mv generator can be taken to be 50—60 cm without sulfur hexafluoride and 35—40 cm with sulfur hexafluoride. The use of compressed gas has completely eliminated the difficulties that prevented increase of the voltage of a generator in the open air.

Immediately afterward another problem arose — that of increasing the breakdown field strength along the generator column.

In apparatus in the open air, in which the supporting column was a cylinder several meters high, the operating field strength along the column was 3 to 4 kv/cm. The use of a compressed gas and an imposed potential distribution along the height of the column obtained by spacing rings placed 3 to 6 cm apart increased the working gradient only by a factor of two (up to 6 or 7 kv/cm). At this field strength flashovers along the belt set in. The belt was under especially unfavorable conditions, since the charge it was transporting and the charge on the collector produced a sharply nonuniform potential distribution along the belt. The insertion of spacing planes and special rods at the sides of the belt (Fig. 4) sharply changed this distribution (Fig. 8). This made it possible to increase the working gradient along the height of the generator to 8 kv/cm. Further increase of the field was prevented by breakdowns in the tube.

During the last ten years a great many researches have been devoted to the phenomena occurring in the tube, but the cause of breakdowns in the tube has not yet been made clear. It is therefore natural that each constructor of generators puts forward his own construction of the electrodes and his own shape of the insulators of which the tube is made.

The working pressure in the tube is $5\text{-}6\cdot10^{-6}$ mm Hg. At this pressure the breakdown depends not on the medium but on the electrodes. For smooth and specially prepared electrodes the breakdown field strength in a uniform field is ~ 250 kv/cm. But in practice a breakdown in vacuum occurs at much smaller intensities, because of microscopic irregularities on the electrodes (coldemission of electrons), oxide films (lowering of the electron work function), liberation of gases from the electrodes, and so on.

A particularly sharp reduction of the breakdown field strength in vacuum is observed in ion tubes. As a rule the breakdown (complete or partial) takes place along the surface of the porcelain insulators that make up the tube, since the breakdown voltage along the surface of a dielectric in vacuum is much lower than that through the evacuated space.

The flashover process is favored by the secondary electron current; this effect was found by Turner in 1950 [12]. Secondary electrons are produced in the tube as a result of partial breakdown in chinks at the

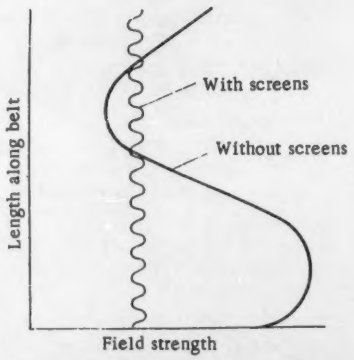

Fig. 8. Field distribution along the belt with and without field-spacing planes (screens).

joints, where residual gas lingers. This electron current increases rapidly with increase of the voltage, and the operation of the tube becomes unstable. Just this process has been the obstacle to the further increase of the voltage of ESG's (above 5 to 6 Mv). From the table and Fig. 9, it can be seen that even now the field along the height of the generator, as limited by the use of a tube, has a scatter over values from 9 to 24 kv/cm.

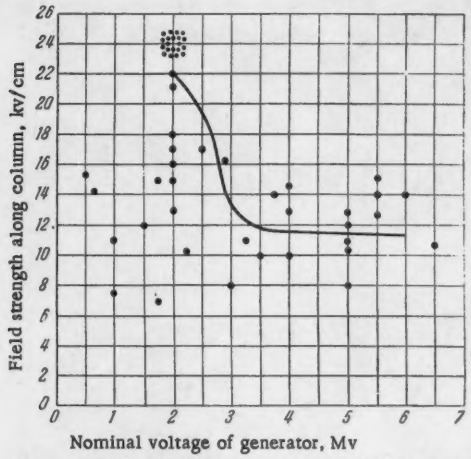

Fig. 9. Field strength along column plotted against voltage of the ESG (constructed from data on 60 ESG's [5]).

Extensive studies made in laboratories with tube components and entire tubes have shown that discharges in them depend on the height, shape, and material of the insulating cylinders, the way they are joined together, the shape of the electrodes, the degree of focusing of the beam, the reduction of the electron current, and perhaps other factors that have not yet been established.

The first ion tubes consisted of porcelain cylinders of height 50 — 60 cm and had an operating field strength of about 2 kv/cm. The inside surfaces of the cylinders were not protected against electron impacts, and therefore breakdowns occurred through tubes that were inadequately aged.

In generators operated under pressure, the height of the individual sections was first decreased to a few centimeters, and then about 1947, to 0.8 cm [13]. The increase of field strengths with a decrease of the distrance between the electrodes (an effect characteristic for all kinds of electric breakdown) brought with it an increase in the number of "weak" places in the tube -- places where the sections are joined, and where discharges may occur. Therefore the height of the sections was increased to 2.5 cm [14]. Recently satisfactory operations have been secured with tubes having a section height of 5 cm [15]. Bench tests have shown that reduction of the height of a section from 5 to 2.5 cm increases the flashover field strength by 15 to 20 percent.

The opinion has been expressed in French papers that the use of unglazed porcelain leads to an increase of the flashover voltage. A test made in the U.S.S.R. by A. A. Tsygikalo has not confirmed this assertion. It has also been found that replacement of smooth porcelain by wavy porcelain leads to an increase of the flashover voltage, in particular the voltage at which partial discharges appear, by about 25 percent.

The method of joining the individual sections is of great importance. The following considerations can be given: any joint in which there is a crease or chink can be a source of electrons when voltage is applied to the tube. Since gas remains in the chink when the tube is pumped out, its breakdown strength is less than for good vacuum, and the field strength is increased because of the redistribution of the potential cause by the difference of the dielectric constants. If furthermore the formation of partial discharges occurs in the cylindrical part of the tube, the discharge goes over into a gliding type, and flashover begins on the whole tube element. In order to reduce the danger of partial discharges, the end surfaces of the porcelain sections are metallized, or lead gaskets are placed between the sections. The porcelain sections and electrodes are glued together with BF-4 cement. The flashover voltage of a section in vacuum depends on the shape of the field between the electrodes near the porcelain. Some weakening of the field is secured by a flange on the cathode electrode (Fig. 10).

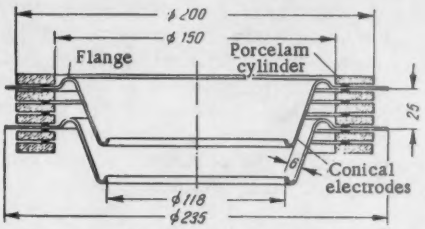

Fig. 10. Shape of the tube electrodes (dimensions in mm).

The distribution of voltage along the height of the tube is secured by the use of intermediate electrodes connected to the field-spacing planes of the generator. The shape of the electrodes is so chosen that they hinder the bombardment of the inside surface of the dielectric by charged particles. The shape of electrode generally used is conical (Fig. 10). The electrodes are crimped over at the inside edge, the radius of curvature and the aperture of the cone being computed so that the electric field at the summit of the cone will always send electrons formed on the electrode surface by impacts of positive ions toward the center of the tube.

As a result of a number of such measures tubes have been operated in ESG's with potential difference 3 -- 5 Mv with average gradients of 10 kv/cm along the tube; in some cases the gradient is 15 kv/cm. Even with these relatively small gradients, however, it has not been possible to get the generator voltage higher than 6 Mv.

Alvarez [16] has proposed the construction of an electrostatic generator using charge transfer between ions. We shall give the basic figures of the plan for an English apparatus [17]. The acceleration of the particles occurs along two successive tubes whose axes coincide. A potential of 6 Mv is applied to the place where the tubes are joined together. Negative ions are introduced from the grounded end into the first tube and are accelerated to energy 6 Mev. Inside the collector the negative ions pass through a thin gas or metal target and are converted into positively charged ions. Having 6 Mev of energy to begin with, the posi-

tive ions are accelerated to twice this energy in the second tube, which is grounded at the output end. Thus in the charge-transfer accelerator, the ions receive an energy of 12 Mev, but the insulation is for 6 Mv. Difficulties arise, however, with the production of significant numbers of negative ions. The proton current in the charge-transfer accelerator is much smaller than in the usual case; but it must be kept in mind that cross sections for reactions increase much more rapidly with increase of the energy than the number of particles. To produce the negative ions one uses a high-frequency discharge or charge transfer to positive ions.

It must be noted that the construction of a charge-transfer generator uses the components and fittings of ordinary generators.

A brief note appeared recently about the production of particles of energy 9 Mev in a charge-transfer generator.

The Power of an Electrostatic Generator

Not only the energy of the accelerated particles, but also their number is of great importance in nuclear researches. An increase of the strength of the beam leads to a shortening of the time spent in carrying out a physical investigation, and to better exploitation of the accelerator. Increase of the current in a beam of mono-energetic particles is not a simple problem.

The limiting value of the current is determined by the following factors: the amount of charge taken up and transported by the belt, and the leakage current; the current received by the tube from the ion source; the degree of focusing of the ion beam; the load at the target and the losses in the analyzer.

The belt is charged by sending it through a region of ionized air at a relatively low potential U_1. The charge is carried to the collector at potential U_2 (cf., Fig. 2). The value of the specific charge on the belt is determined by the intensity of the electric field E in the charging-up region:

$$\sigma = \frac{E}{4\pi \cdot 9 \cdot 10^{11}} \text{ coulomb/cm}^2$$

The value of the field intensity is usually about 60 percent of that found theoretically. An increase of the gas pressure does not produce a proportional increase of E: when the pressure is increased by a factor of 10 to 15 the value of E is increased by a factor of only 2–2.5. The calculated value of σ for generators operated under pressure can be taken to be $5-6 \cdot 10^{-9}$ coulomb/cm^2. The current in a pressurized generator, which also depends on the width and speed of the belt, does not exceed 500 to 800 μ a.

German research workers have made persistent efforts to increase the specific charge on the belt. In the generator of Becker [18] the charging of the belt was produced by friction of the belt against a dielectric roller. Because the approaching and receding sides of the belt were close to each other (the distance between them was 0.1 – 0.2 mm) it was possible to get a considerable increase of the specific charge: at a small distance the lines of force of the electric field are directed perpendicular to the belt, and the breakdown strength of air at atmospheric pressure in a uniform field between electrodes very close together is more than 30 kv/cm. But the close approach of the sides of the belt caused attraction between them and led to a decrease of the linear speed of the belt, so that there was no increase of the current.

A diagram of the charging device employed in generators being produced serially in the Soviet Union is shown in Fig. 11. At the beginning of the column sharp points are placed on the inner side of the belt, and a metal screen is placed on the opposite side. Ions from the corona discharge fall on the belt. Inside the high-voltage electrode there is a similar arrangement, but with the opposite polarity. The charge brought by the belt is taken off by the points, and a charge of the opposite sign is put on the receding side of the belt. The voltage required to charge the belt is 50 to 60 kv.

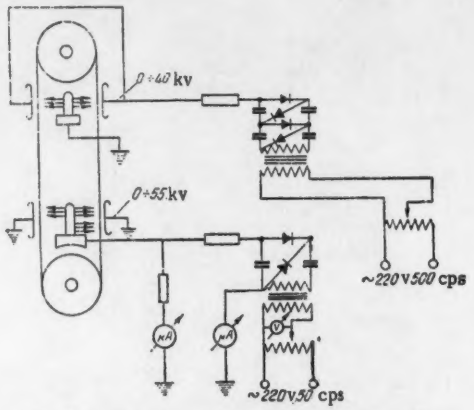

Fig. 11. Diagram of charging system of an ESG.

A considerable part of the current supplied to the collector by the belt is taken up by the current through the ohmic potentiometer, that through the electron gun for the voltage stabilization, and the leakage current. Therefore the useful current usually does not exceed 100–200 μ a.

To increase the useful current, measures are taken to reduce the parasitic electron current that arises from the impacts of the ions on the target and on the elements of the tube; retarding fields are inserted at the end and in the middle of the tube.

The particles accelerated in the tube are produced by the ion source. For a long time there was competition between two types of source: the cold-cathode source and the high-frequency source. The total current of the former is larger, but the fraction of atomic ions does not exceed 6 to 8 percent. Moreover, the cold-cathode source produces a beam with a considerable spread of energies (± 500 ev). High-frequency sources are now used almost exclusively in ESG's and cascade generators; the amount of ion current is as much as 15 ma [19] with 70 to 90 percent atomic ions in the beam, and an energy spread that does not exceed 100 ev.

In a high-frequency source with its tube made of pyrex a ring and linear discharges are excited at pressure $\sim 15\mu$. A transverse or longitudinal magnetic field intensifies the discharge. The system for extracting the ions from the discharge was proposed by Thoneman [20]. The metal cathode, 2, (Fig. 12) is pierced by a channel to let the ion beam out while maintaining the pressure difference between the discharge chamber and the accelerating tube. The cathode is usually made of aluminum. The lateral surface of the

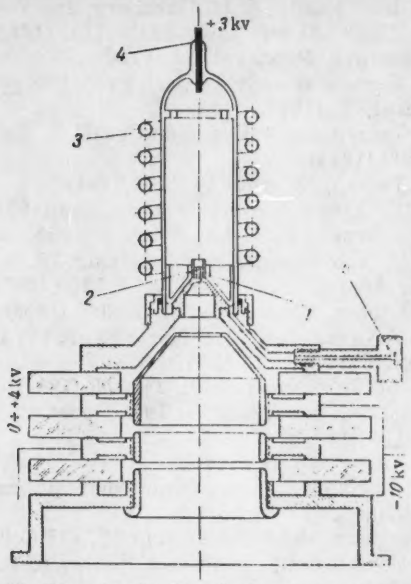

Fig. 12. Diagram of a high-frequency ion source and devices for focusing the beam. 1) quartz cylinder; 2) metallic cathode; 3) high-frequency coil; 4) anode; 5) tube for gas supply.

cylindrical cathode is covered by a quartz cylinder, 1. Gas is supplied through the tube, 5. The removal of the ions from the source occurs through the action of the potential difference between the cathode, 2 and the plasma, to which a positive potential is applied through the anode, 4. The emitting surface of the plasma and the extracting electrode form, as it were, an immersion objective. For definite ratios of the length L and width d of the exit channel and the diameter D of the quartz cylinder the beam is focused at a point in the middle of the channel's length. Experiments have shown [21] that for a source with a gas consumption of 4 cm^3/hr, power consumption 80 w, and ion current 100 μ a the most favorable ratios are $D/d = 2$, $L = 6d$, and $l = 0.6-0.8\ D$, where l is the height of projection of the quartz cylinder above the electrode. The frequency of the high-frequency generator exciting the discharge was 40 Mc. Figure 12 also shows the devices for focusing the ion beam on its emergence from the channel. The passage of the beam through the accelerating tube is mainly determined by its initial focusing in the region where the energy of the ions is small. A beam that has been well focused in the channel falls entirely on the target.

Removal of heat from the target on which the ion beam falls is difficult, since it is in a vacuum. For (d, d) reactions in the ESG, use was made of freezing onto a plate of ice made of heavy water. Such a target required constant cooling and additional pumping out of gas, and did not assure stable operation. The development of targets of zirconium or titanium with gases (deuterium, tritium) adsorbed in them greatly facilitated the work and increased the power dissipated at the target to 100 w/cm^2. Further increase of the power is achieved by motion (rotation) of the target relative to the beam, or vice versa.

It has already been remarked that part of the beam current falls on the jaws of the input and output slits of the monochromator. In a 5-Mev generator the current to the target can be 10 to 15 μ a with an energy spread of 0.01 percent, and up to 100 μ a with a spread of 0.05 percent.

Cascade Generators

A region of interest for nuclear research is that of large currents (up to 10 ma) at relatively low particle energy (about 2 Mev). The problem of producing such beams is solved by means of accelerators based on the use of systems of voltage multiplication — so-called cascade generators.

The usual scheme of voltage multiplication is shown in Fig. 13, a. The voltage drop in the system and the pulsation of the output voltage are given by the formulas:

$$\Delta U = \frac{2in^3}{3fC},$$

$$\delta U = \frac{in(n+1)}{2fC},$$

where i is the current, n is the number of stages (cascades), f is the frequency of the circuit, and C is the capacity of the condenser in a stage.

Up to very recent times cascade systems have been composed of a small number of high-votage condensers, each for a potential difference of a few hundred kilovolts. For example, the Siemens cascade generator has four stages, condensers with capacity 0.003 μ f and potential difference 300 kv (power-supply frequency 500 cps, current 2 ma). Even with such a small number of stages the energy spread of the accelerated particles is 2 percent, and the voltage drop is about 6 percent. With increase of the number of stages the pulsation of the energy of the accelerated particles is strongly increased ($\delta U \sim n^2$).

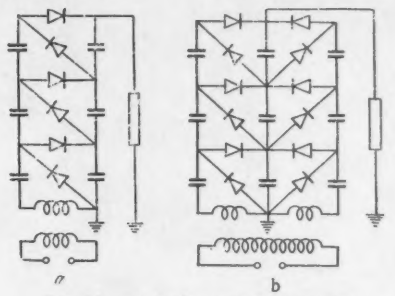

Fig. 13. Caseade generator systems a) Ordinary b) symmetrical.

The height of the apparatus is determined by the value of the breakdown field strength for the potential difference per condenser; for $U = 300$ kv it is 2–3 kv/cm; for $U = 100$ kv, 5–6 kv/cm; and for $U = 30$ kv, 6–7 kv/cm. From this point of view it is helpful to increase the number of stages, but this leads to large pulsations of the voltage. Nevertheless attempts have been made to design a generator with increased n, large capacity C, frequency of some tens of kc, and with a compressed gas as the insulating medium. But then the main advantage of the cascade generator disappeared — the possibility of producing a large current — since there was an increase of ΔU.

In 1955 Heilpern [22] proposed a symmetrical scheme of voltage multiplication (Fig. 13, b). An analysis of this system shows that δU is proportional to the first power of the number of stages, and for identical capacities in the stages and the same number of stages the voltage drop ΔU is smaller by a factor 8 than in the usual scheme. We give an example taken from

reference [23]. The calculated data for the generator are: $i = 5$ ma, $f = 10$ kc, $C = 0.1\,\mu$f, voltage per stage 50 kv, $n = 25$. In this case δU for the usual scheme is 0.82 percent, for the symmetrical scheme 0.03 percent, and the respective values of δU are 20 and 4 percent.

It can be seen from this example that with the right choice of system for a cascade generator, despite the considerable increase in the current the fluctuations of the voltage can remain the same as in an ESG.

Received September 4, 1958

Literature

1. B.M. Gokhberg, J. Tech. Phys. 10, 177 (1940) [USSR].
2. R. J. van de Graaff, Phys. Rev. 38, 1919 (1931).
3. W. Kossel and K. Herschenbach, Naturwissenschaften 6a, 166 (1951).
4. M.S. Livingston, Accelerators [Russian Translation]. (IL, Moscow 1956) p.144.
5. American Institute of Physics Handbook, pp. 8–182 (1957).
6. V.G. Brovchenko, B.M. Gokhberg, and V.V. Morozov, Dokl. Akad. Nauk SSSR 101, 1023 (1955).
7. B. Jennings, Proc. IRE 38, 1126 (1950).
8. R.L. Fortescue and P.D. Hall, Proc. IEE 96, No. 98, General, 77 (1949).
9. J.G. Trump and R.J. van de Graaff, J. Appl. Phys. 19, 599 (1948).
10. J.G. Trump, El. Eng. 70, 781 (1951).
11. V.N. Glazanov, Élektrichestvo, 3, 40 (1958).
12. C.M. Turner, Bull. Am. Phys. Soc. 25, 17 (1950).
13. W.W. Buechner et al., Rev. Sci. Instr. 18, 754 (1947).
14. M. Beckman, Tekn. tidsskr. 44, 1109 (1950).
15. S.D. Winter, L'onde electr. 35, 995 (1955).
16. L.W. Alvarez, Rev. Sci. Instr. 22, 705 (1951).
17. Electr. Rev. 161, 72 (1957).
18. E.W. Becker, Nat. forsch. 2a. 395 (1947).
19. J. Coutant, F. Prévot, and R. Vienet, J. Phys. et Rad. 18, 644 (1957).
20. P.C. Thoneman, Nature 158, 61 (1946).
21. A.N. Serbinov, Instruments and Experimental Techniques, 3, 99 (1958).
22. W. Heilpern, Helv. Phys. Acta 28, 485 (1955).
23. B.S. Novikovskii, J. Atomic Energy (U.S.S.R.) 4, 175 (1958).

THE BIOLOGICAL EFFECTS OF RADIATION

A. V. Lebedinskii

A review is given of the demonstrations shown at the Second International Conference on the Peaceful Uses of Atomic Energy (Geneva, 1958). The lines along which various problems in world science are being tackled is discussed.

In the section in which biochemical and biophysical reactions are described, a description is given of the outstanding advances made in the study of the primary mechanisms of the action of radiation, and in particular of the effects of radiation on protein and on nucleic acids.

In sections dealing with reactions on the cell itself, attention is paid to results found on the changes induced in the microstructure of the cell and the cell organoids.

The effect of the radiation on the whole organism is also considered, and particular emphasis is placed on the study of indirect changes mediated by the nervous and endocrine systems.

In the section on the effect of radiation on the species, changes induced in the offspring of irradiated animals are described, and these include both genetic changes as well as those induced directly in the embryo.

Finally, in the last section, a review is given of the problems of chemical defense against radiation, and new ways and means of therapy and prophylaxis are described.

To conclude, a summary is given of certain general theoretical conclusions reached at the Conference.

Introduction

Biological problems are closely related to those encountered in the peaceful utilization of atomic energy in science and engineering. Facts concerning the biological effects of radiation are used to establish the permissible levels of radiation for industrial workers and for the local population, in the areas concerned.

The problem of the biological effect of radiation has acquired considerable importance in recent years because of the general rise in the natural level of radiation.

In this connection, interesting data were presented at the Second Geneva Conference, where the mode of action of the different kinds of radiation on the organism was described, and new results on the relation between dose and effect were given, and numerical values for the biological roentgen equivalent presented. However, our knowledge of the biological effects developing in response to small radiation doses is as yet insufficient. This is particularly so in the case of so-called somatic effects of radiation. The general physiological basis of radiobiology has not been sufficiently well founded to allow the necessary interpolations to be made. For this reason, particular importance is attached to the results of the genetic effects of radiation, which were well presented in the demonstrations of the Conference and which are important for scientifically estimating the consequences of a general rise in the background level, and for foretelling future changes.

The problems of the biological effects of radiation have come to acquire considerable importance in utilizing atomic energy for medical purposes. In this section, the results demonstrated were of great value, especially in connection with the problem of chemical defense, which is widely used in radiation therapy. The characteristic feature of these investigations is the theoretical foundation for the measures recommended.

The large amount of additional factual material pertaining to ionizing radiation and the organism makes it impossible to include a full report of all the valuable information presented in the reports.

[1]The reference numbers given indicate the number of the report presented at the Conference. Those marked with an asterisk refer to reports quoted from the abstracts.

Study of Phenomena at the Biophysical and Biochemical Levels

In studying phenomena at the biophysical level, investigations of certain physical and biological factors were carried out, determining the relative biological effect from x-rays and from fast neutrons.

Tradescantia microspores were used, and the development of chromosomal aberrations showed that the relative biological effectivity of x-rays and of fast neutrons, having energies of 14.1 Mev, depends on the dose and on the type of aberration investigated and is greater at low temperatures [1652][1]. Results close to those previously published in the literature were obtained for the values of the relative biological effects of x-rays, γ-rays, and fast neutrons on the suppression of mitotic activity of the cells of the intestinal epithelium [1533]*. Precisely the same biological effect on the survival of male mice and on the reduction in ovary weight in females was found for bremsstrahlung having energies of 400 kev and 31 Mev, for equal amounts of energy absorbed [244].

Among the well-studied processes of radiolysis of water and the formation of free radicals and peroxides, great importance is attached to many biophysical mechanisms, such as the migration of the absorbed energy and the development of persistent metastable states [2237]. It is advantageous to use a biological method of evaluating the changes occurring in the experimental animal, and in particular to evaluate their electrical equivalent [2237] and the electronic paramagnetic resonance spectra, a procedure which allows conclusions to be reached regarding the electronic mechanism for the migration of energy in irradiated protein systems [2079]. Models have been made which consist of chemical systems reproducing the phenomena found in living organisms (Bacillus megaterium) as related to irradiation dose, water content, and gaseous constituents of the medium [908].

Several publications deal with the problem of changes induced by radiation acting on protein systems. On irradiating solid purified egg albumen with a dose of 20 -- 100 ev per molecule, the peptide bonds are opened up, so that the spatial relationships of the specific active groups are destroyed [859]. By making

use of the liberation of thiol groups as an index of the denaturation of irradiated serum albumen and serum γ-globulin, it has been found that this process is a primary effect of the action of the radiation. The degree reversibility of the denaturation is associated with the reversibility of the transition of sulfhydril into disulfide groups [1052]. Particular importance attaches to the oxidative opening of the heme ring in the hemoglobin molecule, when irradiated in aqueous solution [1657].

Radiolysis of various amino acids may be induced by several means, and amino acids show varying sensitivities to radiation; for instance, amino-butric acid and lysine are more resistant than are the other amino acids. It is interesting, that among the amino acid breakdown products, there are found amino acids having a longer carbohydrate chain than in the original substance, and this may indicate a condensation of newly formed radicals. As Barron has previously pointed out, radiolysis of certain amino acids resembles the changes occurring as a result of enzyme action [2117].

Attention is drawn to the lipides as a possible substrate for the oxidative reaction, as they may form branched chain reactions, whose part in the development of the radiation effect has attracted so much attention in recent times [2248], [920].

Careful *in vivo* and *in vitro* studies [2248] of the chemical changes induced by radiation in the lipides of the living organism have been made, including an attempt to analyze the phenomenon of the increased content of these substances in the serum, which occurs immediately after irradiation. In chick embryos, this phenomenon is associated with the increased water requirements [901].

A comparatively small amount of work has been done on the action of radiation on enzyme systems. Thus, when the spleen was irradiated outside the organism, it was found that there was an increase of 2 – 4 times in the activity of kathepsin C, which is one of the precursors of proteinase. The authors [2414] suppose, that in this case, there is not a true activation of the enzyme, but simply that it is freed from its combined form. The general problem of the fate of irradiated enzymes is being worked out on cytochrome C, where the reduction of the pure material, as well as the denaturation and auto-oxidation show a definite relationship to the presence of various other substances [1618]. From the study of a large number of enzyme systems, using doses of $5\text{-}20\cdot10^3$ r, the resistance of unpurified enzymes, including thiols (in liver extract and in homogenates) has been demonstrated. A protective action is exerted both by soluble proteins and by nonproteinous aqueous extracts of liver tissue. These enzyme systems, if irradiated when pure, are highly sensitive to the radiation [994].

After giving a general radiation dose over the range of 25 – 1000 r, it was found that for doses up to 100 r, in the spleen and bone marrow there was an increase in the activity of the thiolic enzyme which takes part in the biosynthesis of the porphyrin ring of the dehydrase of delta-amino-levulinic acid, while for greater doses, the activity was reduced. In the liver and kidneys, there was little change in the activity of this enzyme [1586].

In the co-enzyme *A* molecule, even when using special methods, no changes of any kind have ever been reported. Results have now been obtained which indicate that there is a suppression of the acetylating action of co-enzyme *A* in the liver of irradiated pigeons (dose $2 - 3\cdot10^3$ r). This is due to both the reduction in the amount of co-enzyme *A* and to the suppression of the activity of the acetyl groups of the enzyme, which take part in the process [2239]. In microorganisms, a reduction in the activity of dehydrase and of reductase has been found, whereas the activity of cytochrome oxidase undergoes very little change [2320].

Considerable attention has been paid to the study of the fate of desoxyribonucleic acid in the irradiated organism, and this interest is to be expected, because the changes in the content of this acid in cells, tissues, and organs are very well shown and represent an aftereffect of the radiation which has been very thoroughly investigated. The recognition of desoxyribonucleic acid as the basic informational system of the nucleus, leads to a legitimate interest in this compound, in connection with attempts to explain the suppression of mitosis and the origin of the genetic and other somatic effects of radiation. Following the work of Kheveshi, a fairly good correlation has been established between the radiation sensitivity of the cell and the metabolism of desoxyribonucleic acid. Finally, the ability of the nucleic compounds to stimulate hemopoiesis, which was discovered 50 years ago, continues to attract attention at the present time, because this is one of the ways of postponing death following radiation damage to the bone marrow.

Confirmation has again been obtained of reductions of 45% and 65% in the synthesis of desoxyribonucleic acid in the rat thyroid following radiation doses of 500 and of 1000 r, respectively [994]. The absolute content of desoxyribonucleic and ribonucleic acids in the bone marrow and in the spleen is also greatly reduced, the former showing the greater change. The maximal reduction is found on the fourth day after a dose of 325 – 1500 r. A similar effect in the reduction of nucleic acids is found on injecting P^{32} in a dose of 100 – 400 in mC [1236].

Following an irradiation dose of 2000 r, a frog's liver shows a marked temporary increase in the ribonucleic acid content, which is greatest in the skin [1687].

One of the reasons for the reduction in the content of nucleic acids is the suppression of their synthesis, as shown by the reduced amount of labelled phosphorus [1236] and adenine taken up, as well as by the smaller number of cells [886]. The possibility of a dissociation of the nucleo-protein complexes under the influence of radiation must not be underestimated. After further work has been done in this province, it may be useful to make a careful study of the different fractions of these compounds, and to follow their fate in the several different cell organoids. Ionizing radiation has the greatest effect on the ribonucleoproteins of the mitochondria, and then on those of the nucleolus and ergastoplasm [2319].

New experimental evidence, obtained by comparing the changes in mitotic activity with the desoxyribonucleic acid in cells of the intestinal epithelium, has further clarified our ideas concerning the part played by desoxyribonucleic acid in the suppression of mitosis induced by radiation [913].

Studies of Phenomena at Cellular Level

Investigations continue of cellular reactions to radiation, for instance of the reaction epithelium of the oral cavity to x-ray therapy [1654]. One undoubted achievement of recent work on the problem of the biological effects of radiation on the cell has been the investigation of the fate of the different cell organelles, and of the significance of the changes that they undergo in relation to the final damage caused.

Mention must be made of an interesting method of selective intranuclear radiation, using nucleic acids containing tritium. This substance is introduced into the nucleic acid molecule by growing a tissue culture in a nutritive medium containing the tritium form of the precursor of desoxyribonucleic acid -- nucleozide (thymidine). As a result, a level of activity is easily reached in the nuclei which leads to the inhibition of cell division [842].

Some interesting information has become available explaining the effect of damage of the nucleus and of the protoplasm on subsequent cellular changes. Many facts indicate that there is not much difference in the sensitivity of these two parts of the cell to radiation. However, damage to the nucleus is more readily revealed, because it contains the mechanism which controls the most important manifestations of the vital activity of the cell. The irradiated nucleus depresses the metabolism of the cytoplasm. It is interesting to note that in turn, irradiation of the cytoplasm may cause radiation damage to the unirradiated nucleus. Irradiating the nuclei of thyroid cells suppresses the processes by which phenylalanine is incorporated into protein and adenine into ribonucleic acid, the evident reason being that these disturbances chiefly concern the nucleolus. Similar results were obtained for liver cells; there may be some damage to the mitochondria and microsomes [1695]. The importance of nuclear damage in the development of subsequent radiation changes, is illustrated by experiments on the action of x-rays or neutrons on the giant amoeba. Grafting nuclei of unirradiated animals into those which have been irradiated, may prevent their death [907].

The action of radiation on the nucleus and on the chromosomal apparatus is no less interesting. Electron microscopical investigations have shown that in Steatococcus, after the action of x-rays, there is a change in the degree of twisting of the molecules of desoxyribonucleic acid lying in the microfibrillar spaces of the chromosomes [1846]. Chromosomal aberrations developing in plant cells under the influence of ionizing radiations are better shown in response to the far red end of the spectrum [884]. Results obtained on the effect of visible light on mutation in plants are included in the report [2074].

A study has been made of the relationship between the suppression of mitotic activity and the synthesis of desoxyribonucleic acid in ascitic cancer cells. Ehrlich has shown that the synthesis of desoxyribonucleic acid continues after the mitotic activity of the irradiated cells has ceased [886].

Considerable attention has been paid to problems of localized damage and fracture occurring in the chromosomes of the sex cells. For short periods of irradiation, manifest structural alterations in spermatids and late oocytes are related to the dose by a three halves power law, as has previously been established for spermatozoa [893]. In the fruit fly, the frequency of translocation resulting from irradiation of the oocytes is less than for the irradiation of sperms. Repair of chromosome fractures in oocytes may take place in the absence of oxygen, and occurs shortly after irradiation and before fertilization [170].

For the cells of Vicia faba there is a very well shown linear relationship between dose and incidence of simple chromosomal fractures, while a square law represents the case for fragments followed by exchange. The number of primary fragments is reduced in the presence of oxygen [290].

In the case of a single dose of 150 -- 450 r of x-rays applied to the animal, marked cytogenetic effects are found in some of the dividing sex cells. A comparison of the radiation sensitivity of the embryonic cells in the monkey with those in the mouse shows that the former is the more sensitive. Nuclear disturbances in monkeys irradiated with 150 r were found two years later [2476].

One universal manifestation of radiation damage to the cell, and in particular to its superficial structures and energy systems is the increase in cell permeability. In this connection, investigations of the effect of ultraviolet light on the transfer of Na^{24} and K^{42} have been made [111]. Reports were presented describing the permeability of the vascular walls in irradiated rats [903].

A detailed description has been given of genetic mutations as related to the present-day conception of radiation genetics, its advances, and future problems [893], [95], [1391], [897], [2281], [2074].

Studies have been made of mutations in the sex cells of Drosophila as related to different modes of action of the radiation; a comparison has been made of the number of lethal recessive mutations following a single irradiation with a dose of 20 or of 40 r and the same dose, fractionated, by being given in quantities of 1 or 2 r at intervals of 45 seconds. Not only was there no reduction in the number of mutations, but there was actually an increase [237], which demonstrates the occurrence of aftereffects and summation of traces of induced changes. Observations were also made on features of mutations induced by internal irradiation of male fruit flies using P^{32}. The end effect of the radiation as related to the activity of the isotope and sensitivity on each day of the experiment is given [588].

A great deal of factual material is presented which describes the relation between mutation rate and dose. Particular attention is drawn to the reduction in the number of mutations on irradiating with doses greater than 600 r [897]. An explanation of the shape of the curve showing the total effects for the sex glands of the fruit fly is given in terms of the existence of cells at different stages of development, and therefore having different sensitivities [2074]. From calculations of the deviation from direct proportionality between dose and mutation rate, it is recommended to use the optimum value, obtained with a dose of 300 r ($28 \cdot 10^{-8}$ per 1 r at each locus) [897].

Among the factors determining mutability, particular importance attaches to loci showing an inherent high spontaneous mutation rate [893]. An unsuccessful attempt was made to produce less harmful mutations in lethal genes, with respect to which the process of natural selection probably operates. Both facts may be

interpreted as consistent with the idea of a common mechanism of spontaneous radiations and those induced by radiation.

One of the most important subjects of present-day radiobiology is the study of mutations in somatic cells. According to some current concepts, these mutations which develop as a result of damage inflicted by radiation, may turn out to be the ultimate cause of the development of malignant growths. Unfortunately, little work has been done on this subject.

A study of the effect of ultraviolet light and of x-rays on mutation rate in bacteria has revealed a number of factors common to all the mutagenic processes including in particular, the necessity for the presence of amino acids and the precursors of nucleic acids in the cell, at the time of the radiation. It is natural that the suppression of protein synthesis (by chloramphenicol) affects the mutation process, which also requires oxidative phosphorylation [896]. Many of the changes in an irradiated population of yeast cells are transmitted to the offspring [1844]. One result of mutation may be an increase in the rate of division in the offspring of the irradiated population, as has been found in yeast cells [1844].

Effects on the Whole Organism

Among the characteristic features of reactions of intact organisms to radiation, those which concern the description and explanation of the mechanisms of the indirect action of radiation deserve special attention [1278]. There is no doubt that this line of investigation, which has developed from results obtained on the part played by the nervous and endocrine systems in determining the reaction to radiation, has been very successful. At the present time, it is possible to distinguish reflex reactions, endocrine factors, and the entry of toxic products into the bloodstream as distinct indirect modes of action.

Changes in the functional condition of all parts of the central nervous system have been demonstrated experimentally [2315], including cases where the radiation was given in small doses [2068]. I. P. Pavlov's conditioned reflex methods [1289], and electrophysiological techniques [2315], have made these advances possible.

On irradiating peripheral nerves, including the long axons of the rainworm and the crab, with 1-5 kr a marked increase in the peak voltage of the action potential is observed, and this later becomes reduced until the reaction has ceased altogether. Studies have also been made of the change in latent period and conduction rate [892].*

A study of the local reaction of the brain to the radiation revealed the presence of ultra-low frequency variations of the direct potential [2237]. Some time after a general dose of radiation has been given to small animals, a reduction in the amplitude of the waves of the electroencephalogram with subsequent increase, and slowing of the rhythm, is observed [891]. Systematic descriptions have been given of changes in electrical activity and of the development of neurological symptoms in apes at various times after irradiating the head with doses of from 1.5 to 6,000 r. Typically, slow waves and high voltage peaks were found. Changes in the electroencephalogram and in neurological symptoms were compared with histological investigations and with the distribution of trypan blue [891]. Studies were made of the electrical activity of various parts of the cortex and of various subcortical structures after irradiation with lethal doses of x-rays [473].*

Careful studies were made of cerebellar dysfunction in mice, and of the morphological, cytological, and histochemical changes in response to the local action of doses of up to 60 thousand r applied to the cerebellum [1053].

There are important indications of the existence of a possible relationship between the results of radiation damage in rabbits and the animal's type of higher nervous activity. In these investigations, use has been made of some indexes of autonomic function as indicating the reaction of the animal to irradiation [2480].

Interesting results have been obtained in studying the aftereffects of irradiating young rats with doses of 125 – 300 r. The greatest mortality was found in animals irradiated at 1 – 2 days of age; older animals were more resistant [891].

New comparative physiological results have been obtained which show that in mollusks, coelenterates, arthropods, and echinoderms a motor reaction may be obtained just as with mechanical, light, or chemical stimuli. The different classes have widely different thresholds: 1.5 – 2.0 r/second for Helicella candidans Pfeifer; 1.5 – 2.0 r/second for Arion empiricorum, and about 15 r/second for Helix Pomatia [992].*

At the present time, the part played by the endocrine glands in the reaction of the animal to radiation has been well studied. It was found that I^{131} acted on the rat thyroid so as to reduce the metabolic rate; the extent of the reduction was found to be proportional to the amount of radioactive substance injected. Thus for 100 mmc the basic metabolic rate was reduced by 10 – 15%, and for 300 mmc – by 31%, and so forth [479].

A study was made in guinea pigs and rats of the change in weight of the thyroid and of the size of the follicles after a general dose of 500 r. In the pancreas, changes in the ratio of the numbers of the different kinds of cell in the island of Langerhans were found, and these may be correlated with the observed change in the blood sugar curves [469].

Interesting results were obtained in analyzing the physiological mechanisms brought about by changes in the activity of the suprarenal cortex. Besides the previously established importance of the adrenocorticotrophic hormone, there have also been indications of the existence of a direct reflex effect on the suprarenals [2132]. The reaction of the adrenal cortex is found in 14 – 17-day-old rats, and is absent before the 10th day after birth. It is in this latter group that the adrenocorticotrophic hormone exerts the most favorable effect on survival [489]. Many new facts, for instance the excretion of the posterior pituitary hormone in irradiated animals under the influence of stimulation of the adrenal cortex [2132] confirms the previous hypothesis of activation as affected by irradiation of the reticular formation. This phenomenon has not yet been sufficiently investigated.

Gonadotrophin, androgen, and diethylstilbestrol applied locally exert a favorable effect on the course of skin damage developing in response to locally applied radiation in guinea pigs [1405].

TOXIC PRODUCTS. The developing toxic products in the irradiated organism have attracted the attention of many workers. Information is given in report [2316]. In experiments with parabionts, it was found that in the blood of irradiated mice substances appeared which inhibited the mitotic activity of the corneal epithelium [2080]. In the blood of 10–16-day-old rats, irradiated with a dose of 700 r, a factor was found which had the property of inducing an increase in the number of reticulocytes; the amount of this factor increases with increase of dose [494].

There is a great deal of experimental evidence which indicates that the appearance of toxic products is associated with oxidation of lipides induced by the radiation [2248].

An indirect demonstration of the formation of toxic products in the irradiated organism and of their lethal role has been provided by experiments in which a study was made of the phasic changes in the passage of tritium into the aqueous phase of the blood and organs in irradiated animals [2070]. On the basis of experiments with irradiated yeast, it is stressed that the products are not only formed at the time of the irradiation, but that they also continue to appear subsequently [2320].

An important part in the development of certain symptoms of radiation sickness is ascribed to a sensitization of the irradiated organism which develops as a result of the formation of various allergens (for instance breakdown products of the intestinal mucous membrane). The injection of extracts of irradiated organs into the tissue of the lip, induces a strong hyperergic reaction [2073].

Results are obtained which allow the changes of serological activity of the irradiated proteins to be related to the signs of their structural degradation which are revealed in this way [859].

Toxemia in irradiated animals may develop through an infectious process which is secondary to the radiation sickness. Besides studies of various endogenous and exogenous infections, results are also given of the use of antibiotic therapy (bacitracin, thiocymetin, circulin, and others) and different methods of applying these antibiotics are described [1509].

Interesting attempts have been made to activate the formation of antibodies in rabbits exposed to radiation doses of 400 r and immunized to heterogeneous erythrocytes. Experiments showed that the favorable effect on the formation of antibodies obtained by giving yeast extracts or preparations from spleen or epithelial cells, appears to be due to the action of derivatives of nucleic acids [909]. Some results indicate the possibility of facilitation of antibody formation in irradiated animals by implanation of hemopoietic cells [894].

Some mention must be made of the cardiovascular system, whose reaction to ionizing radiation has attracted the attention of so many workers. As far as the blood system is concerned, particular attention is drawn to the fact that in mice irradiated with doses of 301 -- 742 r, there are two periods at which the lukopenia and neutropenia are most marked, and these coincide with the period of bacterial infection of the bloodstream which in turn coincides with the time of highest mortality [1697]. A peripheral leukocytosis, found in rats exposed to the action of fast neutrons (doses of 50% lethal amount given over 30 days) coincides during its development with the expansion of the sinusoids of the bone marrow [1007]. One of the indications of disturbance of function in the hemopoietic tissue is the abnormally high retention in the bone marrow of Fe^{59} in the irradiated animals, which is found to occur 24 hours after giving radiation doses of 100–600 r [1797]. In the final stages of radiation sickness in rats and mice, the anemia associated with liver damage is of considerable importance [2481].

Confirmation has been obtained of the occurrence of binucleate lymphocytes following irradiation of human subjects with small doses of γ-rays (0.1–0.2 r/week, or a single dose of 2.4 or 2.6 r) [888].

In considering the origin of changes in the bone marrow which occur as a result of radiation, it is essential to consider not only the local action on the bone marrow itself, but also indirect effects. This is particularly true in the case where there are changes in the nucleic acid content of the nuclei of the bone-marrow cells. The beneficial influence of the unirradiated parts of the body depends on the action in them of hemopoietic zones [2080]. Recovery processes in the lymphatic nodes of rats irradiated with a general dose of 300 r from γ-rays of Co^{60} are found several days after irradiation. In the new cell population, changes are found in the total amount of desoxyribonucleic acid, and the nucleus is enlarged [1390].

Preparations of desoxyribonucleic acid and ribonucleic acid prepared from different organs and free from albumen, increase survival in rats irradiated with lethal doses of 750 -- 800 r. Best results are obtained from spleen and liver preparations. A negative effect is found when using heterologous nucleic acids [490].

There are many reports of attempts to stimulate hemopoiesis in irradiated animals. It must also be noted that the addition of chick embryo extracts to bone marrow taken from guinea pigs irradiated with a dose of 600 r increases the rate of synthesis of desoxyribonucleic acid, which under these conditions is depressed, from 13 – 35 to 90% of the normal value. The nucleotide fraction of the extract exerts a similar action.

The injection of pirimidine desoxyribonucleotides had a favorable effect on the blood of mice irradiated with a dose of 500 r; a similar effect was shown also by desoxycytidylic acid [2121]. A favorable stimulating effect on survival was also effected by the serum of normal horses or of horses rendered anemic by bleeding [487]. In reference [2238] a favorable result is reported from using leukocytic and thrombocytic masses for radiation sickness therapy.

Work continues on injecting irradiated animals with suspensions of bone marrow, spleen, and lymphatic nodes. Characteristics of the chromosomal apparatus are used as a control over the fate of the transplanted cells, and confirm that it is possible to transplant both homologous and heterologous cell material [97]. The transplanted cells afford useful protection to the host during the time of acute radiation sickness, but subsequently may be the cause of complications brought about by immunity reactions [555].*

Granulocytosis may be induced in mice and in guinea pigs which have been irradiated with lethal doses, by giving a single injection of bacterial toxins prepared from Salmonella typhosa or Escherichia coli [889].

Detailed descriptions have been given of the changes in the activity and functional condition of the heart in partially and in totally irradiated rats; the conclusion reached pointed to the significant effect on changes in heart muscle of irradiating different parts of the body; i.e., attention was drawn to the importance of the indirect effect of the radiation [903].

In the reports, great importance is attached to investigations dealing with the study of remote somatic effects: these include shortening the length of life by inducing early aging, the development of leukosis and other malignant growths.

Another problem is that of whether it is possible to shorten life through aging following a single exposure to radiation, or by the chronic effect of small doses [1857]. A large amount of material has been collected from experiments on mice [4] which were given a single dose of 50 – 850 rads. A shortening of the life span was found in animals given large doses, and a careful study was made of their symptoms and of the causes of death. The results were systematically related to dose, to time of action, and to the age of the animal. For determining the animal's condition, a number of tests were used which included recording the motor activity [292].

The life span of the offspring of irradiated individuals is also reduced by the action of x- and of γ-rays [897]. Similar results were obtained using neutrons.

In studying the effect of injections of Sr^{90} on the length of life in mice, statistically significant results were obtained when injections of about 44 mC kg of Sr^{90} were given [911]. Remote consequences resulting from the continuous action of small amounts of Sr^{90} on dogs are given in report [2077]. Attempts have been made to analyze the mechanism of the "aging" effect of x-rays, and of the therapeutic effects of the process of aging [109]. It is supposed that the reason for the reduction of the life span of an amoeba is due to nuclear damage [1695]. New experimental results on the aging process resulting from the action of radiation are given in report [912], where, incidentally, by observing the different biological effects of neutrons and x-rays on aging, the conclusion is reached that different sources of radiation produce different effects [292].

In spite of the great scope of the tests, which included measurements of the physiological age of the animals, difficulties still remain. It is unfortunate, for instance, that insufficient attention was given to evaluating the condition of the connective tissue as an age index. In general, connective tissue is not sufficiently studied. Only a single report gives experimental results describing the condition of the mast cells of the connective tissue in irradiated animals [1130]. Certain papers, reporting results of the study of malignant growth and leukoses in animals exposed to radiation, deserve special attention.

Insufficient attention has been paid to the problem of the development of osteosarcoma following injections of small doses of radioactive substances. The amounts accumulated in the skeleton at the end of the arbitrarily selected period of one year are given for various isotopes. For instance, for amounts of Ca^{45}, Sr^{89}, and Sr^{90} giving the highest incidence of tumors, the skeletal dose for mice was 40 – 60 krad. The minimal tumor-inducing dose was 150 – 1000 rads [61]. In studying osteosarcomas in mice, for average doses there was no linear relationship between the amount of radioactive substance induced and the tumor incidence. It is therefore thought not to be possible to interpolate to the region of small doses, and the threshold nature of reactive tumor growth is proposed [911].

From statistical results obtained between 1949 and 1955, tests have been made in the USA of a presumed relationship governing the incidence of osteosarcomas. It appears that there has been no recent increase in mortality from this cause. No linear relationship was found between the incidence of the illness and the small amounts of radioactive matter accumulated. The graph of the mortality from sarcomas has the usual appearance of a Gompert's curve, whose shape has not shown any change in the last few years [1060].

In connection with the problem of osteosarcomas originating as a result of radiation, particular attention has been paid to changes induced in bone in this way. It is found that after local irradiation of one limb of a rat with 2000 r one week after irradiating both limbs, a well-marked reduction in the rate of uptake of Ca^{45} can be observed in the proximal ends of the femurs [241]. This result not only illustrates the relatively high sensitivity of bone to radiation, but is also evidence of the considerable part played by the indirect effects in inducing trophic distrubances. The importance of general factors in controlling local changes preceding tumor development is clearly shown by the fact that for Ra^{226} no direct relationship was found between its localization in the bone and the extent of the changes induced [910].

Of the special problems concerning radiation and cancer, the quantitative relationship between the incidence of bronchogenic cancer in rats, following the irradiation of their lungs, deserves attention. It is found that there is a special danger of the formation of complexes consisting of the radioactive substance and tissue proteins [900].

In experimental leukoses, particular importance is paid to the size of the dose as a controlling factor; the author concludes [96] that the development of a leukosis represents a threshold reaction. An investigation of great practical importance related to the development of leukosis in children to the irradiation to which the mother has been exposed in the prenatal period [890].* Confirmation is given of a relation between the profession of radiologist and the incidence of malignant tumors, including leukosis [99].* Results are given of the incidence of leukosis in human subjects exposed to radiation (Hiroshima, Nagasaki), and the effects are related to dosage [905].*

As has already been shown, the threshold nature of the tumor growth reaction has been noted by many investigators. However, in studying the relationship between tumor incidence of the mammary glands in rats and the radiation received by the animal (25–400 r), the relationship is found to be linear, and the straight line graph intersects the ordinate in the small dose region [885].

Thus, the problem as to whether the reaction is threshold or nonthreshold, appears to be quite complicated on account of: The existence of a considerable latent period in the appearance of tumors; for instance renal tumors in mice may be found 10–32 months after irradiation: it is probable that the duration of the latent period increases with reduction in dosage;

The death of the animals prevents the tumor incidence from being established for moderate doses; increasing survival causes an increase in the number of tumor cases [1696];

The marked effect on tumor incidence (even with localized radiation) of hormonal factors, and such general aftereffects of radiation as disturbance of endocrine balance. In this connection results have been given on the importance of the hypophyseal growth hormones, thyroxin [61], and of the ovarian hormones ([110], [85], and others). Further, if the reaction of tumor growth is of a threshold type, then the value of the threshold is very different for tumors of different origin, varying, for instance, in white mice, from 50 to 600 r; i.e., each tissue has its own malignancy threshold [110].

Effect of Radiation on Developmental Processes

Results of considerable importance describing the effect of ionizing radiations on gonads and on the processes of development have been intensively studied in recent times.

Investigations have been made of the harmful effects of radiation on the rabbit ovary, and the number of marginal follicles before and after radiation had been counted. It is very probable that the recovery processes follow an exponential law [1684].

The irradiation by γ-rays of silkworms and the treatment with P^{32} causes males to lose the power of fertilizing females. Histological investigations and the use of radio-autography show that this effect is produced by irradiation of the testis, but only at a certain period of spermiogenesis [1344]. Changes in the testis of the fruit fly may be greater with continuous irradiation (100 r per week) than when a single dose of 600 r is given [237].* Rabbit sperm and the fertilized and unfertilized rabbit ova were irradiated *in vivo*, and the radiation sensitivities of the sperm and ova were determined by observing the subsequent development of the offspring. It was found that the order was as follows: spermatozoa, unfertilized ova, fertilized ova. No unfavorable effect on these tissues resulted from the action of doses of 45--800 r [899].*

In experiments on rats, the pregnancy dates were determined during which irradiation of the animal or injection of P^{32} caused the death of the fetus, or which interfered with its development. By comparing the aftereffects of x-rays or of P^{32}, definitive qualitative and quantitative relationships concerning the development were established, and a good correlation found between the effect and the metabolic condition of any particular organ at the time of irradiation [902].

In mice, the parents were irradiated, and the effects on subsequent irradiations, as far as the third, were studied [292].

Chemical Protection

The problem of the protection of plants and animals from the harmful effects of ionizing radiation were well represented at the conference. This is understandable since, firstly, the possibility of such a protection being realized is well established and has been shown to be practicable, and secondly, the degree of effectiveness of certain prophylactic measures, whose mode of action is understood, enables experimental tests to be made of various of the present-day theoretical conceptions of the effect of ionizing radiation on living objects. Finally, active work on this problem in many scientific research centers has undoubtedly led to new advances, as is shown in reports [898], [2121], and [556]. Some further points can now be given. For instance, cysteine has continued to attract the attention of many workers. Good and careful work on the fate of this substance in the body and in various types of tumor cells has been carried out using labelled S^{35} [242]. New criteria for the protective action of cystamine have been employed, and these have consisted of estimating the quantitative effect of the "protection" according to the extent of the effect produced in protected and unprotected irradiated animals, as judged by the suppression of the synthesis of desoxyribonucleic acid and of the reduction in the activity of the enzyme cathepsin. By using this index, it was possible to show that the protective effect on the liver is found in the first 6 hours, and in the spleen and thyroid gland, during the first 24 hours [991].

It is important to determine the value which causes damage to the cell nucleus and to the mitochondria, and here it is important to reveal the S^{35} in the nuclei and mitochondria of the spleen and liver, using microautoradiography [995].

One of the mechanisms of the protective effect of the thiol compounds consists in the formation of complexes of these compounds with proteins, and the formation may be detected polarographically [1694]. Cysteine was found to be the most effective factor for limiting the oxidation of liver lipids [2248].

Hypothermia reinforces the protective action of cysteine [1686]. By this method (which is still in the experimental stage), it is hoped to overcome one principal disadvantage of cysteine, that of the necessity for applying it only a short time before irradiating. It has been shown possible to provide an effective defense for living objects which have been irradiated at a low temperature, even when the cysteine has been given after the irradiation [993].

Cysteine causes no statistically significant difference in the uptake of Fe^{59} in the bone marrow, liver, or kidney [1798]* in the first few hours after irradiating with doses of 100--600 r. Attention is drawn to an unexplained property of cysteine, which consists in increasing the number of mutations induced by radiation [898].

A good medicine may always be improved. It was found effective to use substances with a certain definite distribution of functional groups in the molecule, but having an elongated hydrocarbon chain [2113].

In determining the radiation sensitivity of the nervous system and the part played by it in the course and development of radiation sickness, studies were made of substances having a specific protective effect on it. These included reserpine and indole derivatives; serotonin (5-hydroxytryptamine) was found to be effective [996].* Mercaptobenzothiazole is found to facilitate the restoration of cortical function impaired by the action of radiation [1289].

By using desoxyribonucleic acid in the bone marrow and spleen, as well as the excretion of creatine and methylnicotinamide in the urine as indexes, a favorable effect of methionine on the course of radiation sickness was demonstrated [1655].*

Results on blocking the mitochondria with special dyes and with surface activating substances, as a

method of reducing radiation sensitivity shows promise that methods perfecting protective substances will be developed [2320]. Descriptions are given of the features of the structure of substances favoring the most rapid reaction with radicals [915].

General Theoretical Conclusions

Important theoretical conclusions may be drawn from the results obtained, and these are of great importance for the future progress of radiation biology. Until recently, such work would have appeared useful only as concerning the primary physical and physicochemical mechanisms of the action of radiation. At present, advances have been recorded in formulating and solving problems at a physiological level involving wider biological relationships. Some theoretical postulates concerning the physiological relationships have been noted above, including in particular, problems of the reaction in the form of mutation, of the substrate of the reaction, and of the laws governing its occurrence and development; the problem of whether tumor growth reaction is a threshold or a subthreshold phenomenon; the part played by the indirect effect and by the general reaction of the organism in the production of localized damage, etc. Among other physiological changes, particular attention is drawn to the problem of recovery from radiation damage. It has already been proposed that it is precisely the occurrence of recovery processes following small doses of radiation that stimulates the threshold character of many somatic effects, and that it is for this reason that for complex processes the relation between the effect and dose is expressed by a sigmoid curve.

A valuable attempt has been made to apply the results of histological investigations to compare the course of the destructive, regenerative, and repair processes as phases which succeed each other in the irradiated animal [2324]. Interesting observations have been made on the part played by nonirradiated systems in the course of the recovery process of irradiated tissue, where, evidently, a specific influence is exerted [2080].

Naturally, these considerations concern only a small part of the problem of the recovery process. Ways and means which might lead to a goal necessitate solving many problems, beginning, for instance, with the important effects on the hemopoietic system, before proceeding to the problems concerned with the basic nutrition of the damaged organism [218].

When the recovery process is weak, or absent, a summation may occur of effects which have not been sufficiently studied during the exposure to the radiation. It is necessary to distinguish between recovery from local injury and compensation for irreversible, or for not completely reversible changes. Compensation for destructive changes is brought about by nervous and endocrine mechanisms.

A problem which is of particular importance both from the theoretical and from the practical point of view is that of the different aspects of radiation sensitivity. It is equally important to determine the factors influencing this sensitivity, as to elaborate methods for controlling it, as, for instance by chemical methods of protection [1392].

Attempts have been made to consider radiosensitivity as a result of the operation of a genetic system which determines the sensitivity of an organism to the effect of the environment. Lines which are sensitive to radiation are less uniform phenotypically [1906].

Interesting results have been obtained which demonstrate a correlation between the radiation sensitivity of tissue and the tension of the dissolved oxygen in the immediate neighborhood of the cell. For bacteria, and for the ascitic Ehrlich tumor cells, this relation takes the form of an exponential curve. It is useful to apply this consideration to the analysis of the radiation sensitivity of various tissues, as relate to the different conditions determining oxygen tension. The authors [293] correlate such an oxygen effect with the local chemical changes which may lead to chromosomal damage. Experiments are described which illustrate the reduction in the degree of damage to hair follicles in mice, following reduction of the blood supply or replacement of the air by nitrogen over the irradiated cutaneous areas [1784]. The importance of oxygen for the chromosomal reaction has been considered above.

The question has been raised as to whether there may be a change in radiation sensitivity as a result of the action of the radiation itself. In other words, is it possible for the organism to adapt itself to any extent to changes in the intensity of the action of this physical factor? This question has not yet been answered with respect to the ionizing radiations, which are one of the most important factors of the internal and external environment.

An increase in radiation sensitivity occurring under the influence of radiation might be the outward sign of an adaptation, but for the increase in threshold to represent a true adaptation in the biological sense of the word, it should be permanent. Therefore, despite the interest of the discovery that after relatively small doses of radiation, the ability of Sacharomyces cerevisiae to withstand large doses is increased, this phenomenon cannot be considered as a true adaptation in the strict sense of the word. The acquired resistance is lost after a certain time, and after repeated irradiation [108]. Increased sensitivity in mice, following a preliminary dose, could not be demonstrated [2080].

Since there is no proof of adaptation, it must be admitted that a reaction may develop which consists of a temporary reduction in sensitivity, a reduction which may arise as a result of irradiation. This phenomenon may be arbitrarily referred to as an adaptation, and it is found in cells of the rat sarcoma [108], and has also been studied in the whole animal [1698]. Experiments show that when thyroid cells of control mice, which have previously been irradiated, are grown outside the organism, they show the same sensitivity to radiation, although the same cells in the body of the irradiated animal are more resistant than are those of controls [1698].

The problem of the possibility of adaptation to small doses remains unsolved; however, it is not easy theoretically to admit the existence of this phenomenon, which consists of a maintained increase of threshold induced by the action of a stimulus, if we consider the possibility of the nonthreshold nature of the underlying physiological reactions. This doubt applies to the genetic consequences of the action of small doses of radiation, which may represent a danger to mankind [897].

Experiments with small radiation doses are important, and for the reason that the reactions studied in this way are free from complication due to the superimposition of pathological effects. Attempts to study the effects of small doses hold out just as much promise, as do efforts to understand the action of irradiation by studying the effect of irradiating different parts of the body [109]. The data available at the present time indicate that small doses of radiation may be concerned in many biological effects [2068], [888].

Since the doses used approximate more closely to the naturally occurring level than has been the case in previous experiments, it may be possible to solve experimentally the problem of the biological effect of naturally occurring radiation as a factor of the external and internal environment of the organism, a factor which evidently has a specific biological action. Evidently, success in solving the many fundamental problems of the biological effects of radiation will depend in large measure on the extent to which it will be possible to apply general physiological and biological principles. The present conference marks an important stage in the solution of these problems through international cooperation of scientists.

The author wishes to express his thanks for help in drawing up this report to Professors V. S. Balabukha, N. N. Demin, M. P. Domshlak, N. A. Kraevskii, and to their scientific collaborators Z. N. Nakil'nitskaya and S. I. Krauza.

Received November 13, 1958

THE STEREOTRON — A BETATRON WITH A HELICAL EQUILIBRIUM ORBIT

B. N. Rodimov

The accelerator to which we have given the name stereotron is a variety of betatron with a constant guiding field, in which an accelerated electron gets into stronger fields by being displaced in the axial direction and without increase of the orbit radius. A diagram of one type of stereotron is shown in Fig. 1.

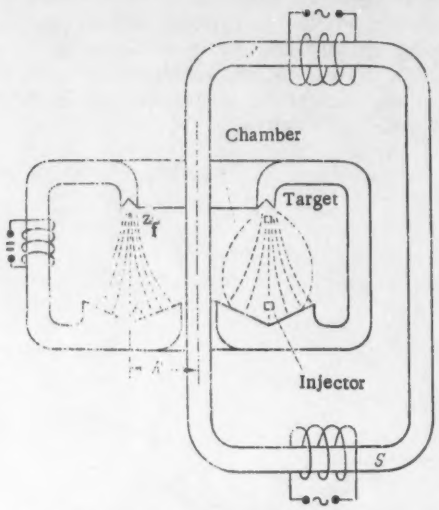

Fig. 1. A type of stereotron — a betatron with a spatial (helical) equilibrium orbit.

The constant guiding field makes it possible to use rather high frequencies in the windings on the central core. Besides this, the capture of electrons into the acceleration process can be more effective than in the usual kind of betatron. For both reasons it should be possible to secure higher average radiation intensity. In the stereotron it is easier to bring the electron beam out of the chamber; the circuits are simpler; the weight of the apparatus is less; and so on.

The magnetic field of the stereotron is axially symmetric. There is a nonvanishing azimuthal component of the vector potential, A_θ, and field-strength components H_r and H_z. Since the guiding and accelerating magnetic fields are separated, we have:

$$\left.\begin{aligned} A_\theta &= A = A_g + A_{acc} \\ H_r &= -\frac{\partial A}{\partial z} = -\frac{\partial A_g}{\partial z}, \\ H_z &= \frac{A}{r} + \frac{\partial A}{\partial r} = \frac{A_g}{r} + \frac{\partial A_g}{\partial r}. \end{aligned}\right\} \tag{1}$$

In the expressions (1)

$$A_g = \frac{1}{2\pi r}\int_0^r 2\pi r H_z\, dr, \quad A_{acc} = \frac{\Phi_0(t)}{2\pi r}, \tag{2}$$

where H_z is the constant-guiding-field component; $\Phi_0(t) = \Phi_m \sin \Omega t$ — is the flux in the central core S (Fig. 1) (Ω — is the frequency of the accelerating field).

The equations of motion of an electron are the usual equations for an axially symmetric field:

$$\frac{d}{dt}\left(\frac{m_0\dot r}{\sqrt{1-\beta^2}}\right) = \frac{m_0 r\dot\theta^2}{\sqrt{1-\beta^2}} - \frac{e}{c} r\dot\theta\left(\frac{A}{r} + \frac{\partial A}{\partial r}\right) = -\frac{e}{c} r\dot\theta\left[H_z - \frac{\overline{H}_z}{2}\right] + \frac{e}{c}\dot\theta\frac{C}{r}, \tag{3a}$$

$$\frac{d}{dt}\left(\frac{m_0\dot z}{\sqrt{1-\beta^2}}\right) = -\frac{e}{c} r\dot\theta\frac{\partial A}{\partial z} = -\frac{e}{2c} r^2\dot\theta\frac{\partial \overline{H}_z}{\partial z}, \tag{3b}$$

$$\frac{m_0 r^2\dot\theta}{\sqrt{1-\beta^2}} - \frac{e}{c} Ar = \frac{m_0 r^2\dot\theta}{\sqrt{1-\beta^2}} - \frac{e}{2c} r^2\overline{H}_z = \frac{e}{c} C, \tag{3c}$$

where $\overline{H}_z$ is the average field intensity inside the circle of radius r, and C is a constant of integration. We require that on the circle of radius R, H_r be zero for all z (Fig. 2). Since this orbit is the equilibrium one for the r direction, on the basis of Eq. (3a) for the motion of the chosen electron the conditions

$$H_z(R) = \frac{\overline{H}_z(R)}{2} + \frac{C}{R^2}, \tag{4}$$

$$\frac{dH_z(R)}{dt} = \frac{1}{2}\cdot\frac{d\overline{H}_z(R)}{dt} \tag{5}$$

will be satisfied throughout the entire time. Since the guiding and accelerating fields are separated, we have

$$\overline{H}_z(R) = \frac{\Phi_0(t)}{\pi R^2} + \frac{1}{\pi R^2}\int_0^R 2\pi r H_z\, dr.$$

From this it follows that

$$\frac{\partial \overline{H}_z(R)}{\partial t} = \frac{1}{\pi R^2}\frac{d\Phi_0(t)}{dt} = \frac{\Phi_m \Omega\cos\Omega t}{\pi R^2}. \tag{6}$$

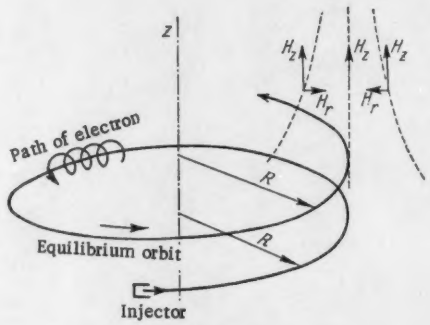

Fig. 2. Path of an electron in the stereotron.

Using Eq. (5), we get

$$\frac{\partial H_z(R)}{\partial z}\dot z = \frac{1}{2}\frac{\partial \overline{H}_z(R)}{\partial z}\dot z + \frac{1}{2}\frac{\partial \overline{H}_z(R)}{dt}.$$

Since on the equilibrium orbit

$$H_r(R) = -\frac{R}{2}\frac{\partial \overline{H}_z(R)}{\partial z} = 0,$$

by using Eq. (6) we find that

$$\frac{\partial H_z(R)}{\partial z}\dot z = \frac{1}{2}\frac{\Phi_m \Omega\cos\Omega t}{\pi R^2}. \tag{7}$$

After integrating Eq. (7) we get

$$H_z(R, z)-H_z(R, z_0)=\frac{\Phi_m}{2\pi R^2}[\sin\Omega t-\sin\Omega t_0]. \quad (8)$$

On the circle of radius R the motion of an electron in the z direction is inertial motion, i.e.,

$$\frac{m_0\dot{z}}{\sqrt{1-\frac{(R\dot{\theta})^2}{c^2}}}=T_z, \quad (T_z=\text{const}). \quad (9)$$

Using Eq. (9) and the relation valid for $C=0$,

$$\frac{m_0\dot{\theta}}{\sqrt{1-\frac{(R\dot{\theta})^2}{c^2}}}=\frac{e}{c}H_z,$$

we find

$$\dot{z}=\frac{T_z}{\sqrt{m_0^2+\frac{e^2}{c^2}H_z^2R^2}}. \quad (10)$$

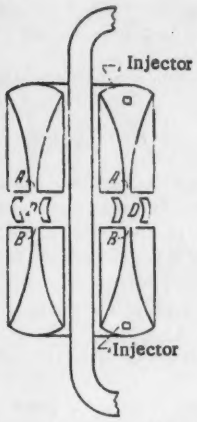

Fig. 3. The synchrostereotron — a type of stereotron with injection of electrons from both sides into the synchrotron mode of acceleration.

Integrating Eq. (10), we get $z(t)$. The constant T_z is determined by prescription of the difference of the final and initial coordinates, $z_f - z_0$ (Fig. 1). Knowing the function $z(t)$ for the "zeroth" electron (for which $C=0$), we can put the expression for H_z in the form

$$H_z(R, z)=\frac{\Phi_0(z)}{2\pi R^2}+\frac{\Phi_{\text{упр}}(R)}{2\pi R^2}, \quad (11)$$

where $\Phi_g(R)$ is the flux of the guiding field through the circle of the equilibrium radius R, and is independent of z.

Examining the field near R we easily convince ourselves that it is a focusing field for the radial direction for any value of z. To get stability of the motion in the z direction, however, we must add to the main magnetic field a supplementary constant azimuthal magnetic field. This field causes the appearance in Eqs. (3a) and (3b) of terms depending on H_0. Therefore an equilibrium electron will move around the former equilibrium orbit in a spiral (a double spiral). Similar spirals will also be followed by electrons displaced from their equilibrium orbits (Fig. 2). By varying the intensity of the field H_0 one can obtain conditions of optimal capture and acceleration of electrons. The technical realization of the supplementary field presents no difficulties.

In the scientific research institute of the Tomsk Polytechnical Institute a stereotron to produce 10-Mev electrons and operate at a frequency of 50 cps has been designed and is being built.

On the basis of the type of stereotron with its guiding field produced by coils one can construct, in particular, a synchrotron with injection of electrons from both sides, through the regions $A-A$ and $B-B$ into the region $D-D$ of synchrotron acceleration (the synchrostereotron, Fig. 3). By using two such assemblages, placed on opposite sides of the accelerating core, one can obtain an apparatus with clashing or intersecting beams of electrons or x-rays. These types of machines are also under study in our institute from the theoretical and engineering points of view.

Received October 9, 1958

THE USE OF AN INHOMOGENEOUS ELECTRIC FIELD FOR THE REMOVAL OF ACCELERATED PARTICLES FROM A CYCLOTRON

A. A. Arzumanov and E. S. Mironov

In many nuclear studies one needs to focus an external beam from a cyclotron on a target of small dimensions in such a way as to have a minimum angle of convergence of the beam and a maximum intensity. This problem can be solved if the current loss and the angles of divergence of the beam when the particles are removed from the cyclotron are small and the divergence of the beam is uniform (the size of the virtual source of the divergent beam is small).

The "plane" condenser removal system usually used in cyclotrons does not assure the fulfillment of these conditions. The deflected beam is strongly defocussed in the horizontal plane by the stray field of the magnet, and this leads either to large current losses or to large angles of divergence.

The removal system with an inhomogeneous electric field that will be described here satisfies the conditions that have been stated. In the development of this system we have made use of the experience provided by the work of N. D. Fedorov, who has carried out calculations and experimental studies of deflecting systems using inhomogeneous electric fields.

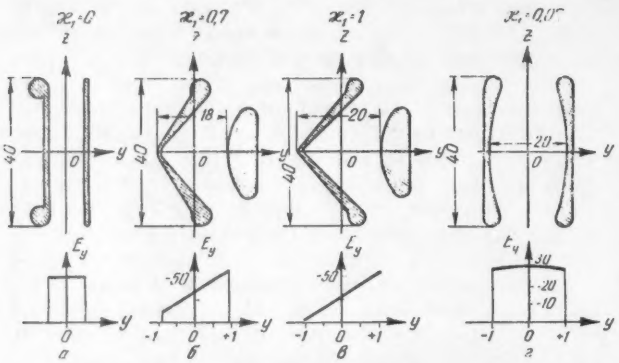

Fig. 1. Transverse section of the electrodes (dimensions in mm) and dependence of E_y on the coordinate y in various parts of the deflecting system (E in cm^2, y in cm).

The deflection and focussing of the beam in the horizontal plane ($z=0$) is accomplished by means of an electric field whose horizontal component E_y is represented by the expression

$$E_y=\frac{V}{2a}\left(1+\varkappa_1\frac{y}{a}\right), \tag{1}$$

where U is the potential difference applied to the electrodes, $2a$ is the distance between the electrodes at $z=0$, and $\varkappa$ is a parameter characterizing the rate of change of the electric field intensity ($\varkappa_1 \leq 1$).

The field represented by the expression (1) is formed between two electrodes (Fig. 1, b, c) that have the shapes of the hyperbolas*

$$\left(\frac{y}{a}+\frac{1}{\varkappa_1}\right)^2-\frac{z^2}{a^2}=\left(\frac{1}{\varkappa_1}\pm 1\right)^2, \tag{2}$$

where the signs $\pm$ refer to the two electrodes. The orientation of the coordinate axes y and z is shown in Fig. 1; the x axis is perpendicular to the plane of the diagram.

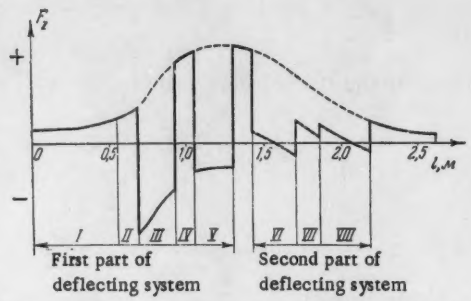

Fig. 2. Dependence of the resultant vertical elastic force F_z on the path l of a particle in the deflecting system.

The vertical component of the electric field intensity

$$E_z=-\frac{U}{2a}\varkappa_1\frac{z}{a}$$

has a defocussing effect on the beam, whereas the stray field of the magnet focusses it.

Our calculation of the focussing is based on the condition of equality of the magnetic focussing and electric defocussing forces acting along the y axis along the whole path of the particles in the stray field:

$$\beta e\frac{\partial H_z}{\partial y}(x,0,0)\,z=e\frac{\partial E_z}{\partial z}(x,0,0)\,z,\ \left(\beta=\frac{v}{c}\right).$$

From this equation it follows that

$$\varkappa_1(x)=-\frac{\beta}{E_0}\frac{\partial H_z}{\partial y}(x,0,0),\ \left(E_0=\frac{U}{2a}\right).$$

This condition gives the maximum focussing of the beam in the horizontal plane without vertical defocussing.

The calculations showed that the nonlinearity of the decrease of the magnetic field leads to an increase of the horizontal dimension of the virtual focus of the beam removed from the cyclotron. A correction for this effect can be produced by means of an electric field

$$E_y=E_0\left(1-\varkappa_2\frac{y^2}{a^2}\right),$$

where

$$\varkappa_2=-\frac{a^2}{2E_0}\frac{\partial^2 E_y}{\partial y^2}.$$

For $\varkappa_2 \ll 1$ such a field can be produced by means of two electrodes of circular shape (Fig. 1, d) with radius of curvature

$$\rho=a\frac{1+\varkappa_2}{2\varkappa_2}.$$

The deflecting system designed for the removal of the 20-Mev deuteron beam from a 150-cm cyclotron consists of two parts. The voltage on the electrodes of the first part, which is inside the dee, is 68 kv, and

*L. M. Nemenov et al., J. Atomic Energy (U.S.S.R.) 2, 1, 36 (1957).

that on the electrodes of the second part (outside the dee) is 80 kv. The total angular extent of the system is 157°; the entrance aperture is 8 mm, and the exit aperture is 50 mm.

The entire system is divided into eight sections (Fig. 2) with electrodes of different shapes. The transverse sections of the electrodes and the variation of the electric field intensity E_y for sections I, III, IV, and V are shown in Fig. 1, a, b, c, d, respectively. The electrodes in sections VI-VIII are like those shown in Fig. 1, d, and those in section II are like the electrodes of section IV.

Figure 2 shows a plot of the elastic force acting on a particle in the vertical plane. The plus sign is for focussing, minus for defocussing. The dotted line shows the component of the elastic force caused by the falling off of the magnetic field. The discontinuities in the resultant elastic force are caused by the action of the electric field of the deflecting system.

The same forces act in the horizontal plane, but with opposite signs. There is another component, however, giving an additional horizontal focussing, proportional to the square of the curvature of the trajectory.

The deflecting system whose parameters have been given makes it possible to decrease the angle of horizontal divergence of the emergent beam, as compared with the action of the system usually employed (the "plane" condenser), by about a factor of 5, without additional losses of beam current and without increasing the vertical divergence. Such a system was first proposed by the writers in 1954, in work on the plans for a cyclotron to accelerate multiply charged ions. Subsequently a similar system (without correcting electrodes) was designed by Associate of the U.A. NIIEFA, I. M. Mator, for a cyclotron with 120-cm pole diameter. Tests of this system carried out by members of the NIIEFA gave good results. With suitable choices of the parameters this type of deflecting system makes it possible to obtain from the cyclotron either a parallel beam or a converging beam.

In conclusion the writers thank L. M. Nemenov for suggesting the subject of this work.

Received October 13, 1958

THE EFFECT OF IRRADIATION ON INSULATORS

Yu. K. Gus'kov and V. F. Sachkov

Much attention is now being given to problems of the changes of the properties of electrical and radiotechnical materials when they are irradiated with neutrons and γ-rays, because of the fact that these materials are widely used in the construction of nuclear reactors [1, 2]. We have studied the dependence of the electric conductivity of porcelain, mica, and quartz on the flux density of neutrons and γ-rays and on the integrated flux of the irradiation.

The irradiation was carried out in a cooled experimental channel in the pile at the Atomic Electric Station. The diameter of the channel was 44 mm. The flux density of neutrons in the channel was $0.8 \cdot 10^{13}$ neutrons cm^{-2} sec^{-1} with cadmium ratio (gold detection) 1.5. Serious difficulties were encountered in measuring the high resistances during the irradiation of the specimens. First, at high radiation fluxes there is considerable leakage current because of the ionization of the air. For instance, at a flux of about 10^{13} neutrons cm^{-2} sec^{-1} the resistance of air is about 10^8 ohm cm. Therefore when the resistances of insulators are measured they have to be thoroughly screened. Secondly, in the lead wires and at the contacts between the measuring electrodes and the insulator the irradiation causes a photoelectric emf, which may either get added to the measured voltage or get subtracted from it. It was found experimentally that the emf depends strongly on the flux density of neutrons and γ-rays and does not depend very much on the time of irradiation. To eliminate the effect of this emf it was necessary to take voltage-current characteristics. All the measurements were made with the circuit shown in Fig. 1. The measuring device used was a type ÉMU-3 vacuum-tube voltmeter, which had a high input impedance ($5 \cdot 10^{11}$ ohm). The battery voltage was checked with a C-95 voltmeter. The resistance R_{sh} could be varied from $5 \cdot 10^4$ ohm to $5 \cdot 10^9$ ohm, so that the sensitivity of the circuit could be varied over a wide range. During the measurements R_{sh} was always smaller by 2 to 3 orders of magnitude than the leakage resistance of the lead-wire insulation and the leakage resistance through the air which restrict the upper limit on the sensitivity of the measuring circuit to $5 \cdot 10^{13}$ ohm.

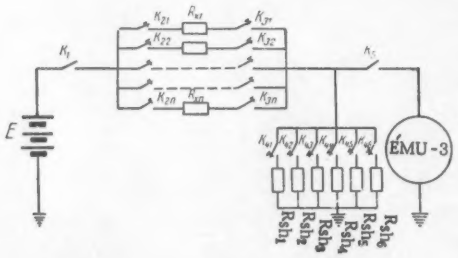

Fig. 1. The measuring circuit.

The voltage-current characteristics for all the specimens studied were taken over the range 0-2000 v, and the resistances of the specimens were determined from them. In addition, the leakage resistance of the cable insulation and the leakage through the air in the measuring unit were checked with a type MOM-3 instrument, with which the sensitivity of the measuring circuit was also checked. The studies of the insulators were made with the measuring circuit that has been described and the measuring-head assembly shown in Fig. 2.

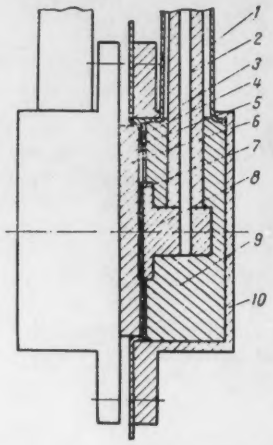

Fig. 2. Assembly for measuring the resistance of insulators under irradiation. 1) BPTE cable screen; 2) BPTE cable insulation; 3) copper conductor of BPTE cable; 4) brass guard ring; 5) aquadag guard ring; 6) specimen to be tested; 7) aquadag or sputtered silver; 8) brass electrode; 9) teflon washer; 10) case of assembly.

The specimens for the measurements were prepared in the form of disks of 20 mm diameter and of 1.5 mm thickness for the quartz and porcelain and 0.5 mm for the mica. Aquadag, or silver evaporated on in vacuum, was applied where the brass electrodes made contact with the specimen; it was found that the two materials gave the same results.

The specimen was placed between teflon washers, into which the brass contacts were pressed and through which the lead conductors were passed. This assembly was then placed in a brass case (Fig. 2). This construction makes it possible to reduce considerably the shunting action of the air and to get a high leakage resistance – about 10^9 ohm in a flux of 10^{13} neutrons cm^{-2} sec^{-1}. Nine such assemblies were constructed, three each for tests of porcelain, quartz, and mica; three of the assemblies served only for checking the temperatures of the specimens. All of the assemblies were placed in an aluminum container.

The temperatures of the specimens were checked at the places where the brass electrodes made contact, by means of copper constantan thermocouples; during a run the temperature was not higher than 160 deg C for the quartz and mica and 130 deg C for the porcelain. The fluctuations of the temperature did not exceed 10 percent and were caused by changes of the temperature of the air in the channel at a given reactor power. The lead conductors used were BPTE cable 0.5 mm in diameter.

The initial resistances of the specimens were not measured precisely, but for the porcelain and quartz it was larger than 10^{14} ohm cm, and for the mica it was larger than $5 \cdot 10^{15}$ ohm cm.

When the container with the specimens was placed in the channel of the pile, the conductivity of the mica and porcelain, and particularly that of the quartz, was considerably increased. The results of the irradiation are shown in Fig. 3. As can be seen from the diagram,

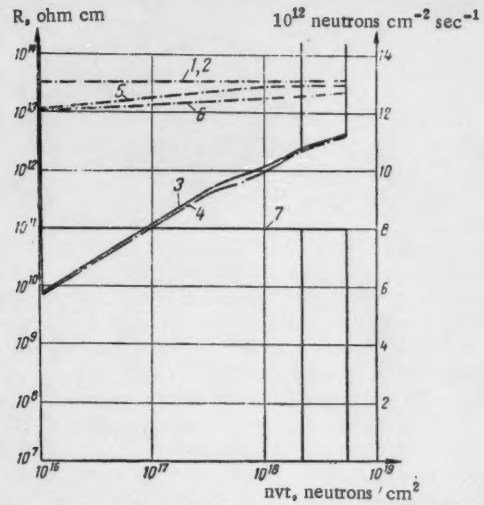

Fig. 3. The effects of the flux of neutrons and γ-rays and of the integrated radiation flux on the conductivity of insulators: 1, 2) porcelain; 3, 4) quartz; 5, 6) mica; 7) variation of the flux density of neutrons and γ-rays with the time.

at the first instant the resistances of the specimens fell to 10^{13} ohm cm for the mica, $3.5 \cdot 10^{13}$ ohm cm for the porcelain, and 10^{10} ohm cm for the quartz. With increase of the integrated flux of the irradiation the resistances of the quartz and mica increased linearly; an increase of the integrated flux by an order of magnitude produced a corresponding increase by an order of magnitude in the resistance of the quartz, and a 50 percent increase in that of the mica. When the radiation flux was reduced by four orders of magnitude the conductivity of the specimens fell to a value less than 10^{-14} ohm^{-1}.

Because of the fact that the resistance of the porcelain specimens remained rather high under irradiation, the measurements were made in a region of small sensitivity of the apparatus. Thus the error in the results is about 30 percent.

The initial fall of the resistance is explained by the effect of the temperature and the ionizing action of the γ-rays and neutrons [3–5]. With an increase of the integrated irradiation flux the accumulation of radiation defects begins to affect the resistance [4–8]. This causes an increase of the resistance of the mica and quartz. When the flux density of the neutrons and γ-rays was reduced by four orders of magnitude (curve 7) the resistance of the specimens increased and became too large for the sensitivity of the measuring circuit we were using.

The results of this work lead to the conclusion that quartz, porcelain, and mica show good retention of their insulating qualities at a flux density of neutrons and γ-rays of about 10^{13} neutrons cm^{-2} sec^{-1} and integrated flux $\sim 5 \cdot 10^{18}$ neutrons/cm^2.

The writers thank Professor A. K. Krasin for proposing the topic and for his constant interest in the work, and also A. V. Zvonareva for assistance in carrying out the experiment.

Received October 8, 1958.

Literature

1. J.C. Pigg and C.D. Bopp, Communications and Electronics 22, 717 (1956).
2. R.D. Shelton and J.G. Kenney, Nucleonics 14, 9, 66 (1956).
3. D.S. Billington, Nucleonics 14, 9, 54 (1956).
4. O. Sisman and J.C. Wilson Nucleonics 14, 9, 58 (1956).
5. A. Charleby, Nucleonics 14, 9, 82 (1956).
6. A.I. Zakharov, Usp. Fiz. Nauk 57, 525 (1955).
7. G.H. Kinchin and R.S. Pease, Usp. Fiz. Nauk 60, 590 (1956).
8. J.W. Glen, Usp. Fiz. Nauk 60, 445 (1956).

THE CALCULATION OF THE THERMAL CONDUCTIVITIES OF MOLTEN METALS

G. F. Butenko and M. I. Radchenko

Because of the limited amount of data on the thermal conductivities of molten metals the extrapolation of these data to high temperatures is of particular interest. The difficulty of graphical extrapolation is increased by the uncertainty in our knowledge as to the temperature dependence of the thermal conductivities of liquid metals. On the other hand there is no great difficulty with the extrapolation of the electric conductivity of molten metals, since the temperature dependence of the resistance can be taken to be linear over a wide range.

Therefore an attempt has been made to obtain a unique temperature dependence of the Lorentz function for a number of thermodynamically similar metals, so that by using values of the electric resistance obtained by extrapolation one can calculate the thermal conductivity:

$$\lambda = \frac{L T}{r}, \tag{1}$$

where λ is the thermal conductivity, L the Lorentz function, T the absolute temperature, and r the electric resistance.

Figure 1 shows the relation $L = f(t)$ for various metals.

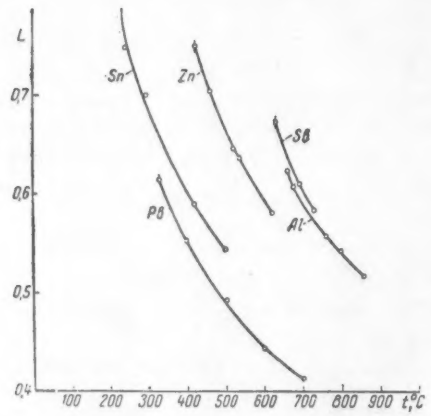

Fig. 1. Temperature dependence of the Lorentz function for various metals.

From the theory of thermodynamic similarity it follows that groups of thermodynamically similar substances must have universal functional dependences on the reduced parameters of state.

Let us write down the well-known equation for the thermal conductivity [1]

$$\lambda = \frac{g^{\frac{1}{2}} (\mu R)^{\frac{5}{6}} p_c^{\frac{2}{3}}}{\mu^{\frac{1}{2}} T_c^{\frac{1}{6}}} f\left(\pi, \tau, \frac{c_{v_0}}{R}\right), \tag{2}$$

where $\pi = \frac{p}{p_c}$ and $\tau = \frac{T}{T_c}$ are the reduced parameters of state; μ is the molecular weight; R is the universal gas constant; p_c and T_c are the critical pressure and temperature; g is the acceleration of gravity; and c_{v_0} is the specific heat at constant volume.

The thermal conductivity of a liquid metal is made up of phonon and electron conductivities:

$$\lambda = \lambda_{ph} + \lambda_e, \tag{3}$$

where λ_{ph} is the phonon thermal conductivity and λ_e is the electronic thermal conductivity. The phonon thermal conductivity can be expressed in the form [4]:

$$\lambda_{ph} = \frac{h \nu_{max} w}{3 s T}, \tag{4}$$

where h is Planck's constant, ν_{max} a phonon vibration frequency, w the speed of sound in the metal in question, s the cross section for scattering of phonons, and T the absolute temperature. Therefore Eq. (2) can be supplemented by certain universal coefficients to take account of the phonon thermal conductivity.

It can be expected that the thermal and electric conductivities have only weak dependences on the pressure. Since the electric conductivity is also a function of the temperature, the following expression will be valid:

$$L = c f_1\left(\frac{T}{T_c}\right), \tag{5}$$

where c is a constant. In order to distinguish a group of thermodynamically similar substances from among the monatomic liquid molten metals, we have drawn a curve (Fig. 2) in the dimensionless coordinates $\frac{L}{L_m}$ and $\frac{T}{T_m}$. The data on which the curve is based are taken from different authors [2, 3]. Assuming that at

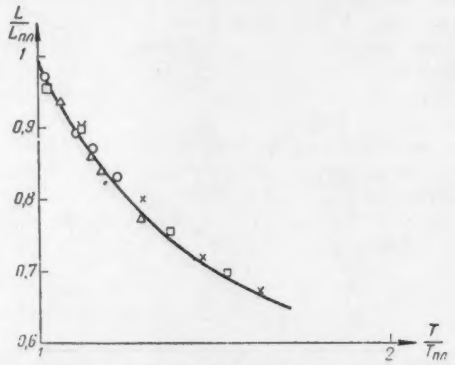

Fig. 2. Dependence of the dimensionless Lorentz function on the dimensionless temperature.

○ — aluminum [2]; □ — tin [3]; △ — zinc [2]; × — lead [3].

the melting point the substances are in corresponding states, we have analyzed the experimental data by reference to this temperature. The small scatter of the points provides a basis for the assumption that these metals belong to a single group of thermodynamically similar substances. All the points fall satisfactorily on the curve given by the equation

$$\frac{L}{L_m} = 0{,}2 \frac{4\frac{T}{T_m} + 1}{2\frac{T}{T_m} - 1}.$$

As a test of this assumption a curve was drawn with the coordinates $\frac{\lambda r}{(\lambda r)_m}$ and $\frac{T}{T_m}$ (Fig. 3). The points for sodium and potassium do not fall on the curve

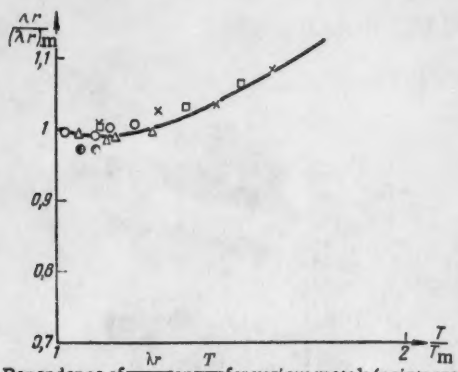

Fig. 3. Dependence of $\frac{\lambda r}{(\lambda r)_m}$ on $\frac{T}{T_m}$ for various metals (points are marked as in Fig. 2; points ◐ are for antimony [2,3]).

$$\frac{\lambda r}{(\lambda r)_m} = 0{,}2\,\frac{T}{T_m}\,\frac{4\frac{T}{T_m}+1}{2\frac{T}{T_m}-1},$$ drawn in Fig. 3.

The anomalous variation of the Lorentz function for mercury, insufficiency of data for cadmium, and contradictions in the data for bismuth, are the reasons we have not included these metals.

Thus we have distinguished a group of thermodynamically similar substances among the simple monatomic molten metals, and for this group we have determined a universal dependence of the dimensionless Lorentz function on the dimensionless temperature.

This group of thermodynamically similar substances, like the corresponding group defined in terms of the viscosity [5], consists of metals occurring only in the right-hand subgroups of the Mendeleev table. This gives a confirmation of the connection of the electric and thermal conductivities with the molecular structure of a liquid. Furthermore, the law we have found is an additional proof of the close relation between the thermal conductivity and the electric conductivity for molten metals.

Our equation is of practical interest for the determination by calculation of the thermal conductivities of liquid metals of this group at various temperatures, if one knows the thermal conductivity, the electric conductivity, and the temperature at the melting point, and also the electric conductivity at the temperature in question. It must be emphasized that the determination of the electric conductivity is a simpler task experimentally than that of the thermal conductivity.

Only a sufficient quantity of experimental data will provide a possibility of confirming the conclusions reached in this paper.

Received April 11, 1958

Literature

1. M.P. Vukalovich and I.I. Novikov, Technical Thermodynamics [in Russian] (Gosénergoizdat, 1955) p. 143.
2. R.W. Powell, Thermal Conductivities of Molten Metals and Alloys [Russian translation] (Translation GNB 17111, 1949).
3. N.T. Gudtsov and M.N. Gavze, "The Action of Mercury as a Heat Transfer Medium on Steel in Power Installations", Proceedings of the A.A. Baikov Metallurgical Institute [in Russian] (AN SSSR Press, 1956) p. 140.
4. Ya. I. Frenkel', Introduction to the Theory of Metals [in Russian] (Gostekhizdat 1950) p. 193.
5. A.N. Solov'ev, J. Atomic Energy (U.S.S.R.) 3, 12, 550 (1957).

A SEPARATION CASCADE OF DIFFUSION COLUMNS

R . Ya. Kucherov and G. A. Tevzadze

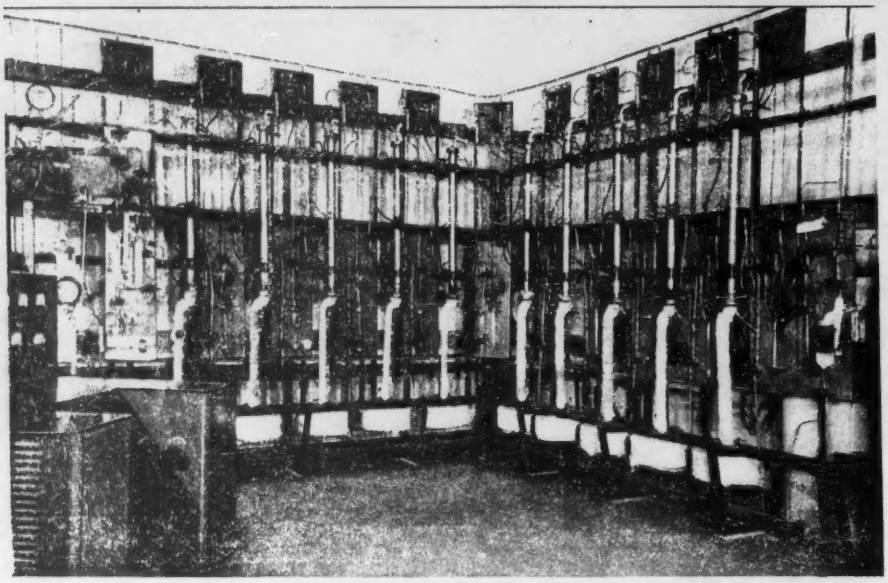

General view of the separation cascade.

The report of G. F. Barvikh and R. Ya. Kucherov at the All-Union Scientific and Technical Conference on the Applications of Radioactive and Stable Isotopes* mentioned the construction of a laboratory separation cascade consisting of 10 diffusion columns. We shall give some of the specifications of this cascade and some results obtained on the separation of the isotopes of neon, argon, and carbon.

The successive individual columns were connected according to the scheme: upper condenser of nth column--lower part of the space between the diaphragm and condenser of the $(n+1)$st column--upper part of the same space in the nth column. The flow of gas in the communicating tubes was assured by the hydrodynamic pressure drop caused by the vapor flowing through the diaphragm. The amount of gas flowing was measured with a capillary flowmeter. Control experiments showed that the flow was sufficient to assure the effective exchange of gas between the columns.

A 200-liter bulb containing the original material was attached to one end of the cascade, and the product gas enriched in the required isotope was drawn off from the other end.

The total diaphragm area in the ten columns of the cascade was 1.25 m^2, and the length of the diaphragm in each column was 1 m. The cascade consumed 7 to 8 kw of electric power. Xylol was used as the working liquid. The cascade could be operated at a pressure of 100 to 300 mm Hg. A general view of the cascade is shown in the photograph.

In the case of separation of the neon isotopes at a pressure of 280 mm Hg the time for establishment of the stationary state was about 60 hours. At smaller pressures this time was shorter in proportion to the reduction of the pressure.

The cascade was used to separate the isotopes Ne^{22}, Ar^{36} and C^{13} (methane). When methane was being separated its large solubility in xylol led to remixing of gas of differing isotopic compositions, which caused a decided lowering of the concentration and a reduction of the amount of product that could be withdrawn. The results obtained are shown in the table.

Gas separated	Isotope	Number of columns in cascade	Amount of gas removed, normal cm^3 per 24 hours	Original concentration of isotope to be separated, percent	Concentration of separated isotope, percent
Neon	Ne^{22}	10	400	9.2	99
Argon	Ar^{36}	9	175	0.31	14
Methane	C_1^{13}	9	500	1.1	12

*See the collection: "Isotope Production, Powerful Gamma-Ray Sources, Radiometry, and Dosimetry" (in Russian), Proceedings of the All-Union Scientific and Technical Conference on the Applications of Radioactive and Stable Isotopes and Radiations in the National Economy (AN SSSR Press, 1957) pp. 120-126.

Received September 9, 1958

PRODUCTION OF Sb^{125} AND In^{113m} WITHOUT CARRIERS

V. N. Rybakov and I. I. Stronskii

In the separation of tin, antimony, and tellurium by the ion-exchange method [1] we discovered the possibility of separating from tin irradiated with thermal neutrons the isotopes Sb^{125} and In^{113m}, formed by the reactions

$$Sn^{124}(n,\gamma)Sn^{125} \xrightarrow[10\ days]{\beta^-} Sb^{125} \xrightarrow[2,7\ hrs]{\beta^-} \rightarrow Te^{125m} \xrightarrow[58\ days]{\text{i.t.}^1} Te^{125}_{stab}$$

$$Sn^{112}(n,\gamma)Sn^{113} \xrightarrow[112\ days]{K} In^{113m} \xrightarrow[1,74\ hrs]{\text{i.t.}} In^{113}_{stab}$$

[1] i. t.—isomeric transition

For complete transition of the Sn^{125} to Sb^{125} it is necessary to store the irradiated tin for four months [2].

There are published papers on the problem of separating radioactive isotopes of antimony and indium without carriers [3-7]. The methods for separating them are described in survey articles [8, 9]. In these papers no use was made of the ion-exchange method for producing Sb^{125} and In^{113m} without carriers. The possibility of using this method is a very interesting subject for study.

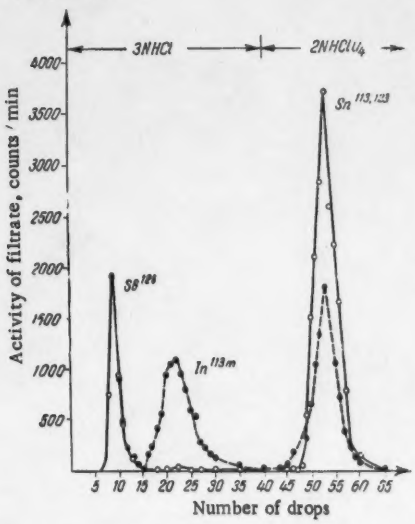

Fig. 1. Separation of Sb^{125}, In^{113m}, and $Sn^{113, 123}$ on anionite ASD-2.

THE EXPERIMENTAL WORK. For the separation of the radioactive isotopes of antimony and indium we used a column of diameter 2 mm and height 100 mm, filled with the strongly basic anionite ASD-2 in chloroform; the particle size was $\sim 30\,\mu$.

The resin in the column was treated with concentrated hydrochloric acid containing 10--20 mg of Br_2 per liter, after which it was carefully eluted with 3N HCl. The experiments were made with a solution of radioactive tin (3N acid with HCl) containing 2.3 mg of Sn^{IV} per ml. About 0.1 ml of this solution was introduced into the column. The elution of the antimony and indium was done with 3N HCl at the rate of 1 drop (0.04 ml) per minute, and that of the tin with 2N $HClO_4$ at the same rate. Figure 1 shows a chromatogram of the separation of the antimony, indium, and tin. The measurements of the activity of the original solution and the filtrate were made with an end-window counter MST-17 two times: the first time directly after the elution (dashed curve in Fig. 1) and the second time 24 hours later (solid curve). The second measurement showed that in one fraction the activity was unchanged, in another it had practically disappeared, and in the third it had increased by about a factor two.

For the identification of the fractions, measurements of the energies of the γ-radiation from the peak drops were made with a scintillation γ-ray spectrometer with a NaI(Tl) crystal*. The first fraction gave the spectrum shown in Fig. 2. Comparison of the γ-ray energies in this spectrum with tabulated values [10] shows that they belong to Sb^{125}. For the second fraction the γ-ray energy was measured with the spectrometer and the half-value period was found with the MST-17 counter. The decay curve of In^{113m} is shown in Fig. 3. The energy of the γ-radiation was found to be 0.42 ± 0.4 Mev, and the half-value period was 105 ± 2 min; within the limits of error of the measurements these values agree with the tabulated values for In^{113m} [10]. The third fraction is identified as $Sn^{113, 123}$.

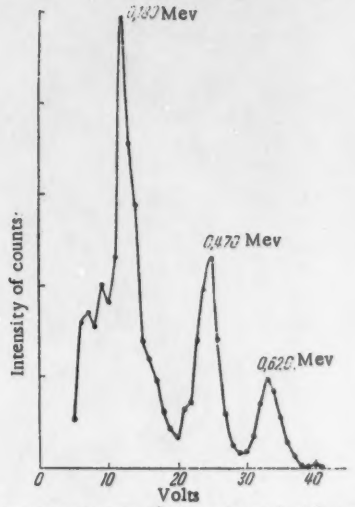

Fig. 2. Gamma-ray spectrum of Sb, measured with a scintillation γ-ray spectrometer with a NaI(Tl) crystal.

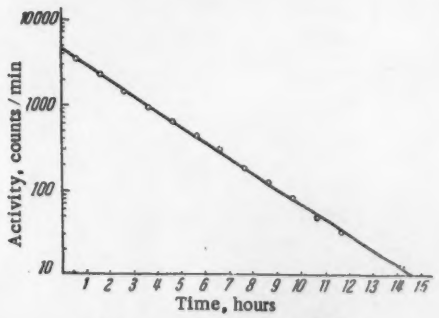

Fig. 3. Decay curve of In^{113m}.

* The measurements with the γ-ray spectrometer were made by V. V. Kuznetsov, to whom the writers express their sincere thanks.

The chromatographic column was also used for the repeated production of indicator quantities of In^{113m}. In this case the tin was not washed out with perchloric acid. After the removal of the radioactive antimony isotope and the establishment of equilibrium between Sn^{113} and its daughter product In^{113m} the radioisotope of indium was taken out in 0.8 ml of 3N HCl filtrate. Control experiments showed that on the first elution the indium fraction contained 1.5 percent of long-lived radioactive contaminations (evidently Sb^{125}), but on subsequent elutions no contaminations were detected.

SUMMARY: 1) an ion-exchange method has been developed for the separation of indicator quantities of antimony and indium from the radioactive tin isotopes, which makes it possible to produce Sb^{125} and In^{113m} without carriers; 2) the chromatographic column has been used for repeated separation of In^{113m}.

The writers regard it as their pleasant duty to express their thanks to V. A. Khalkin for his constant interest in this work and to V. A. Yakovlev for providing the possibility of making measurements with the γ-ray spectrometer.

Received August 20, 1958

Literature

1. V.N. Rybakov and I.I. Stronskii, J. Inorg. Chem. (U.S.S.R.) (in press).
2. A.N. Nesmeyanov, A.V. Lapitskii, and N.P. Rudenko, The Production of Radioactive Isotopes [in Russian] (Moscow, State Chemistry Press, 1954).
3. E. Jacobi. Helv. Phys. Acta 22, 66 (1949).
4. P.T. Barret, Proc. Roy. Soc. 218A, 104 (1953).
5. V.D. Nefedov, S.P. Lepnev, E.N. Sinotova, and M.A. Toropova, J. Inorg. Chem. (U.S.S.R.) 3, 167 (1958).
6. I.D. Robinson and M. Kahn, J. Amer. Chem. Soc. 75, 2004 (1953).
7. N.P. Rudenko, J. Phys. Chem. (U.S.S.R.) 31, 354 (1957).
8. A.N. Murin, V.D. Nefedov, and I.A. Yutlandov, Uspekhi Khimii 24, 527 (1955).
9. N.P. Rudenko, in Coll.: Applications of Marked Atoms in Analytical Chemistry (in Russian) (Moscow, AN SSSR Press, 1955) pp. 155-178.
10. G. Seaborg, I. Perlman, and J. Hollander, [Russian Translation]. Table of Isotopes (Moscow, IL, 1956).

BRIEF COMMUNICATIONS

USSR. A general-purpose device has been designed at the Joint Institute for Nuclear Research, for measuring the intensity of a time-invariant magnetic field over the range extending from 300 to 20,000 oe. The instrument is based on utilization of the phenomenon of nuclear resonance absorption. The allowable inhomogeneity of the magnetic field in the region of the sensing device is 4—5% of the measured value. Measurement accuracy is ± 0.01%. A one-quarter molar (0.25 M) aqueous solution of $Fe_2(SO_4)_3$ is being used as a sample.

USSR. At the Physics and Engineering Institute of the Academy of Sciences of the USSR, a method has been developed for stabilizing constant current or constant voltage, based on the use of the field of a permanent magnet as a reference value. Conversion of the intensity of a constant magnetic field to constant current is realized with the aid of a compensation magnetometer using a magnetically saturated probe as a sensing device. Experimental studies on a current stabilizer designed on the basis of that method, showed that when the supply voltage is varied from 70 to 180 v, the change in the constant current of 220 ma comes to ± 0.027%. When the voltage or load resistance is changed, the change in current does not exceed 0.001%.

USSR. At the Leningrad Institute of Railroad Transportation Engineers, two methods have been developed for measurements of weak magnetic fields. The first method, involving measurement of inhomogeneous magnetic fields, is based on the nutation of the total magnetic moment of protons. The method was verified over the range of magnetic fields from 0.17 to 500 oe, with an inhomogeneity of up to 200 oe/cm. The accuracy of the measurements is determined basically by the inhomogeneity of the field inside the volume of the sensor, which occupies 0.2 cm^3. The second method makes it possible to measure and stabilize weak homogeneous magnetic fields on the basis of the magnetic resonance of protons. The device developed there affords the possibility of measuring magnetic fields with intensities as low as 5 oe. The accuracy achieved in measurements of the intensity of the magnetic field reaches 10^{-4} at the lower limit, and increases as the field intensity increases. Field stabilization is realized beginning with 12 oe. The stabilization factor is ~ 300.

USSR. At the Scientific Research Institute of Nuclear Physics attached to Moscow State University, a multichannel recorder has been developed to record tracings of pulse amplitudes for pulses of $\sim 3 \cdot 10^{-5}$ sec duration or longer. The device is designed in the form of a compact package containing 49 miniaturized 8L029 cathode-ray tubes, the tube screens being photographed on a single over-all frame. Recording accuracy of the amplitudes comes to within ~ 5%.

BELGIUM. Three Belgian firms concluded an agreement with the company "Electricité de France" for the joint construction of an atomic electric power plant near the Franco-Belgian frontier.

CHINA. During its first week, the Soviet science and engineering exhibit on the peaceful uses of atomic energy, which opened up in December 1958 at the Palace of Sino-Soviet Friendship in Shanghai, was visited by more than 70 thousand persons. Other thousands came to Shanghai from scientific research institutions in Peking, Wuhan, Shenyang, and other cities to study the exhibits displayed, to hear lectures given by Soviet specialists, etc. Soviet specialists delivered lectures on thermonuclear processes, on isotope production, the use of isotopes in science and industry, etc. Popular science films were shown to visitors in the movie auditorium housed in the exhibit. This exhibit will also be on display at Hwangchow and Chengtu.

CHINA. Arrangements have been made for the production of nuclear photoemulsions and elementary particle counters. Also being manufactured are 100-channel and 50-channel pulse analyzers and high-power oil diffusion pumps.

BIBLIOGRAPHY

New Literature

PHYSICS OF PLASMA AND THE PROBLEM OF CONTROLLED THERMONUCLEAR REACTIONS. A symposium of articles edited by M. A. Leontovich, appearing in four volumes. Publ. by Academy of Sciences of the USSR, 1958. Vol. I contains 300 pp, Vol. II 356 pp., Vol. II 363 pp., and Vol. IV 400 pp., 50 rubles.

For the opening of the Second International Conference on the Peaceful Uses of Atomic Energy (Geneva, 1958), the publishing house under the auspices of the Academy of Sciences of the USSR released a symposium of articles giving an exposition of theoretical and experimental research on the problem of controlled fusion and on problems of plasma physics associated with it, from research carried out at the Institute of Atomic Energy (IAE) of the Academy of Sciences of the USSR. The symposium includes over one hundred papers reflecting the basic findings of intense research on the study of fusion processes at the IAE since 1951. Papers published during 1956—1957 following the widely publicized report by I. V. Kurchatov at the British atomic center in Harwell are not included in the symposium. Over-all guidance of the research was entrusted to L. A. Artsimovich, while theoretical papers were handled by M. A. Leontovich. The research had its beginnings in contributions by I. E. Tamm and A. D. Sakharov, which took up the possibility of obtaining a high-temperature plasma and self-sustaining thermonuclear reactions in systems incorporating magnetic confinement of the plasma. Articles by I. E. Tamm and A. D. Sahkarov published in the first volume provide general evaluations of the possibilities of containing plasma and the conditions required for achieving controlled thermonuclear reactions, and consider the motion of particles immersed in electric and magnetic fields, suggesting a method for stabilizing toroidal drift with the aid of a strong current induced along the axial circumference of the toroid.

Those concepts acted as a stimulus to the first experimental and theoretical work on obtaining and studying plasmas in toroidal systems. Papers submitted by A. M. Andrianov, O. A. Bazilevskaya, S. Yu. Luk'yanov, N. A. Yavlinskii, S. M. Osovets, Yu. F. Petrov, I. M. Podgornyi, B. I. Davydov (pp. 42-109) take up electrodeless discharges (induction discharges

of methods for investigating plasma, including spectroscopic measurements. The results of the investigations showed that, to avert toroidal drift, what was required was a large axial current to constrain the discharge to contract (pinch effect), i.e., assure the containment of the plasma column forming upon the discharge. On that basis, research was developed and conducted intensively on studies of high-current discharges in straight cylindrical pinch chambers filled with deuterium. Among the papers treating of this trend which appear in the first volume, we duly note the contribution of M. A. Leontovich on studies of the stabilizing action of the conductive sheath surrounding the linear current; a paper by S. I. Braginskii on bottling of current by the magnetic field proper; a study by B.A. Trubnikov on instability of a pinch (buckling and constriction of cylindrical plasma column), and a paper by M.A. Leontovich and V.D. Shafranov on stabilization of the discharge by a longitudinal magnetic field. Of interest also is a paper submitted by G. I. Budker suggesting a betratron method for heating the plasma to high temperatures. All of these papers are included in the first volume, and represent work carried out in 1951–1952.

Further studies on the stabilizing effects of a longitudinal magnetic field and of the conducting sheath are presented in papers appearing in the second volume by L. A. Artsimovich, S. I. Braginskii, V. D. Shafranov, T. F. Volkov (pp. 26, 81, 101, 144). The same volume includes papers by N. A. Borzunov, D. V. Orlinskii (p. 150), S. M. Osovets (p. 165), V. S. Kamel'kov, T. I. Morozova, Yu. V. Skvortsov (p. 170), providing detailed investigations of electric high-current discharges in deuterium and neutron radiation associated with them.

Of interest are papers by S. M. Osovets, Yu. V. Petrov, I. I. Shchedrin and Yu. F. Nasedkin (pp. 238-264), reporting research on the powerful annular discharge induced by a special-configuration variable magnetic field and resulting in the formation of a plasma annulus in the area of a stationary orbit, with the plasma breaking away from the orbit as time passes and converging toward the center. The magnetic energy stored by the ring current is then converted to the kinetic energy associated with the radial motion of the particles. The further development of this line of research is described in articles found in the third volume.

The third volume starts off with an article by G. I. Budker on a theoretical investigation of a plasma trap with magnetic mirrors, and lays the foundations for a new direction of development in thermonuclear research (cf. the article by I. V. Kurchatov, J. Atomic Energy, Vol. 5, August 1958).

A large number of theoretical articles appearing in the third and fourth volumes (S. M. Belyaev, V. V. Babikov, A. E. Bazhanova, S. I. Braginskii, G. I. Budker, T. F. Volkov, B. B. Kadomtsev, V. S. Kudryavtsev, V. I. Kogan, L. I. Rudakov, R. Z. Sagdeev, B. A. Trubnikov, O. B. Firsov, V. D. Shafranov) are devoted to general problems in plasma physics, to the study of electromagnetic oscillations of plasma, and to the use of electromagnetic waves for confining and heating the plasma. Among those contributions one should note a paper by B. A. Trubnikov and A. E. Bazhanova entitled "Magnetic Radiation of a Plasma Layer" (Vol. 3, p. 121), the findings of which call for a re-evaluation of the significance of radiation in the energy balance of the reacting plasma.

Of the experimental papers included in the fourth volume, we note the contributions of A. A. Bezbatchenko, I. P. Golovin, P. I. Kozlov, V. I. Pistunovich, V. S. Strelkov, and N. A. Yavlinskii on studies of high-current toroidal discharges stabilized by a magnetic field (pp. 116-156); E. E. Yushmanov on a cylindrical magnetic trap with plasma injection by magnetron, as proposed by M. S. Ioffe and V. G. Tel'kovskii; I. M. Podgornyi, S. A. Chuvatin, G. A. Bykov, and V. D. Pis'mennyi on the investigation of the process of electrodynamic acceleration of plasma bunches.

This brief review does not afford space to give the gist of the papers appearing in the symposium which touch, to one or another degree, on questions related to the problem of controlled thermonuclear reactions and plasma physics. In addition to papers earlier published, a bibliography of which is provided at the end of the symposium, materials are also included which give the balance sheet of the seven-year efforts of the faculty of physicists and engineers at the Institue of Atomic Energy in the field of controlled fusion. The study of those papers will unquestionably prove of value to all those occupied or interested in thermonucleonics.

The series is written for a fairly sophisticated audience -- physicists and engineers engaged in thermonuclear research, as well as senior and graduate students specializing in that field.

STATIC AND DYNAMIC ELECTRON OPTICS (the theory of focusing in lenses, deflecting systems, and accelerators). P. A. Starrock translated from the English by E. L. Burshtein, edited by M. L. Levin (Foreign Literature Press, 1958), 286 pp. The book takes up, in succession, the use of the general methods of Lagrange, Hamilton, Lyapunov, and Poincaré in the study of image converters and stability in accelerators. Those methods are used to advantage in the analysis of the properties of the most important instruments and facilities: electron lenses, beta spectrographs, mass spectrographs, deflecting plates of cathode-ray tubes, and some types of accelerators (synchrotron, linear accelerator, strong-focusing accelerators).

In the first part of the book, Static Electron Optics, the focusing of charged particles in static electromagnetic fields is treated. This part embraces the following chapter headings: The Variational Equation; Instrumental Electron Optics; Systems Exhibiting Rotational Symmetry; Systems Exhibiting Mirror Symmetry. In the second part of the book, Dynamic Electron Optics, we find a discussion of focusing of charged particles by time-variant electromagnetic fields. This part consists of two chapters on homogeneous focusing in charged-particle accelerators and periodic focusing in accelerators. In the first chapter, it is assumed that focussing proceeds at a slow rate during an acceleration cycle (which explains the term "homogeneous" adopted by the author). Such an assumption is fully valid when treating of cyclic accelerators in which the particle executes a large number of phase and radial oscillations over a single acceleration cycle. In the first chapter, the synchrotron and linear accelerators are considered, and in the second chapter, a discussion is given on the 25-Bev synchrocyclotron now being erected at Brookhaven National Laboratory.

The book will prove a valuable aid for those concerned with applications in the field of charged-particle dynamics. The most attractive part of the book, from the interested reader's standpoint, is the second part, touching on the theory of focusing of charged particles in accelerators.

DAS ZENTRALINSTITUT FUR KERNPHYSIK AM BEGINN SEINER ARBEIT. (Symposium Describing Work Initiated at the Central Institute of Nuclear Physics in East Germany) Barwich, Schintlemeister, Thummler. (Publ. by H. Barwich, Akademie-Verlag, Berlin, 1958) 59 pp. The Central Institute of Nuclear Physics of the German Democratic Republic at Dresden has released a collection of articles devoted to the commencement of research at the Institute.

The symposium presents reports by German scientists read at an enlarged session of the scientific council of the Institute. The session met on December 16, 1957, in Dresden and was dedicated to the official commissioning of the research reactor.

The article by H. Barwich, entitled "Research Reactor of the German Democratic Republic and Its Perspectives," reports that on December 14, 1957, the research reactor, developing 2,000 kw power, went critical. The reactor is of the swimming-pool type, operating on enriched uranium (10%). Fuel elements (in the form of rods) have aluminum cladding. The core is contained in an aluminum tank. Water acts as moderator, coolant, and shielding.

Each working cell of the reactor accommodates 16 uranium fuel rods 1 cm in diameter and 50 cm in height. The initial charge of the reactor is 26 cells. The reactor has 9 experimental channels (passing through a cast iron and concrete shield), a thermal column, channels for the production of isotopes and other facilities.

Alongside the reactor building stands a radiochemical laboratory. It is reported that work has already begun on much of the research contemplated, and that preparations are underway in the remainder of the schedule.

Investigations carried out on the reactor will make it possible to clear up a number of problems related to the building of the German Democratic Republic's first atomic-fired electric power plant, in which a pressurized-water reactor will be employed. Checking of various theoretical aspects of a heavy-water homogeneous reactor will also be of great interest, at a later time.

The article by Schintlemeister, entitled "On the Cyclotron at the Institute of Nuclear Physics and Scientific Plans Dealing with the Physics of the Atomic Nucleus", described the second major facility of the Institute, a cyclotron. The cyclotron is intended for acceleration of alphas to energies of 25 Mev, or deuterons to 12.5 Mev. The cyclotron parameters are: diameter of electromagnet pole piece: 1200 mm; air gap: 170 mm; intensity of magnetic field at center: 14,100 oe; dee voltage 140-150 kv; resonant wavelength: 22--30 meters; capacity of diffusion pumps: 3000 liters/sec.

The article also outlines the operating principles of cyclotrons and describes experiments which may be performed on them.

The article by F. Thummler, "Some Interesting Problems in Materials Technology in Nuclear Power Engineering", discusses briefly the properties of uranium and of the cladding material used for fuel elements, their behavior inside a nuclear reactor and the effect of radiations on materials (fuel, construction materials, high polymers, semiconductors), and explains the phenomenon of radiation damage to solids as a result of thermal spikes and displacement spikes.

SOURCEBOOK ON ATOMIC ENERGY, S. Glasstone, (Van Nostrand Co., 1958) 641 pp. In the second edition of the sourcebook, Glasstone takes up modern theoretical concepts of radioactivity, describes the design and operation of cyclotrons, synchrotrons, and nuclear reactors. New chapters have been added on nuclear reactors, the identification of the fundamental particles, transmutations of new elements and the uses of isotopes.

REACTOR PHYSICS CONSTANTS. (ANL-5800, 1958) 536 pp. The book provides physical constants, theoretical and empirical formulas, results of experiments, tables and graphs needed for performing the complete physical design of reactors of various types (constants published in March—April of 1958 are also included). The book has nine parts.

In the first part, the Fission Process, yields of fission fragments and fission spectra of fast and thermal neutrons are considered. Extensive material is available on delayed neutrons, illustrated with tables and graphs of the reactor transfer functions required in reactor kinetics computations.

The second part, Selected Cross-Section Data, provides data on the energy-transfer cross sections of neutrons in the thermal region, data on inelastic scattering by U^{238} and on averaging of cross sections based on various energy spectra of neutrons.

The third part, Spectrum of Thermal Neutrons in Infinite Homogeneous Media, gives the spectra of slow neutrons in one-atom and many-atom gases, ordinary and heavy water (taking into account chemical bonds), as well as in water with boric acid added. Group physical constants are also given for thermal intermediate neutrons and high-energy neutrons. At the end of this part of the book, information is given on kinetics calculations and control methods for homogeneous reactors.

In the fourth part, Lattice Constants of a Thermal Heterogeneous System, methods are described and the necessary data are adduced pertaining to the design of a thermal heterogeneous reactor using various types of moderator. On the basis of the data presented, it is possible to take into account anisotropy of neutron diffusion, the effect of channels in the lattice, and other features affecting the value of the multiplication constant.

In the fifth part, Intermediate Reactors, information throwing light on some specific features of the design of intermediate-spectrum reactors is given, as well as the constants required for the many-group design of intermediate reactors in the diffusion-age approximation.

In the sixth part, Fast Reactors, together with experimental data on critical masses and the composition of fast-reactor cores, constants are given for the design of reactors in one-, two-, three-, six-, ten- and eleven-group approximations. A procedure is derived for evaluating the accuracy of calculations of the radius of a fast reactor with a reflector.

In the seventh part, Constants for Shielding Design, data are given on radiation yields from the reactor core, neutron, and gamma attenuation in shielding materials.

In the eighth part, Constants Related to the Interpretation of Experimental Data, information is made available on parameters and the procedure to be followed for obtaining physical measurements.

In the ninth part, Properties of Fuel Elements and Reactor Materials, information needed for calculations related to the composition of reactor structural materials and the physical properties of fuel elements (heat conductivities, specific heats, coefficients of linear expansion, melting and boiling points) are made available.

An extensive bibliography is appended to each part. The symposium will serve as a useful manual in the physical design of the majority of existing reactor types.

THE PHYSICS OF INTERMEDIATE SPECTRUM REACTORS. Edited by J. R. STEHN, US AEC, UC-81, 1958, 478 pp. The results of research work on intermediate spectrum reactors carried out at Knolls Atomic Power Laboratory are collected in this book. The book consists of four parts.

The first part, Investigation of the Characteristics of Reactor Critical Facilities, describes in detail the design of critical assemblies, methods for measuring reactivity and calibrating control rods, and compares experimental findings with design data in the multigroup approximation.

The second part, Reactivity Measurements During Reactor Operation, contains calculations of the poisoning of an intermediate reactor, calculations of burnable additives, and a description of the physical processes taking place in the starting up and operation of an experimental intermediate reactor.

The third part, Heat Generation and Design Materials, gives the calculations of heat generation in the reactor core, associated with the absorption of primary and capture gammas. Results of experiments on the determination of residual heat production in intermediate reactors incorporating sodium coolant with a beryllium moderator are presented.

The fourth part, Kinetics and Temperature Coefficients, contains ample experimental material on temperature coefficients of reactivity (related to heating of core features and of the sodium coolant) and data on Doppler broadening of resonance peaks in the cross sections of fissionable materials. Results of experiments performed with different techniques are compared.

The book is written for a readership of specialists engaged in the field of reactor design.

In Press

REPORTS BY SOVIET AND FOREIGN SCIENTISTS AT THE SECOND INTERNATIONAL CONFERENCE ON THE PEACEFUL USES OF ATOMIC ENERGY (Geneva, 1958). Atomizdat, 16 volumes. This edition* consists of 16 books, which include about 250 reports by Soviet scientists (taking up 6 books in the series) and about 500 selected papers by foreign scientists (10 books).

Reports by Soviet Scientists

NUCLEAR PHYSICS, Edited by Academician A. I. Alikhanov, Academician V. I. Veksler, Candidate Phys.-Math. Sci. N. A. Vlasov.

NUCLEAR REACTORS AND NUCLEAR POWER ENGINEERING, Edited by Corresponding Member of Academy of Sciences of the USSR N. A. Dollezhal', Prof. Dr. Phys.-Math. Sci. A. K. Krasin, Acting Member of Acad. Sci. Ukrainian SSR A. I. Leipunskii, Corresponding Member Acad. Sci. USSR I. I. Novikov, and Prof. Dr. Phys.-Math. Sci. V. S. Fursov.

NUCLEAR FUEL AND REACTOR MATERIALS, Edited by Acadamician A. A. Bochvar, Acadamician A. P. Vinogradov, Corresponding Member Acad. Sci. USSR V. S. Emel'yanov, and Dr. Tech.-Sci. A. P. Zefirov.

CHEMISTRY OF RADIOELEMENTS AND OF RADIATIVE TRANSMUTATIONS, Edited by Academician A. P. Vinogradov.

RADIOBIOLOGY AND RADIATION MEDICINE, Edited by Corresponding Member Acad. Med. Sci. USSR A. V. Lebedinskii.

PRODUCTION AND USE OF ISOTOPES, Edited by Academician G. V. Kurdyumov and Corresponding Member Acad. Sci. USSR I. I. Novikov.

Reports by Foreign Scientists

PHYSICS OF HOT PLASMA AND THERMONUCLEAR REACTIONS, Edited by Candidate Tech. Sci. V. F. Kalinin.

NEUTRON PHYSICS, Edited by Cand. Phys.-Math. Sci. N. A. Vlasov.

PHYSICS OF NUCLEAR REACTORS, Edited by Acting Member Acad. Sci. Ukrainian SSR A. I. Leipunskii and Prof. Dr. Phys.-Math. Sci. V. S. Fursov.

NUCLEAR REACTORS AND NUCLEAR POWER ENGINEERING, Edited by Corresponding Member Acad. Sci. USSR N. A. Dollezhal', Prof. Dr. Phys.-Math. Sci. A. K. Krasin, and Corresponding Member Acad. Sci. USSR I. I. Novikov.

CHEMISTRY OF RADIOELEMENTS AND OF RADIATIVE TRANSMUTATIONS. Edited by Academician A. P. Vinogradov.

NUCLEAR FUELS AND REACTOR MATERIALS, Edited by Academician A. A. Bochvar, and Corresponding Member Acad. Sci. USSR V. S. Emel'yanov.

TECHNOLOGY OF ATOMIC RAW MATERIALS, Edited by Dr. Tech. Sci. A. P. Zefirov.

GEOLOGY OF ATOMIC RAW MATERIALS, Edited by Academician A. P. Vinogradov.

RADIOBIOLOGY AND RADIATION MEDICINE, Edited by Corresponding Member Acad. Med. Sci. A. V. Lebedinskii.

PRODUCTION AND APPLICATIONS OF ISOTOPES, Edited by Academician G. V. Kurdyumov and Corresponding Member Acad. Sci. USSR I. I. Novikov.

ENGLISH-RUSSIAN RADIO AND ELECTRONICS ENGINEERING DICTIONARY, (Atomizdat) compiled by N. I. Dozorov. The dictionary is printed in accordance with the American edition, supplemented by approximately 2000 new entries. It contains a grand total of

* "Prospectus of proceedings of the Second International Conference on the Peaceful Uses of Atomic Energy," (Atomizdat, 1958) 24 pp.

about 24,000 terms and definitions in radio engineering and electronics, with applications in the following branches of science and engineering: automatic control, acoustics, antennas and waveguides, military systems, railroad communications, signaling, block systems and automatic traffic control, measurements and measuring devices, radio power supplies, semiconductor devices, radio astronomy, navigational aids, radar, radio communications links, radio broadcasting, radio engineering, radio physics, radio-wave propagation, x-ray applications, television telegraphy, remote control, telemetry telephony, infrared and ultraviolet techniques, amplifiers, facsimile, electrical machinery, vacuum-tube techniques and devices, medical electronics, electrical engineering. Terms relating to nucleonics applications, guided missiles, meteorology, and geophysics are also partially covered.

ELECTROSTATIC GENERATORS, (Atomizdat). A. K. Val'ter et al. This is a symposium of reports by a team of authors headed up by Acting Member of the Academy of Sciences of the Ukrainian SSR A. K. Val'ter. It is devoted to the general principles of the design of electrostatic generators and fields in which they find application, and also to particular problems arising in designing, testing and operating them. A number of articles deal with various subassemblies incorporated in electrostatic generators (power sources, apparatus for voltage measurement and stabilization, accelerator tubes, etc.).

COMPENDIUM OF PROBLEMS IN ATOMIC PHYSICS (Atomizdat). I. E. Irodov. The compendium consists of 12 chapters, embracing all of the basic subdivisions of a course in atomic physics. Answers are provided to the problems, as well as solutions of the most complicated problems presented. At the beginning of each section, resumes of the basic formulas and physical concepts are given.

The present compendium is the only available adequately complete textbook especially devoted to atomic physics. It is written for students in the pertinent specialities.

SOVIET SCIENTISTS TAKE THEIR STAND AGAINST TESTING OF ATOMIC WEAPONS. (Sovetskie uchenye protiv ispytanii atomnogo oruzhiya) (Atomizdat). This symposium of reports by the prominent Soviet scientists, V. M. Klechkovskii, B. V. Kurchatov, A. V. Lebedinskii, and others, is devoted to the problems arising from contamination of the earth's surface due to radioactive products of fallout from nuclear explosions. The symposium provides data on the extent of contamination of the territory of the USSR, as well as on the harmful effects of radioactive substances on human and animal organisms. It is prefaced by remarks of Academician I. V. Kurchatov.

ATOMIC ENGINEERING ABROAD, No. 2 (1959). This issue contains translated articles on various aspects of atomic engineering.

In an article by Ramon L. Ashley, Effective-Energy Method for Spent-Fuel Shielding, Nucleonics 16, 10 (1958), a method of replacing the complex spectrum of gamma radiation of fission fragments by a single group of gamma quanta with effective energy is provided.

Graphs provided, make it possible to perform in a short time, a fairly accurate calculation of the shielding. The results of the computations are compared with experimentally observed data.

An abridged translation of an article by M. Daniels and J. Weiss, "Effects of Ionizing Radiations on Solids," Research 10: 9, 341; 10, 396 (1957), contains a brief description of findings of the latest theoretical and experimental work on the study of the chemical effects of various types of radiations on the structure of matter (halides of alkali metals nitrate and cyanide crystals, ice, ammonia, carbon dioxide, and organic substances).

An article by J. Sharp, "Neutron Detectors," Nucl. Engng. 3, 27 (1958), deals in brief with available types of detectors used for slow, intermediate, and fast neutrons. Particular attention is given to the detection of neutrons with energies $\lesssim$100 kev in the presence of a background of thermal neutrons and gammas, and the possibility of greater speed in reaching evaluations of the energy spectrum of neutron flux is also pointed out.

Articles by M. Nachman, L. Sechter, H. Totia appear in The Use of Spark Counters for Fast Neutron Detection, a report presented by Roumania at the Second International Conference at Geneva on the Peaceful Uses of Atomic Energy. The efficacy of three particle detectors discussed which serve as detectors of neutrons with energies of several megaelectron-volts, varies, depending on the filling gas, from $5 \cdot 10^{-5}$ to 10^{-3}%.

An article by R. Bock, A. Dering, and others, "A Single-Dee Fixed-Frequency Cyclotron," Z. fur angew. Phys. 10, 2, 49 (1958), provides a description of the subassemblies of the machine, as well as a description of the operating characteristics of the redesigned single-dee cyclotron at Heidelberg (West Germany).

An article by H. Albers and B. Walter, "Simulation of the Dynamic Behavior of the Swiss D_2O Reactor DIORIT" (Geneva paper No. 231), provides a description of the facilities for simulating neutron kinetics and the temperature coefficient of reactivity of the Swiss heavy-water reactor DIORIT. Reactor characteristics obtained by simulation of various modes of reactor operation are disclosed.

Geneva paper No. 2402, USA, "The Physics of Boiling Water Reactors," provides a review of theoretical and experimental work in research on the effect of the control system on the volume power distribution in a boiling water reactor, and also reviews work on the study of the dynamics of power installations using boiling water reactors. Two theoretical methods are considered: the "inverse method" for two-dimensional problems, allowing the possibility of obtaining a power distribution with the density of a neutron sponge taken into account, and the WKB method (Wenzel-Kramers-Brillouin), which makes it possibility to quickly find the neutron density distribution and the steam coefficient of reactivity associated with it.

An article by D. S. Arnold, P. W. Henline, and R. H. Sisson, "Utilization of a Moving-Bed Reactor for the Production of Uranium Tetrafluoride" (Geneva paper No. 1015, USA), deals with the characteristics of a reactor installation built to process UO_3 into UF_4. As an example, a moving-bed reactor with a product capacity of 5000 tons annually is considered. The process of manufacturing UO_3 pellets as reactor raw material is described.

NUKLEONIKA (Polish Nucleonics Journal) Vol. 4, 1 (1959): L. Infield, "Impressions of the Second Geneva Conference"; J. Zlotkowskii and M. Zelinskii, "Observation of Isotope Effect in Displacement Process by

the Van Slyke Method of C^{14}-Tagged Aliphatic Alcohols and Acids"; A. Selecki and R. Broszkiewicz, "Ultracentrifuge Separation of Isotopes"; Use of Ionizing Radiation for Sterilizing Foodstuffs and Medicinals; J. Wasiliuk, "Review of the Most Important Isotopes in Use at the Present Time in Biology and Medicine"; K. Kowalska, "Nuclear Research in Brazil", S. Minc and Z. Libus, "Investigation of Extractive Properties of Tributylphosphate."

COMMUNICATIONS: A 14-channel pulse height analyzer with counter attachment; LE-1 model E electronic counting circuit; LE-3 model A electronic counting circuit; LE-4 electronic counting circuit; LE-2 high-speed attachment.

Book reviews. Chronicle. Bibliography.

Articles from the Periodical Literature

M.A. Abdulkabirova, "Thorium in Several Granitoids of Kalba and Altai." Izvestiya akad. nauk kazakh, SSR, Seriya geol. No. 2 (1958).

A. I. Akishin, "Recording of Ion Beams by Photoelectronic Multipliers in Mass Spectroscopy and Nuclear Research," Uspekhi fiz. nauk XVI, 2 (1958).

I.P. Alimarin and G.N. Bilimovich, "Use of Method of Isotope Dilution for Determination of Various Rare Elements." Trudy komis. po analit. khim. Akad. nauk, SSSR 9 (1958).

S.I. Alyamovskii et al. "On Lower Oxides of Niobium," Zhur. neorgan. khim. 3, 11 (1958).

S. V. Balmukhanov, "Chronic Radiation Effects and Problems Facing Workers in the Health Service Field," zdravookhranenie Kazakhstana, 8 (1958).

Yu. N. Barabanenkov, "Hydrodynamic Approach to the Compression of a Rarefied Plasma in an Axisymmetric Magnetic Field," Zhur. eksptl. i teor. fiz. 35, 11 (1958).

N. G. Belen'kii, et al., "Study of Alteration of S^{35}-Labeled Meat Proteins in the Process of Thermal Denaturation," Doklady vses. akad. s.-kh. nauk (Proceedings of All-Union Academy of Agricultural Sciences), 9 (1958).

B.I. Boltaks et al., "On the Absorption Coefficient of Gammas Emitted by Co^{60} in Semiconductors," Doklady akad. nauk SSSR 123, 1 (1958).

S.E. Bresler and G.E. Pikus "Contribution to the Theory of Isotope Separation and Separation of Alloy Constituents in the Passage of Current Through Molten Metal," Zhur. tekhn. fiz. 28, 10 (1958).

Yu. I. Bykovskaya "Niobium Assay in the Presence of Large Amounts of Titanium," Trudy komis. po analit. khim. akad. nauk SSSR 9 (1958).

Yu. V. Vandakurov, "Contribution to the Theory of Focussing in Accelerators with a Magnetic Field Periodically Varying in Azimuth," Zhur. tekhn. fiz. 28. 11 (1958).

A.G. Vasil'ev et al.. "Study of Ground Waters Using the Technique of Isotope Analysis." Trudy Khar'kovsk. otdeleniya vsesoyuz. khim. obshch-va (Proc. of Kharkov Section of All-Union Chemical Society) 1 (1958).

I.A. Vasil'ev and K.A. Petrzhak. "Radiochemical Study of Photofission in Th^{232}." Zhur. eksptl. i teor. fiz. 35. 11 (1958).

V.I. Veksler and L.M. Kovrizhnykh. "On the Cyclic Acceleration of Particles in High-Frequency Fields," Zhur. eksptl. i teor. fiz. 35. 11 (1958).

A.A. Glazov and D.L. Novikov, "Investigation of a Resonance High-Frequency Discharge," Zhur. tekhn. fiz. 28, 10 (1958).

A.I. Danilin, "Radioactive Snow Meter for Field Snow Surveys," Trudy NII gidrometeorol. priborostroeniya (Proceedings of Scientific Research Institute for Hydrometeorological Instrument Design), 6 (1958).

Kh. A. Dzherpetov, "Effect of Permanent Magnetic Field on Ignition and Quenching Characteristics of a High-Frequency Discharge," Vestnik Mosk. un-ta. (Bulletin of Moscow University) Seriya matem., mekhan., astronomii, fiz., khim. (Mathematics, Mechanics, Astronomy, Physics, Chemistry Series) 1 (1958).

T.T. Drobyazko, "Electromechanical Mortar for Separating Radioactive Powders," Zavodsk. Laboratoriya 24, 10 (1958).

A.N. Ermakov et al., "Anion Exchange Studies of Complexing of Zirconium and Hafnium with Oxalate Ion," Trudy komis. po analit. khim. (Akad. nauk SSSR), 9 (1958).

V.M. Zaporozhets and E.M. Filippov, "Use of Charged-Particle Accelerators in the Study of Oil Field Bore Holes, Employing Radioactive Logging Techniques," Prikladnaya geofizika, 20 (1958).

I.E. Zimakov and G.S. Rozhavskii, "A Technique of Multiple Radioactive Dilution for Assay of Trace Impurities," Trudy komis. po analit. khim. (Akad. nauk SSSR) 9 (1958).

N.A. Izmailov and V.S. Chernyi, "Investigation of Solubility of Salts in Nonaqueous Solvents by Means of Tagged Atoms," Trudy komis. po analit. khim. (Akad. SSSR) 9 (1958).

I.A. Kakovskii and V.I. Revnivtsev, "Separation of Zircon and Apatite by the Method of Electrical Separation," Otdel. tekhn. nauk (Izvestiya akad. nauk SSSR), 9 (1958).

L.B. Kaminir and G.N. Orlovskii, "On Some Features of the Operation of The High-Frequency System of a Synchrotron with a Large Number of Electrons Accelerated per Cycle," Zhur. tekhn. fix. 28, 11 (1958).

K.I. Karasev and T.N. Mukhina. "Use of the Labeled-Atom Technique for Determining the Effectiveness of the Fractionation of Gaseous Hydrocarbons." Trudy komis. po analit. khim. (Akad. nauk SSSR) 9 (1958).

I.M. Kol'tgof. "Use of Radioactive Isotopes in the Study of Aging of Crystalline Precipitates (articles from USA)." Trudy komis. po analit. khim. (Akad. nauk SSSR) 9 (1958).

A.N. Komarovskii, "Concrete with Increased Water Content for Shielding from Nuclear Reactor Radiations," Beton i zhelezobeton (Concrete and Reinforced Concrete), 8 (1958).

E.V. Kopchenova and K.V. Skvortsova, "On Collomorphic Molybdenite and Uranium-Molybdenum Black Rocks in Uranium Deposits," Doklady Akad. nauk SSSR 123, 1 (1958).

S.M. Kochergin and G.R. Pobedimskii, "Use of Radioactive Isotopes in the Study of the Conditions Governing the Formation of Electrolytic Alloys," Zhur. prikl. khim. 31, 9 (1958).

I.V. Krapivina, "Propagation of a Plasma Beyond the Range of the Discharge Space," Trudy vses. elektrotekhn. in-ta (Proc. of All-Union Electrical Engng. Inst.), 63 (1958).

V.I. Kuznetsov et al., "Acid Decomposition Technique in Thorium and Uranium Assay in Sandstones," Zavodsk. laboratoriya 24, 10 (1958).

A.K. Lavrukhina, "Several Features of Radiochemical Analysis," Trudy komis. po analit. khim. (Akad. nauk SSSR), 9 (1958).

L.A. Nisel'son, "Separation of Tantalum, Niobium, and Zirconium by the Method of Rectification." Nauchnye doklady vysshykh shkol. Metallurgiya (Scientific Reports of Higher Schools, Metallurgy) 3 (1958).

L.I. Pivovar and V.I. Gordienko. "Microdischarges and Pre-Discharge Currents Between Metal Electrodes Immersed in a High Vacuum." Zhur. tekhn. fiz. 28. 10 (1958).

I.A. Piontkovskii. "On Several Features of the Higher Nervous Activity of Adult Animals Exposed to Prenatal Bombardment by Ionizing Radiations; Contribution to the Effects of Ionizing Radiations on Heredity," Communication 1. Byull. eksperim. biol. i med. 46, 9 (1958).

R.F. Post, "Energy from Fusion," Uspekhi fiz. nauk 65, 2, 314 (1958). [Russian translation].

E. Ya. Pumper "Absorption of Gases in a Low-Pressure Arc," Zhur. tekhn. fiz. 28, 10 (1958).

N.P. Rudakov, "Labeling of Fish by Radiocerium," Rybnoe khozyaistvo (Fish Husbandry) 9 (1958).

S.A. Rudenko, "On the Nature of Zircon Found in Alkaline Pegmatites of the Azov Sea Region," Zapisi. Leningr. gorn. in-ta (Memoirs of Leningrad Mining Institute) 33, 2 (1958).

E.F. Simonova, "Radioactive Isotopes and Their Role in the Solution of Problems in Biology and Agriculture," Zapisi Voronezhsk. s.-kh. in-ta (Memoirs of the Voronezh Agricultural Institute) 28 (1958).

M.F. Skalozubov and V.I. Matsokin, "Radiometric Determination of Surface of Disperse and Porous Substances," Zhur. prikl. khim. 31, 9 (1958).

V.P. Skripov, "Heat of Mixing of Ordinary and Heavy Water," Zhur. eksptl. i teoret. fiz. 35, 11 (1958).

I.E. Starik, et al., "Carbonate Method for Separating Trace Quantities of Uranium from Iron," Trudy komis. po analit. khim. (Akad. nauk SSSR) 9 (1958).

K.N. Stepanov. "Low-Frequency Plasma Oscillations in a Magnetic Field " Zhur. eksptl. i teoret. fiz. 35 11 (1958).

R.V. Teis et al.. "Isotope Composition of Naturally Occurring Phosphates," Doklady Akad. nauk SSSR 122, 6 (1958).

A.M. Ushakova, "Determination of Small Amounts of Uranium in Potassium Salts by the Luminescence Technique," Ukrains'ki khimichni zhurnal (Ukrainian Chemical Journal) 24, 4 (1958).

E. Hang-Tse and L.V. Vechorek, "State of Matter at High Temperatures and Pressures," Priroda, 10 (1958).

V. P. Shvedov and L. M. Ivanova, "Isolation from Complex Mixtures and Purification of Several Short-Lived Isotopes," Trudy komis. po analit. khim. (Akad. nauk SSSR), 9 (1958).

V. P. Shvedov and N. A. Pavlova, "Coprecipitation of Zirconium with Cerium Oxalate in Nitric Acid Medium," Trudy komis. po analit. khim. (Akad. nauk SSSR), 9 (1958).

N.I. Shtela, "Graphic and Analytic Plotting of Paths of Charged Particles in Electrostatic and Magnetic Fields," Zhur. tekhn. fiz. 28, 11 (1958).

K.B. Yatsimirskii and E.N. Roslyakova, "Radiometric Titration Using Solutions of Cobalt-60 Complexes," Trudy komis. po analit. khim. (Akad. nauk SSSR) 9 (1958).

J.W. Allison, "Gamma-Radiation Absorption Coefficients of Air in the Energy Range 0.01 to 100 Mev," J. Appl. Phys. 29, 8, 1175 (1958).

S.K. Allison, "Experimental Results on Charge-Changing Collisions of Hydrogen and Helium Atoms and Ions at Kinetic Energies above 0.2 kev," Rev. Mod. Phys. 30, 4. 1137 (1958).

J.C. Allred et al., "Critical Measurements on UO_3-H_3PO_4 Solutions," Nucl. Sci. and Engng. 4, 3, 498 (1958).

W.K. Anderson and D.N. Dunning. "Radiation Damage Resistance of Some Rare Earth Cermets." Nucl. Sci. and Engng 4. 3. 458 (1958).

W. K. Anderson, "Broad Aspects of Absorber Materials Selection for Reactor Control," Nucl. Sci. and Engng. 4, 3, 357 (1958).

W.H. Arnold. "Two-Group Calculation of Prompt Neutron Lifetime." Nucl. Sci. and Engng. 4. 4, 598 (1958).

N. Balai, "Materials, Fabrication and Performance of the EBWR Control Rods," Nucl. Sci. and Engng. 4, 3, 429 (1958).

M. Balicki, "Absence of Irradiation Growth in α-Uranium above 430° C," Nucl. Sci. and Engng. 4, 3, 502 (1958).

M.M. Bayet, "Fusion of Light Nuclei: General Considerations Pertaining to Thermonuclear Power Production," J. Phys. et Radium 19, 8-9, 62S (1958).

G.A. Behman, "Table of Particle-Acceleration Facilities," Nucl. Instruments 3, 4, 181 (1958).

J.A. Brimson, "Sources of Radiation Injury in Naval Medicine," Arch. Industr. Health 18, 3, 186 (1958).

A.M. Brues, "Criticism of the Theory of a Linear Dependence of the Development of Malignant Neoplasma on the Radiation Dose," Science 128, 3326, 693 (1958).

L.F. Bates and R.G. Loasby, "Magnetic Susceptibility and Electrical Resistivity of Several Uranium Alloys," Proc. Phys. Soc. 72, 467, 757 (1958).

S. Cohen et al., "Mu-Meson Molecular Ions and Nuclear Catalysis." Phys. Rev. 110, 6, 1471 (1958).

G.W. Cunningham et al., "Development of a Composite Control Rod," Nucl. Sci. and Engng. 4, 3, 449 (1958).

M.I. Deverall "Solution of the Time-Dependent Thermal Neutron Diffusion Equation." Nucl. Sci. and Engng. 4 3 495 (1958).

D.J. Donahue et al. "Determination of k_∞ from Critical Experiments with the PCTR." Nucl. Sci. and Engng. 4. 3 297 (1958).

D.N. Dunning et al., "Boron Containing Control Materials." Nucl. Sci. and Engng. 4, 3 102 (1958).

R.E. Dunway and J.A. Phillips, "Neutron Generation from Straight Pinches." J. Appl. Phys. 29, 8, 1137 (1958).

J.H. Ebersole, "Shipboard Medicine on board the Submarines 'Nautilus' and 'Seawolf' ", Arch. Industr. Health 18, 3, 200 (1958).

U. Farinelli et al., "Measurement and Automatic Control of Energy in the 31-Mev Betatron," Nucl. Instruments 3, 4, 218 (1958).

J. Giacobbe and D.N. Dunning, "New Developments in the Fabrication of Hafnium Control Rods," Nucl. Sci. and Engng. 4, 3, 467 (1958).

G. Goertzel, "The Method of Discrete Ordinates," Nucl. Sci. and Engng. 4, 4, 581 (1958).

M.A. Greenfield, "Computing Absolute Thermal Neutron Flux from Measurements Made with Indium Foils," Nucl. Sci. and Engng. 4, 4, 563 (1958).

G.A. Heath and R.M. Hobson, "Modified Ion Source of Mass Spectrometer for Investigation of Solid Samples," J. Sci. Instrum. 35, 11, 429 (1958).

J.D. Jones, "Radiation Shielding (Review article covering Geneva conference reports)," Engineering 186, 4834, 568 (1958).

J. Inorg. and Nucl. Chem., 8 (1958). The entire issue is devoted to papers read at the International Symposium on the Chemistry of Coordination Compounds (Rome. Sept. 15-21, 1957).

D.M. Keaveney et al. "Effects of Low-Lying Europium Resonances on the Temperature Defect in Water-Moderated Reactors." Nucl. Sci. and Engng. 4. 3, 332 (1958).

G. Leibfried. "A Remark on Neutron Thermalization Theory," Nucl. Sci. and Engng. 4, 4, 570 (1958).

J.W. Lucas and D.C. Pickering, "Direct Absorption of Sr^{90} and Y^{90} in Solution by Frog Tadpoles (rana temporaria)," Nature 182, 4644, 1242 (1958).

J. McPhee, "The Kinetics of Circulating Fuel Reactors," Nucl. Sci. and Engng. 4, 4, 588 (1958).

P. Ohlin et al., "Study of Neutron Production in a Linear Deuterium Pinch," Nucl. Instr. 3, 4, 237 (1958).

S. Pearlstein, "Application of the Absorption Area Method to Three-Group Diffusion Theory Problems," Nucl. Sci. and Engng. 4, 3, 322 (1958).

W.G. Pettus and I.E. Dayton, "Mutual Shielding of Lattice Pins in the Resonance Energy Region," Nucl. Sci. and Engng. 4, 4, 522 (1958).

L.B. Prus et al., "Boron Stainless Steel Alloys," Nucl. Sci. and Engng. 4, 3, 415 (1958).

W.E. Ray and C.J. Beck, "A Method of Hot Coextruding Complex Shapes Through Round Dies." Nucl. Sci. and Engng. 4. 3 481 (1958).

W.E. Ray et al., "Discrete Fixed Poison Rods Containing Boron," Nucl. Sci. and Engng. 4, 3, 386 (1958).

E.C. Ridley, "Quantitative Study of the Wave Function of Metal Uranium," Proc. Roy. Soc. 247, 1249, 199 (1958).

M.T. Robinson et al., "The Behavior of Fission Products in Molten Fluoride Reactor Fuels," Nucl. Sci. and Engng. 4, 3, 288 (1958).

M.T. Robinson "Xenon Poisoning Kinetics in Gas-Sparged, Molten Fluoride Fueled Nuclear Reactors," Nucl. Sci. and Engng. 4, 3, 270 (1958).

M.T. Robinson "On the Chemistry of the Fission Process in Reactor Fuels Containing UF_4 and UO_2," Nucl. Sci. and Engng. 4, 3, 263 (1958).

P.A. Roys and K. Shure, "Production Cross Section of N^{16} and N^{17}," Nucl. Sci. and Engng. 4, 4, 536 (1958).

V. Spiegel et al., "Age to Indium Resonance for D-D Neutrons in Water," Nucl. Sci. and Engng. 4, 4, 546 (1958).

R. Steiger et al., "Erection of the European Center for Nuclear Research," Atomkernenergie no. 10, 375 (1958).

H.E. Stevens "Nuclear Requirements for Control Materials," Nucl. Sci. and Engng. 4, 3, 373 (1958).

P.G. Vendryes, "Will Industrial Use of Thermonuclear Energy Be Feasible in the Near Future?," J. Phys. et Radium 19, 8-9, 724 (1958).

G. H. Vineyard, "Scattering of Thermal Neutrons in Water," Phys. Rev. 110. 5, 999 (1958).

J. T. Weber, "Effect of Alloying on the Critical Mass of a Plutonium Spherical Fast Reactor," Nucl. Sci. and Engng. 4, 3, 341 (1958).